Hydrodynamics of jumping in archer fish, Toxotes microlepis

by

Anna Margaret Shih

B.S., Mechanical Engineering
Tufts University (2008)

Submitted to the Department of Mechanical Engineering
in partial fulfillment of the requirements for the degree of

Master of Science in Mechanical Engineering

at the

MASSACHUSETTS INSTITUTE OF TECHNOLOGY

June 2010

Author .....
Department of Mechanical Engineering
May 7, 2010

Certified by .....
Alexandra H. Techet
Associate Professor of Mechanical and Ocean Engineering
Thesis Supervisor

Accepted by .....
David Hardt, Professor of Mechanical Engineering
Chairman, Department Committee on Graduate Theses

Hydrodynamics of jumping in archer fish, Toxotes microlepis

by

Anna Margaret Shih

Submitted to the Department of Mechanical Engineering
on May 7, 2010, in partial fulfillment of the
requirements for the degree of
Master of Science in Mechanical Engineering

Abstract

The maneuvering of fish is not only of interest to those wishing to better understand how fish function, but also is a great inspiration for designing underwater vehicles. This thesis provides the first characterization of the behavior of *Toxotes microlepis*, the archer fish, as it jumps for bait above the water surface. Two separate studies provide information on both the kinematics and hydrodynamics associated with the jump. The kinematic study makes use of high speed backlight videos and image processing, while the hydrodynamic study relies on high speed digital particle image velocimetry (DPIV).

The kinematic study is able to successfully break the jumping behavior into three parts: (1) hovering, (2) thrust production and (3) gliding. Hovering is when the fish is beneath the surface of the water and is trying to maintain position. Thrust production occurs when the archer begins to perform tail strokes and exit the water, resulting in a sharp spike in acceleration and a subsequent increase in velocity. Gliding happens after the archer has partially left the water and is no longer flapping its tail, at which point the archer refrains from any motions until after it has captured its bait. Detailed velocity and acceleration plots are presented. The number of times an archer flaps its tail is shown to increase with the height of the bait, as is the maximum velocity it attains. Additionally, an energy balance is explored.

For the hydrodynamic study, PIV shows that each time the archer fish performs a tail stroke during the thrust production phase, a jet is formed that provides impulse to enable jumping. Additionally, the anal fin is shown to have a significant impact on the thrust production, as it also produces a jet. Numerical results for the circulation and impulse created by these jets are presented.

Thesis Supervisor: Alexandra H. Techet
Title: Associate Professor of Mechanical and Ocean Engineering

Acknowledgments

Clearly, none of this thesis would have been possible without my adviser, Alexandra Techet, who supported my thesis not only financially but also was kind enough to give me advice and tolerate my dreams of turning the lab into a giant aquarium. My UROP student, Elli Pauli was also very supportive and helpful when I needed assistance building my set up or was unwilling to measure the fish, among other things.

My labmates provided tons of help as well as comic relief from the fish. Tadd Truscott was the master of the inspirational pep talk, dispenser of useful advice, and all around fun and helpful. Jesse Belden and Brenden Epps provided Matlab codes, valuable pointers and general technical advice, while Rod La Foy would come up with useful suggestions when I was stuck on something. Jenna McKown made sure to provide advice and fun distractions when needed.

Additionally, my parents and friends listened to hours of random thoughts on fish, reassured me when I was convinced I was a bad fish caretaker, and made sure I stayed sane through all of the hours of waiting for archer fish to jump.

Finally I would like to acknowledge the archer fish. They are adorable and I want to take them home with me.

Contents

1 Introduction **15**

1.1 Archer Fish; *Toxotes* 16

1.2 Literature Review 17

1.2.1 Fast Starting Kinematics, Performance and Fluid Mechanics . 17

1.2.2 Swimming and Fluid Mechanics 19

1.2.3 Fish Jumping 21

1.2.4 Archer Fish 22

1.3 Outline of Thesis 25

2 Experimental Methods **27**

2.1 Fish and Aquariums 27

2.2 Kinematic Analysis 28

2.2.1 Data Processing 30

2.3 Flow Visualization 30

2.3.1 Image Processing 32

3 Archer Fish Behavior **35**

3.1 Introduction 35

3.2 Swimming 35

3.3 Station Keeping 36

3.4 Prey Approach 36

3.5 Jumping 37

3.5.1 Sequence of Jumping Motions 37

3.5.2 Body Kinematics 41
3.5.3 Angle of Initial Inclination 43
3.5.4 Tail Strokes 46
3.5.5 Dimensionless Parameters 51

4 Kinematic Analysis **57**
4.1 Introduction 57
4.2 Position, Velocity and Acceleration Data 58
4.2.1 Data Processing 58
4.2.2 Maximum Velocity and Acceleration 61
4.2.3 Velocity and Acceleration Variation Throughout Jump 63
4.3 Jump Duration 73
4.4 Over Shooting 74
4.5 Energy Analysis 77

5 Hydrodynamic Analysis **93**
5.1 Introduction 93
5.2 Hovering 93
5.3 Thrust Production 95
5.3.1 Anal Fin Contribution 95
5.3.2 Caudal Fin Contribution 97
5.4 Circulation 103

6 Conclusions **109**
6.1 Kinematics of Jump 109
6.2 Fluid Mechanics of Jump 110
6.3 Consideration for Future Studies 111

List of Figures

1-1 Images of jumping versus shooting. 16

1-2 Toxotes microlepis 17

1-3 Toxotes microlepis leaping for food. 18

2-1 Particle Image Velocimetry set up 31

2-2 Example PIV image, pre and post processing. 33

3-1 Flow chart of actions leading up to shooting. 37

3-2 Image series of an archer jumping. 38

3-3 Hovering before a jump. 39

3-4 Thrust production during the jump. 40

3-5 The glide portion of an archer's jump. 41

3-6 Body traces of archers through time while jumping. 42

3-7 Additional body traces of archers through time while jumping. 44

3-8 Schematic side view of archer's jump. 45

3-9 The angle that a fish is from vertical compared to the height of bait the fish was jumping for. 46

3-10 Example of a tail stroke. 47

3-11 Jump height in body lengths vs the number of tail strokes. 48

4-1 Nose position over time. 59

4-2 Nose velocity over time. 60

4-3 Nose acceleration over time. 61

4-4 Maximum velocities of various fish with jump height. 62

4-5 Maximum accelerations of various fish with jump height. 63
4-6 Jumping velocity and acceleration, Archer 1 66
4-7 Jumping velocity and acceleration, Archer 2 67
4-8 Jumping velocity and acceleration, Archer 3 68
4-9 Jumping velocity and acceleration, Archer 3 69
4-10 Jumping velocity and acceleration, Archer 10 70
4-11 Jumping velocity and acceleration, four archers 71
4-12 Repeatability of jumping velocity and acceleration, three archers . . . 72
4-13 Fish maximum jump heights versus the time it took to reach maximum height. 73
4-14 Percentage overshoot that fish overshot based on fish size. 75
4-15 Percent bait height that fish overshot versus bait height. 76
4-16 SolidWorks model of Archer 1 78
4-17 Comparison of maximum kinetic and potential energies for all archers. 80
4-18 Archer 1 energy analysis for highest jump. 81
4-19 Archer 1 energy analysis for lowest jump. 82
4-20 Archer 2 energy analysis for highest jump. 83
4-21 Archer 2 energy analysis for lowest jump. 84
4-22 Archer 3 energy analysis for highest jump. 85
4-23 Archer 3 energy analysis for lowest jump. 86
4-24 Archer 4 energy analysis for highest jump. 87
4-25 Archer 4 energy analysis for lowest jump. 88
4-26 Archer 10 energy analysis for highest jump. 89
4-27 Archer 10 energy analysis for lowest jump. 90

5-1 PIV for an archer fish hovering. 94
5-2 PIV for a jump with bait height of 0.5 BL, laser aligned with anal fin. 96
5-3 PIV for a jump with bait height of 0.5 BL. 98
5-4 PIV for a jump with bait height of 1.0 BL. 99
5-5 Bottom view PIV for a jump with bait height of 0.5 BL. 101

5-6 Bottom view PIV for a jump with bait height of 1.0 BL. 102

List of Tables

2.1 Fish Dimensions 28

2.2 Archer fish used in this study 29

3.1 Inital Angles for Jumps 45

3.2 Tail strokes versus jump height trends 48

3.3 Stroke Information, Archer 1 jump of 0.41 BL 49

3.4 Stroke Information, Archer 2 jump of 0.93 BL 49

3.5 Stroke Information, Archer 3 jump of 1.97 BL 50

3.6 Stroke Information, Archer 4 jump of 1.27 BL 50

3.7 Stroke Information, Archer 10 jump of 2.15 BL 50

3.8 Stroke comparison between similar height jumps 51

3.9 Another stroke comparison between similar height jumps 52

3.10 Froude Number 53

3.11 Strouhal Number 54

3.12 Length and Velocity Ranges 55

4.1 Maximum velocity versus jump height trends 63

4.2 Jump velocity and acceleration reliability 65

4.3 Jump heights versus time trends 74

5.1 Hovering circulation and impulse data for the vortex ring that is shed off the pectoral fin that appears on the left of the images. 105

5.2 Hovering circulation and impulse data for the vortex ring that is shed off the pectoral fin that appears on the right of the images. 105

5.3 Jumping circulation and impulse data for anal fin vortex, bait height 0.5 BL. 106
5.4 Jumping circulation and impulse data for caudal fin vortex, bait height 0.5 BL. 107
5.5 Jumping circulation and impulse data for caudal fin vortex, bait height 1.0 BL. 107
5.6 Jumping circulation and impulse data for caudal fin vortex as viewed from below, bait height 0.5 BL. 108

Chapter 1

Introduction

In southeast Asia there is a diminutive family of fish with a very unusual skill. Not only can these fish find food underwater, but they also are able to forage above the surface of the water. The members of this family are collectively known as archer fish, scientific name Toxotes. The seven species of Toxotes can be found in a variety of conditions, from mangrove-estuaries to freshwater streams. However, despite their varying habitats, all archer fish share a fascination with prey located above the surface of the water. While many people know of Toxotes because of their ability to shoot jets of water at aerial prey, archer fish also have the ability to jump out of water and catch food located close to the surface. Images of both of these behaviors can be found in Figure 1-1. Many researchers are interested in this shooting ability, but the jumping of archer fish should not be ignored as it can also provide valuable insight.

Fish that can jump out of water are of great interest to engineers who draw inspiration from the biological performance of animals. Whales have provided inspiration for flapping foil technology, while squids and salps have given rise to vortex jet thrusters. However, present-day technology has yet to master rapid escape maneuvers for underwater vehicles. In particular, there is no efficient way for these vehicles to surface rapidly and while still functioning efficiently. Water exit is a aspect of underwater maneuvering which could be greatly enhanced by mimicking archer fish and their ability to capture prey above water.

This thesis focuses on Toxotes' ability to jump in order to better understand how

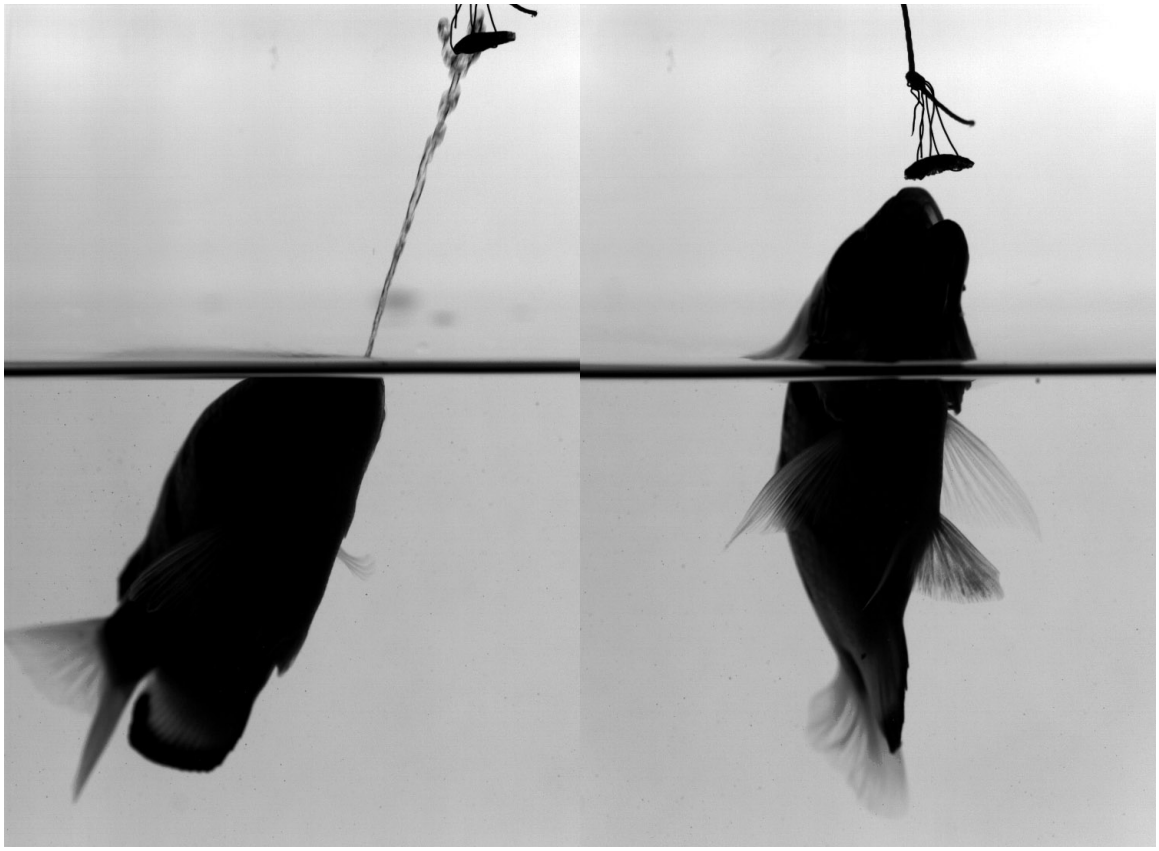

Figure 1-1: On the left, a Toxotes microlepis shoots a jet of water at a dried brine shrimp. In the image on the right the same fish jumps for the prey.

the fish generates the force to propel itself out of the water. Determining the force is done through two methods: first through analysis of high speed video of a fish jumping, then using particle image velocimetry (PIV) to better understand the fluid mechanics of the jump.

1.1 Archer Fish; *Toxotes*

This family of fish is named after the Toxotai, or Greek archers, because of their ability to shoot streams of water at aerial prey. They are members of the class Actinopterygii, which include all the ray finned fishes, and are classified under the order Perciformes, or perch like fish. There are seven species of Toxotes that have been identified in southeast Asia, all of which are normally found in salt water in mangrove swamps or river mouths, however they also have been known to live upstream in freshwater

or out at sea [6]. Toxotes mainly eat insects or small aquatic animals that live near the surface of the water. For all seven species of archers, the fish grow up to be a maximum of 25 cm long. They are distinctive due to their silver bodies with four to six black stripes and also because of their yellowish green dorsal fins and tails. An image of one of the archer fish used in this study can be found in Figure 1-2, while Figure 1-3 provides a more detailed view of an archer fish jumping.

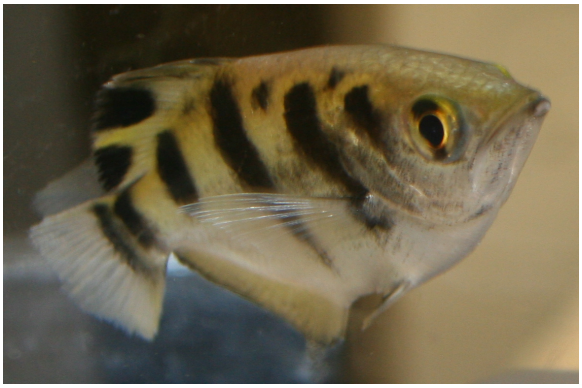

Figure 1-2: Toxotes microlepis

1.2 Literature Review

1.2.1 Fast Starting Kinematics, Performance and Fluid Mechanics

Biologists and engineers alike have studied fish during regular activities such as steady swimming, turning, or accelerating. Maneuvers that involve the brief, sudden acceleration of a fish are considered fast starts. These normally take place during predator-prey interaction, on either side. A notable initial contributor on this subject is Weihs, who developed a general three stage kinematic pattern for C-shape fast-starts [36]. This pattern involves a preparatory stroke (stage I), a main propulsive stroke (stage II) and finally a variable phase (stage III) that changes depending on the type of maneuver being performed. Initial movement begins at the rear of the body as well as the base of the tail, while the head moves in the opposite direction. A good review

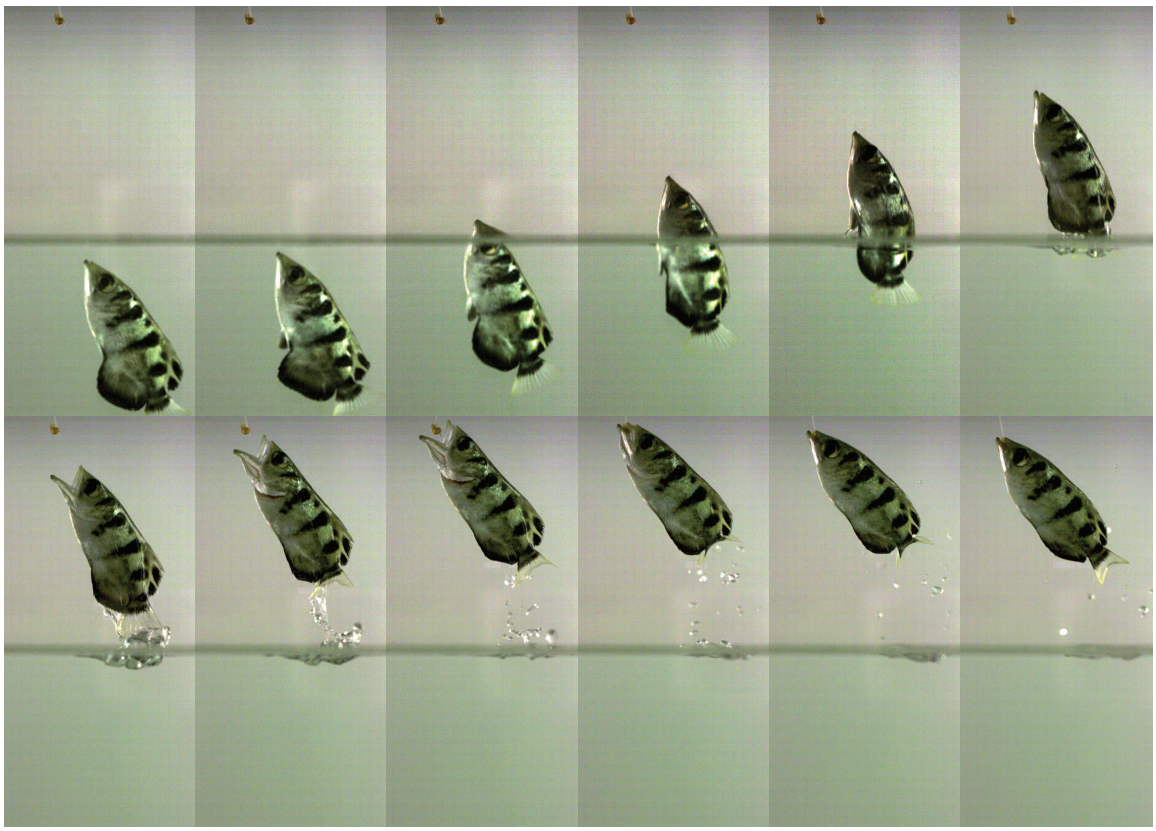

Figure 1-3: Toxotes microlepis leaping for food. Images are 0.01 seconds apart and were taken using a Phantom V9.0

of fast starting by Domenici and Blake [10] summarized the main points developed in the 25 years following Weihs' 1972 investigation. Fast starts are either classified as C or S-starts depending on the shape the fish bends into at the end of the first lateral muscular contraction. C-starts tend to be escape responses; while S-starts are more common for predator strikes [10]. In regards to C-starts, fast C-starts rely on Mauthner neurons in order to be activated and they cover a wide range of behaviors from social interactions to post-feeding turns or escapes. The control system for C-starts and S-starts is not known, but they can both be escape starts, in addition to S-starts being used for predator strikes.

Fast C-starts typically display maximum acceleration during stage I and early in stage II. However, S-starts often persist for multiple tail beats, providing several instances of maximum acceleration (1-4). Larger fish generally have longer duration starting maneuvers and attain slower maximum *specific* speeds (body length/s). Ad-

ditionally, fish observed in laboratory tanks perform better when they are in water that is a temperature they have been acclimated too.

To get an idea of how performance varies between different types of fish, P.W. Webb compared seven species of teleost fish and their fast starts. He selected the species to study based on their varying body shapes [35]. He noted the relationship between maximum velocity and also distance covered in fast-starts is dependent on fish length, as was stated above, but it varies between species.

Since fast-starts are often considered to be different from prey capture, Harper and Blake [17] compared the mean performance of the two maneuvers for northern pike, Esox lucius, and found that acceleration and velocity were greater for the escapes than the feeding strikes. Additionally, they discovered that prey-capture acceleration increased as targets got larger, and also increased for closer prey. However, as is mentioned later, this may not apply for archer fish [38].

In biological terms, the fast start has been ascribed to the Mauthner-initiated startle response in many teleost fish [12]. This type of response is a biphasic process, where the first portion of the reaction is characterized by a rapid increase in displacement and velocity and then the second segment features the fish returning zero angular velocity but still experiencing significant linear velocity for a period of time. Eaton et al. [12] compared the Mauthner-initiated response to other startle responses and found an additional category; "fast-forward displacement". Fast-toward displacements have similar response latencies, but lack the angular velocity component. This type of start also had no early peak in displacement velocity, and thus was categorized as a different type of neurophysiological process that they only found in calico rockfish.

1.2.2 Swimming and Fluid Mechanics

Swimming has also been looked at from the point of view of fluid mechanics. There is a well established body of work on the "footprints" (e.g.[11, 21, 31]) left behind a steadily swimming fish. Muller et al. [21] looked at the overall wake left behind a continuously swimming mullet using two dimensional particle image velocimetry.

From this PIV data the mullet could be seen to shed a vortex every half tailbeat at the most lateral position of the tail. The overall wake viewed in two dimensions is consistent with what would be seen for a three dimensional vortex chain resulting from jet flow. It was determined that some of the circulation of the vortices had been generated by a transverse body wave that travelled down the body, however this was less than half of the energy in the wake. That means that the rest of the energy came from the tail itself. Additionally, the spacing between the shed vortices matched the tailbeat amplitude as well as the stride length of the fish (distance travelled per beat).

In the study by Drucker and Lauder, [11] the vortices that are shed off the pectoral fin of a fish when it is swimming continuously are analyzed through the use of digital particle image velocimetry. This body of experimental work focuses specifically on bluegill sunfish (*Lepomis macrochrius*), but should be extendable to other fish (such as archers) that use their pectoral fins when swimming. For low swimming speeds, the pectoral fins were found to create discrete vortex rings that were fairly symmetrical and uniform. When swimming speeds reached, or passed, the maximum rate of one body length per second that applies to labriform swimmers, there was addition vorticity on the pectoral fins' upstroke. Interestingly, for biphasic responses, splaying of fins occurred when the body bend did.

Triantafyllou, Triantafyllou and Yue [31] summarized the hydrodynamics of swimming. They nicely summarize the work that has been done on the fluid mechanics of real fish and how the vortex wakes behind swimming fish resemble a reverse von Kármán street (vortices are the opposite direction but in the same pattern as behind a bluff body).

Epps and Techet [15] investigated maneuvering kinematics and resultant vortical wakes for Giant Danios that were C-starting. From this 500 Hz PIV data it was possible to see the "maneuvering" and "propulsive" vortices that allow the fish to complete this fast start. Additionally, a linear momentum balance was enacted to compare the change in momentum of the fish's swimming with the impulse of the two vortex rings that were shed. The first vortex to be shed by the fish's tail was the maneuvering one, which had a circulation of 17 cm^2/s and a total impulse of

51 gcm/s. The second, propulsive vortex had a circulation of 34 cm^2/s and a total impulse of 157 gcm/s. In order to calculate these total impulses Epps and Techet used the theory that was set forth by Dabiri [7]. This paper theorizes that the impulse of a vortex ring is composed of three terms; the impulse of a vortex ring moving steadily ahead, an additional term for the thickness of the vortex core and finally a term for the added mass of the ring.

In a similar study, Tytell and Lauder [34] found three fluid jets during escape responses of bluegill sunfish, *Lepomis macrochirus*. An important finding of this paper is that the caudal fin motion opposes the body bend's propulsive momentum during the first stage of the escape. Also, a significant portion of the propulsive momentum is derived from the dorsal and anal fins, which places a new found importantance on the location of these fins compared to a fish's ability to fast start.

1.2.3 Fish Jumping

Archer fish are not the only species of fish that are known to jump out of water. Fish such as salmon and trout also jump, in order to travel upstream. Studies on trout jump height have been used to understand better how to manage trout migration aids. Kondratieff and Myrick evaluated the maximum height a brook trout could jump up two different types of artificial waterfalls [18]; their results were dependent on body length as well as plunge pool depth. This work is representative of the studies on trout, which for the most part are more concerned with the migration of trout than the fluid mechanics or biomechanics of their jumping.

Great white sharks and blacktip sharks are two types of sharks known to jump out of the water. Brunnschweiler [5] studied the water-escape velocities of video-taped blacktip sharks, as well as their maximum height, angle of penetration and duration of jump. From these values the speeds of two sharks studied were calculated at $6.3 \pm 1.2 m/s$ for one shark and $6.3 \pm 2.2 m/s$ for the other shark studied. The angles of escape were either 30 or 45 degrees, with maximum heights of 1 and 1/2 meter respectively. As for great white sharks, they are known to ambush prey by swimming at high speeds and hitting the prey, resulting in a large amount of free

surface disturbance before the attack. Tricas [32] refers to this as the "surface-charge". Unfortunately, this is a difficult behavior to study analytically, so most of the work focuses on the kinematics and timing of surface attacks.

African butterfly fish (*Pantodon buchholzi* Peters) have gained a reputation as fish that need to live in tanks with secure lids because of their propensity to jump out of water. In 2004 Saidel et al. [23] studied the startle response of 26 african butterfly fish and determined that the fish jump upwards, making use of their pectoral fins, in a ballistic-like motion that only has linear acceleration. Saidel et al. use video taken at 30 frames per second, recording . For the fish studied, the average jump was no more than twice the fish's height and the horizontal distance covered was about five times the standard length of the fish. While the butterfly fish might twist in mid-air, the study concludes these motions do not increase the distance of the fish's flight. Additionally, this same pattern of jumping occurs within the water column, indicating that this is a general escape response not limited to aerial excursions.

Freshwater hatchetfish (*Gasteropelecidae*) exhibit behaviors similar to the African butterfly fish for their escape maneuvers. High speed video by Wiest [37] determined that hatchetfish also follow projectile like trajectories after their escape from the water. Additionally, the jump of these fish also makes use of the pectoral fin in a similar abduction to a C-start startle response.

Perhaps the most relevant previous work on fish jumping is the work done by Lowry et al. on silver arawanas [19] . This paper compares the underwater and aerial feeding behaviors and determines that all aerial feeding excursions rely on an S-start posture. They reach the conclusion that all jumping events had larger displacements and faster motions than with underwater feeding strikes as a result of different behaviors associated with each kind of maneuver.

1.2.4 Archer Fish

One key behavior of the archer fish is their ability to shoot jets of water at their prey, and there has been a portion of the scientific community devoted to studying their shooting skills. Working on the cognitive side of the archer fish's prey capture,

Goldstein and Hall [16] demonstrated that shooting is maintained through a variable ratio schedule of reinforcement due to competitive situations, which is sufficient to keep fish shooting in schools. In terms of other cognitive portions of the shooting behavior, Schuster et. al [26] concluded that archer fish are able to learn how to successfully hit moving targets at great heights just from watching a group member. Additionally, when prey is dislodged, archer fish are able to use the initial prey trajectory to successfully predict the direction, speed and distance at which the prey will land, and turn accordingly in less than 100 ms [22].

Research on the main physical mechanism that allows the fish to spit was performed by Milburn and Alexander [20], who analyzed forces on muscles and reached the conclusion that there might be a catapult mechanism responsible. Elshoud [13] showed that the mouth of the archer fish acts like a flutter valve which directs the trajectory of the jet caused by the tongue. Schlegel et. al [24] affirm the mechanism, presented by Elshoud, by showing an image of the archerfish "blowtube" used to shoot jets of water. Finally, while the tongue and lips of the fish are important for creating the jet of water, they are unable to direct the jet. That role is left to the angle and aim of the body of the fish itself, which is supported by the fact that when the fish is aiming, the eyes remain steady but the body rotates [29].

Researchers have examined the sight of archer fish in an effort to better understand how Toxotes is able to accurately locate prey despite the change in index of refraction between water and air. Dill [8] was the first to do any work on archer fish vision in 1977. He took video at 200 frames per second and concluded that archers can compensate for refraction at a variety of angles and elevations, although there were fewer successful shoots when the prey was higher. This was backed up in his research by the fact that the bait was hit by the larger water droplets, rather than smaller drops that break off, implying that the fish also somehow correct for the effects of gravity on their water jets. Timmermans and Vossen [30] determined the locations of shots that missed the prey. If the target is considered to be in a plane that is perpendicular to the water being shot at it, the shots would pass through the target plane anywhere in an ellipse centered on the prey. This ellipse has its major axis

along the vertical, indicating that most of the misses were more likely to be affected by gravity than by poor aiming. From this they drew the conclusion that archer fish do not appear to learn a correction for refraction. Schuster et al.[25] showed that archer fish could be trained to aim for the same size target consistently, which they say is indicative of the ability of Toxotes to account for viewpoint dependency. Temple[27] calculated the effect of changing index of refraction on the archer fish's vision and determined that the change in location of the image due to the variation in the salinity would result in the same amount of misses as the natural variation of spit widths would. The reader is directed to Braekevelt [4] for a detailed description of the retina of the archer fish.

In terms of other aspects of Toxotes' lifestyle, however, there has been very little research. Bekoff and Door analyzed the sequence of motions leading up to an archer fish attempting to capture prey [3]. The steps involve orienting and swimming towards the prey. The fish then rotates vertically a variable number of times when near their prey and either jump or shoot at the prey. Bekoff and Door never seemed to witness the fish successfully capturing the prey by jumping, so the sequence of steps always ends at shooting. In their study the prey was typically 30 centimeters above the free surface.

Wohl and Schuster compared the C-start of an archer fish to rapid turn the fish makes when it is capturing prey and noted an unexpected similarity [38]. For archer fish, there was no difference between the maximum speeds attained in feeding strikes and that of fast starts resulting from being startled. Additionally, the fast starts of archer fish were discovered to be some of the fastest among teleost fish. Wohl and Schuster measured peak linear speeds above 20 $bodylength/s$, angular speeds over 4600 deg/s and a maximum linear acceleration up to 12 times that of gravity. The peak angular acceleration exceeded 450,000 deg/s^2. However, other than Wohl and Schuster, there has been an absence of study on the mechanics of archer fish maneuvering, and in particular, there has been no work on their jumping out of the water.

1.3 Outline of Thesis

Chapter Two focuses on the experimental methods that were used in this thesis. It gives the set up information for both kinematic videos of the archer fish and also the particle image velocimetry experiments that were run. This chapter also highlights some of the key points of the data processing for the entire thesis, although often specific details are included in the results sections.

Chapter Three is concerned with the behavior of archer fish in general. It touches on the way they swim and other behaviors, such as station keeping and prey approach. This chapter also provides the reader with a detailed description of the sequence of motions required for a jump. Any jumping details here are purely descriptive, the analysis comes in later chapters.

Chapter Four starts taking the raw jumping data and converting it into more useful information through kinematic analysis. Height and duration of the jump are covered here, as is position, velocity and acceleration data and patterns. Additionally, this chapter discusses the energy considerations and forces at play during the leap.

While kinematic analysis is useful, Chapter Five starts delving into the particle image velocimetry data, which provides more information on the fluid mechanics of the jump.

A conclusion to all of this is provided in Chapter Six, as well as suggestions for future work.

Chapter 2

Experimental Methods

2.1 Fish and Aquariums

For this thesis there were ten (10) archer fish studied; they were all of the species *Toxotes microlepis*. These fish were obtained from Mr. Ellis London at Tropic Isle Aquarium in Framingham, MA. Home for the archer fish was a 55 gallon tank that was maintained by a Eheim Ecco 2236 canister filter. The water was kept at a pH between 7.0 and 8.0, and the salinity of the water was held between 8.5 and 9.5 mS, while the temperature was kept between 76 and 84 °F. Thirty percent of the water in the tank was changed every three weeks. All of the fish were fed a daily diet of dried brine or mysis shrimp and the occasional live cricket.

Each archer was weighed and its length, width and height were recorded upon acquisition. In order to find the mass of an individual fish, a 1000 mL beaker partially filled with brackish water from the fish's home tank was weighed. Then the fish was placed in the beaker and it was weighed again. For the length and height measurements, the fish was placed in a narrow acrylic aquarium also filled with brackish water. A piece of gridded paper was taped to the back of the tank, as well as to the bottom of the tank, and then the fish's picture was taken. Another image was taken of an object of known length in the same location as the fish, so that any image distortion due to the tank or salinity of the water could be compensated for. From these images the length, height and width of each individual fish could be determined.

Maximum sizes of the fish and their respective weights can be found in Table 2.1. The table and images also show the difference in angle between the body centerline, which is used in this thesis, and the body axis, which is relied on by Timmermans and Souren [28, 29]. The body centerline runs from the tip of the nose to the middle of the caudal peduncle. Timmermans and Souren define the body axis as running from the bottom of the eye along the black stripes that naturally occur on the archers. For the purpose of comparison the body axis was drawn from the bottom of the eye to the middle of the caudal peduncle, since all of the stripes varied greatly between the different archers used in this study. More information on angles can be found in the section about jumping behaviors.

Table 2.1: Fish Dimensions

Archer No.	Length [cm]	Height [cm]	Width [cm]	Weight [g]	Difference between body axes [°] [29]
1	11.1	4.3	2.6	28.3	3.0
2	9.8	3.8	2.0	23.6	4.4
3	7.0	2.6	1.2	7.9	4.9
4	6.8	2.5	1.1	10.2	3.6
5	7.3	2.7	1.1	8.2	N/A
6	7.5	2.7	1.2	10.3	N/A
7	7.3	2.9	1.1	9.9	N/A
8	7.9	2.8	1.2	9.9	N/A
9	8.3	2.8	1.2	10.6	N/A
10	7.6	2.6	1.4	9.3	4.4

For the experiments detailed here, only archers one through four and ten were used since they were the only archers that would jump under experimental conditions. Images of each fish studied can be found in Table 2.2.

2.2 Kinematic Analysis

When studying the kinematics of archer fish jumping, the fish were left in their home tank in order to minimize stress. To isolate a fish for studying in the home tank, laser cut plastic dividers were used to separate one fish while still allowing it to swim freely. The slots cut in the dividers allowed the tank filtration to continue uninterrupted. In

Table 2.2: Archer fish used in this study

Archer 1

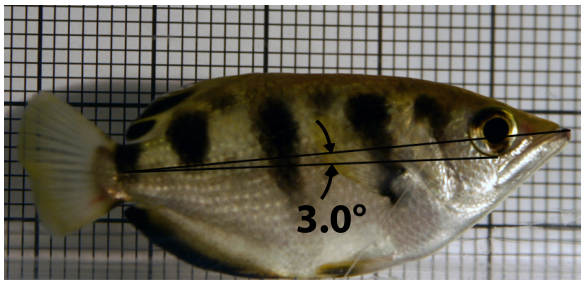

Archer 2

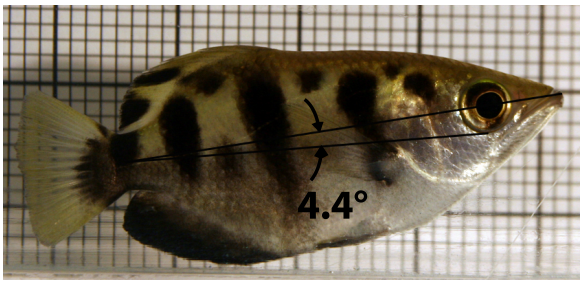

Archer 3

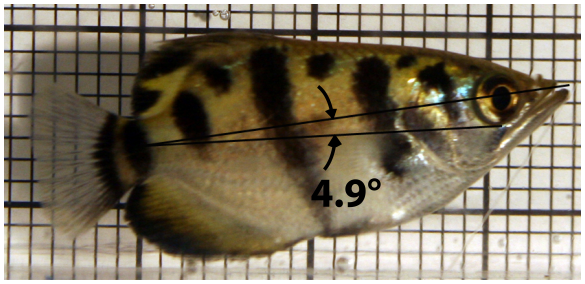

Archer 4

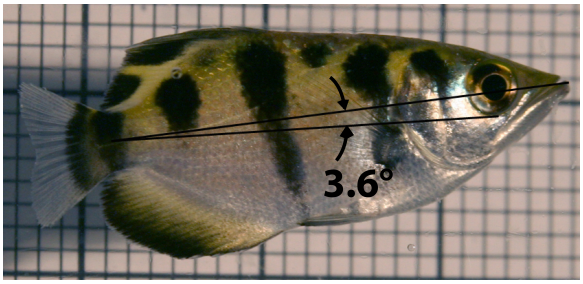

Archer 10

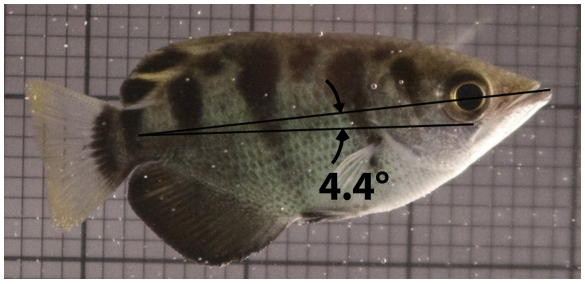

order to elicit the maneuver, a dried gammarus shrimp was held above the surface of the water on a wire, far enough from the edge of the tank to negate wall effects. The lighting consisted of a panel of 32 fluorescent light bulbs with a white diffuser between the panel and the tank. An IDT Motion Pro X3 (resolution 1280 x 1024 pixels) was set up in front of the tank, so that the fish would be backlit when it jumped. A 50mm Nikkor lens with aperture between f4.0 and f5.6 was used. The frame rates ranged from 700 to 900 frames per second, while the exposures went as high as 1008 μs and as low as 900 μs. For all runs, a calibration image was taken so that the conversion between pixels and centimeters was known.

2.2.1 Data Processing

Much of the statistical data on jumping was manually collected using Adobe Photoshop® (Adobe Systems Inc., San Jose, CA, USA) to find angles of inclination, or Matlab R2008a® (Mathworks, Natick, MA, USA) for most other data. In order for data to be collected from a run, the final height of the fish had to be visible. Five fish were examined (N = 5),with 18 to 35 runs for each fish, resulting in a total of 127 runs. Time equal to zero (t = 0) was set as the frame when motion was first detected in the fish's fins (both pectoral and caudal fin motions are synchronous), indicating the initiation of the jump maneuver. The frame where the fish reached maximum height was also recorded, as was the distance above the water surface.

The position, velocity, and acceleration were digitized using custom software in Matlab. This software found the location of the nose of the fish in each frame and then fit a smoothing spline [14] to these locations in both x and y, as will be discussed in more detail later on. From the spline, velocity and acceleration were calculated. Only runs where the nose was easy to track were used for the position, velocity and acceleration data, which reduced the total number of runs from the previous total. This narrowed down the previous total of 127 runs from the 5 fish studied to between 5 and 9 velocity data sets per fish, for a total of 33 sets.

2.3 Flow Visualization

Particle Image Velocimetry (PIV) of the archer fish was done in a separate PIV tank. The PIV set up consisted of a 10 gallon tank situated on a stand which was tall enough to allow the laser to be mounted on an 80/20 frame underneath the tank. The height of the laser was adjustable. A basic schematic of this set up can be found in Figure 2-1.

This thesis used high speed, digital, two dimensional (2D) PIV in order to gain information on the wake dynamics of jumping archer fish. The same IDT Motion Pro X3 camera with a 50mm Nikkor lens from the kinematics portion was used, as well as a Lasiris Magnum diode laser. Since the combination of the X3 and the diode laser

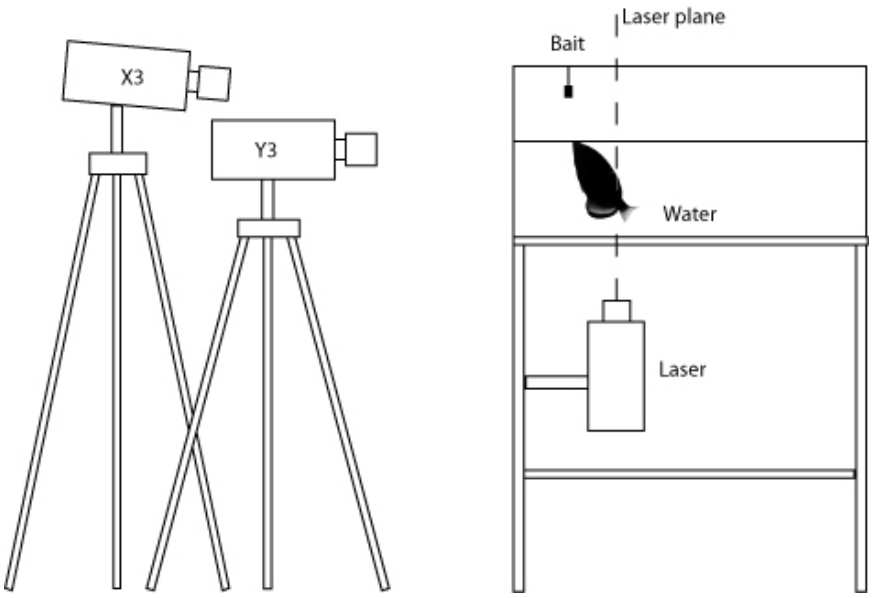

Figure 2-1: Particle Image Velocimetry set up

did not provide good enough data when studying the archer's tail, an additional IDT Motion Pro Y3 camera with similar 50mm Nikkor lens was also used for some trials. Dantec Dynamics polyamide particles of average diameter 50 μm were seeded into the tank and illuminated by the laser. In order to reduce motion blur, the 50mm lens was set at f1.8 for both cameras during all of the trials. To illuminate enough of the tank for the jumping event to be captured, the Lasiris Magnum diode laser, which produced a maximum of 2.0W at 810 nm, was fitted with optics so that its light was transformed into a 10° fan.

For the data presented here, independent of the size of the tank, the laser was located far enough from the bottom of the tank so that it would illuminate the field of view. The tank had between 6 and 12 cm of water inside. The camera took images in the range of 500 to 900 frames per second, or equivalently, had a time step greater than 0.0011 seconds but less than 0.002 seconds in between frames. PIV runs presented in this thesis had exposure times between 275 and 957 μs for jumping, while the hovering data presented had an exposure time of 1997 μs. Each image's resolution was 1,260 x 1,024 pixels with a field of view and zoom dependent on each individual trial. Since archer fish jump for prey, it was easy to ensure the fish were

in the right location, however the exact orientation of the fish's body was not always predictable. There were many runs that were taken, however only the runs where the fish jumped through the laser sheet and was still oriented so that it faced the camera head on were processed.

Additionally PIV data was captured using the X3 camera, which was was located under neath the experimental tank. The laser plane in this configuration, was horizontal and located less than 3 cm from the bottom of the tank. The amount of water in the tank was calculated based on average jumping angles of the fish being studied so that the laser would line up with the fish's tail when it jumped. Comparing this to Figure 2-1, the major change is that the camera and laser have switched positions.

2.3.1 Image Processing

PIV data were processed in order to extract the desired maneuvering information. For the velocity vector extraction, LaVision DaVis 7.2® software package provided a multi-pass, cross-correlation processing algorithm. The data presented here had a final interrogation window size of 32 x 32 pixels and used a 50% overlap between windows. In addition, the data was post processed by DaVis® in order to median filter and smooth the data and then iteratively fill up any empty spaces. The end result was a time series of data that had 64 x 69 vectors. From this output, the velocity data was taken and postprocessed in Matlab in order to determine the vorticity and circulation. An example of the PIV image is shown in Figure 2-2. On the left is the raw image taken by the camera, on the right is the result of the DaVis processing of the velocity vector between the image shown and the image immediately preceding it in the time series of images.

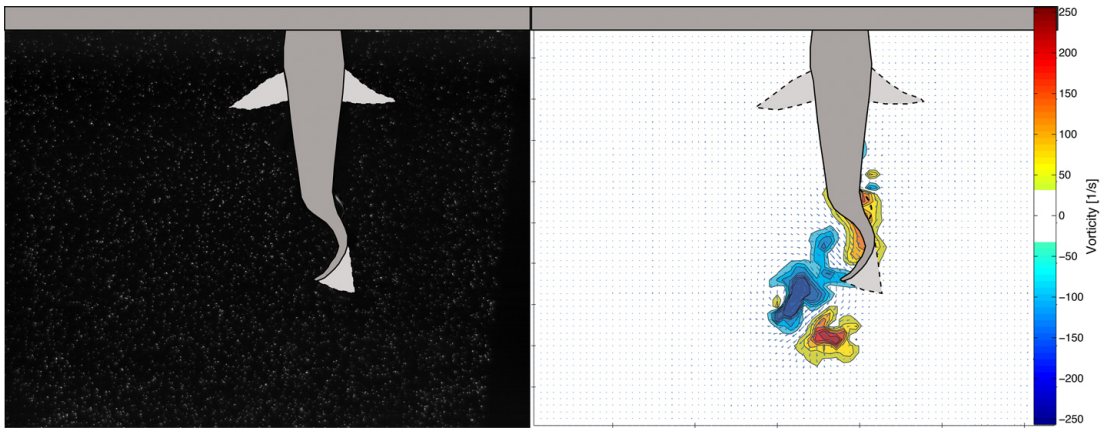

Figure 2-2: A sample PIV image taken by the Y3 camera (left) with the fish body superimposed. On the right is the resultant PIV velocity and vorticity fields, also with the fish body superimposed. Lighter dashed outline fins are in front of the laser sheet.

Chapter 3

Archer Fish Behavior

3.1 Introduction

This chapter gives a brief overview of how archer fish behave. It describes swimming and station keeping so that their common behaviors can be compared to other species of fish, and then delves deeper into their unique ability to jump. The jumping behavior is broken down into three parts; hovering, thrust production and glide. Additionally, key features of jumping, such as the angle of initial inclination and the number of times the archer moves its tail are described.

3.2 Swimming

When archer fish swim normally, without any escape or feeding responses, they experience both body and/or caudal fin (BCF) and median paired fin (MPF) locomotion depending on the speed at which they are traveling. For slow swimming, the archer uses its pectoral fins and an oscillatory wave in the caudal fin, however there is less movement of the caudal peduncle, making this similar to median paired fin locomotion. Alternatively, for motion at a constant faster rate, the archer relies less on its pectoral fins and does not display the same wave in the caudal fin. Instead, the majority of the motion in the fish's body occurs in the caudal peduncle, which is body/caudal fin type motion.

Interestingly enough, at slow speeds the archer is as capable of swimming backwards as it is forwards. The motion involved in swimming backwards appear to be similar to that of slow forwards swimming, with the pectoral fins doing a majority of the work.

3.3 Station Keeping

Archers need to station keep in order to maintain their position during a variety of events, based on their current circumstances. In order to successfully do this the archer relies on paired pectoral fin motions. The pectoral fins beat alternately in an out of phase motion while the oscillatory wave seen in the caudal fin during slow swimming is also present.

3.4 Prey Approach

Bekoff and Dorr (1976) [3] provided a flow chart of actions for when archer fish are shooting jets of water at prey, as seen in Figure 3-1. This chart provides a good reference for actions that archer fish may take when attempting to capture above water prey; however it is not entirely representative of actions taken for lower bait heights. While the actions listed by Bekoff and Dorr were seen during experiments, they never observed jumping capture. Based on the fact that they only performed trials where the bait was 30 centimeters above the water and never provided the length of the four archers used in this study, it is impossible to tell if this is out of the range of an archer's jump. If the fish used by Bekoff and Dorr were the same size as the fish used herein, 30 cm would be 2.7 to 4.4 body lengths. We only considered bait at less than 3 body lengths above the free surface. In our studies the fish occasionally spit but usually jumped. Therefore, in order for this sequence of actions to be more complete it should include the possibility of starting with a jump, options for jumping capture, and the possibility of multiple jumps before capture for lower bait heights.

Additionally, it should noted that jumping and shooting behavior seemed to vary

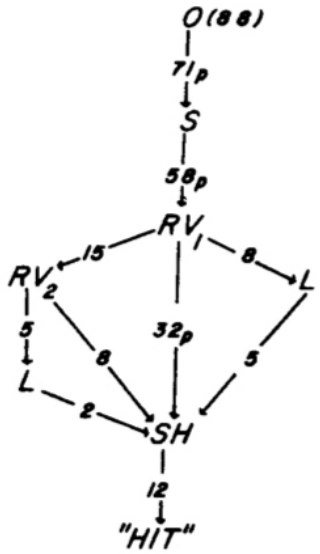

Figure 1. This figure shows the frequency of occurrence of the various actions making up a shooting sequence (orient, O; swim, S; first vertical rotation, RV_1; second vertical rotation, RV_2; leap, L; shoot, SH; the transition between the two acts connected by the arrow occurred significantly more frequently than expected by chance [$p < .001$; chi-square analysis]).

Figure 3-1: The series of actions leading up to an archer fish shooting at its prey, from Bekoff and Door, 1976. [3]

between animals. It was also dependant on the short term history; whether or not the archer had just missed the bait appeared to impact its choice of next action. While the sequence of actions followed could have been further refined, that past was not further pursued in favor of focusing on hydrodynamics rather trying to untangle the animal dependent pattern of actions. This is still a useful flow chart for the general series of actions that take place, the limitations just need to be kept in mind.

3.5 Jumping

3.5.1 Sequence of Jumping Motions

Archer fish follow a similar sequence of actions when they jump out of the water. Figure 3-2 provides an overview of a typical jumping behavior pattern. It is convenient to break the description of archer fish jumping into three parts; (1) hovering, (2) thrust

production and (3) gliding.

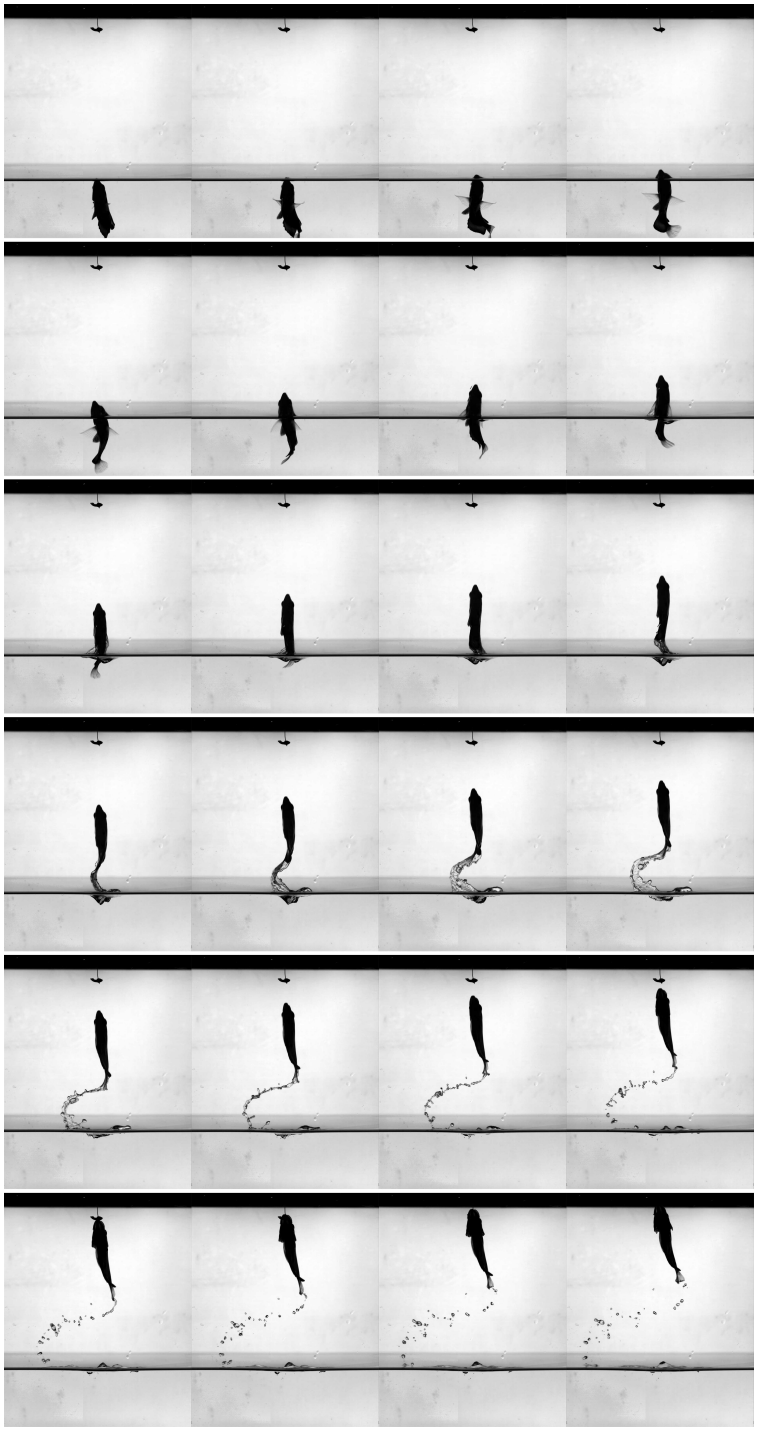

Figure 3-2: A sample series of images of an archer fish jumping for its prey, showing thrust and glide production. Every 5th image is shown and time equals zero (t = 0) would occur between the first two images. A more detailed view of t = 0 is shown in Figure 3-4. The images were taken at f5.6, with a frame rate of 900 frames per second, so the images shown are 0.0056 seconds apart.

Hovering

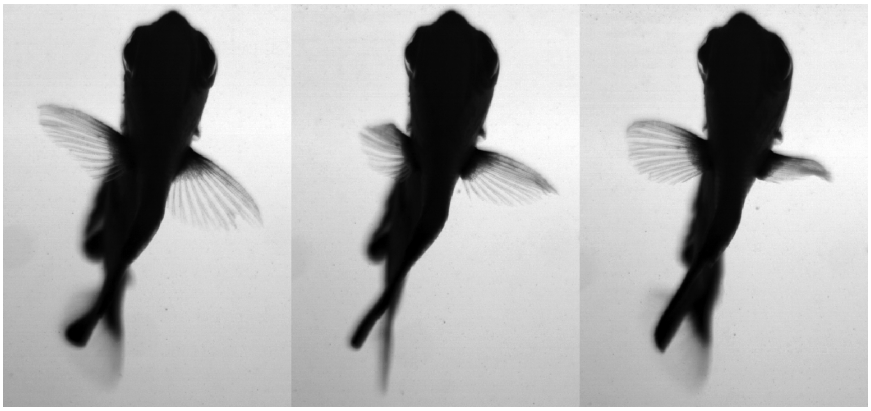

Figure 3-3: One cycle of pectoral fin motions when an archer is hovering before jumping for its prey. The images are 0.0533 seconds apart.

Before each jump the fish lines up with its nose at the free surface to maintain position. Hovering motions are similar to those involved in station keeping. The fish is inclined at an angle (β) relative to the water surface; further discussion of approach angle can be found in Section 3.5.3. Out of phase pectoral fin motion and an oscillatory wave in the caudal fin provide the stabilizing forces that allow the archer fish body to remain motionless. Figure 3-3 shows parts of one cycle of the pectoral fin motions during hovering. PIV of the hovering event is presented in Chapter 5 with the other PIV data.

Thrust Production

In order to jump 0.5 - 3.0 body lengths out of water the fish must generate sufficient thrust (Figure 3-4). The pectoral fins are extended before the start of thrust production and remain that way until they break through the water surface. In all data that references time, time equal to zero is set to be at the first discernible motion of the archer's pectoral fins. Once the pectoral fins have assumed the necessary position, the archer starts to flap its tail back and forth. The number of flaps varies from jump to jump, however there is a minimum of one flap.

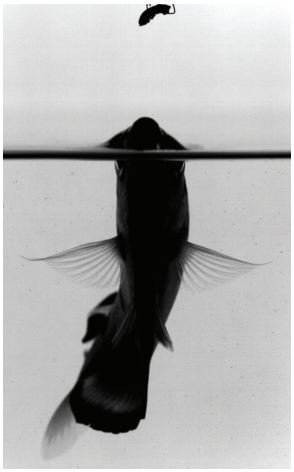

Figure 3-4: An archer fish beginning its thrust production. It has brought its pectoral fins into a position perpendicular to its body that it will maintain until the fins leave the water.

Glide

After thrust production there is a third "glide" phase which is not always evident. After a fish has finished flapping its tail and is partially out of the water it will hold its body almost entirely motionless and glide until it reaches the bait. An example of two moments during a glide can be seen in Figure 3-5. The appearance of the glide portion of the jump depends on which fish is being studied. For the five fish used herein, one showed a distinctive glide behavior in only 56% of 35 jumps. However, for the other four fish from the study, there was no glide behavior only 3% of the time. Lacking the glide behavior meant that the tail of the archer was never motionless and the fish continued to flap its tail in the air.

Archer 10 was the fish that lacked the glide phase most often, however it also jumped the highest and was seen to flap its tail in air when jumping for unusually tall bait heights. If the bait was lower than 1.55 BL the archer had a definite glide for all of its 15 jumps studied. However, above 1.55 BL the archer only had a definite glide in 2 out of 20 trials, there were 10 runs where the glide was definitely missing, and the rest of the jumps were difficult to classify.

The other archers also showed glides for low bait heights. The jumps that lacked glide behavior all occurred for bait heights of 1.0 BL or higher. From this compar-

Figure 3-5: An archer fish glides after it has left the water. The two images are 0.0256 seconds apart on the same jump, where the bait was 2.1 body lengths above the water surface.

atively small sample size of five archers, it is hard to make a definite conclusion on whether or not this is a normal pattern of actions, however it seems to be individual dependent since there was an overlap in jump heights for multiple fish around two body lengths and only Archer 10 did not glide regularly.

3.5.2 Body Kinematics

To determine the overall motion of a fish in a given jump, backlit video was taken of the fish jumping. Then the video was processed using Matlab® in order to show the position of the fish's spine over time. This relied on a custom code that allowed the user to manually input points along the spine. Once the points were recorded for a particular image, a spline was interpolated in the horizontal direction. If desired, the user can overwrite the spline with new locations and a corresponding new spline. After location data was collected for a series of images, skipping a set number of frames in between each trace frame, the resultant traces were plotted so that the

change in location could be seen over time.

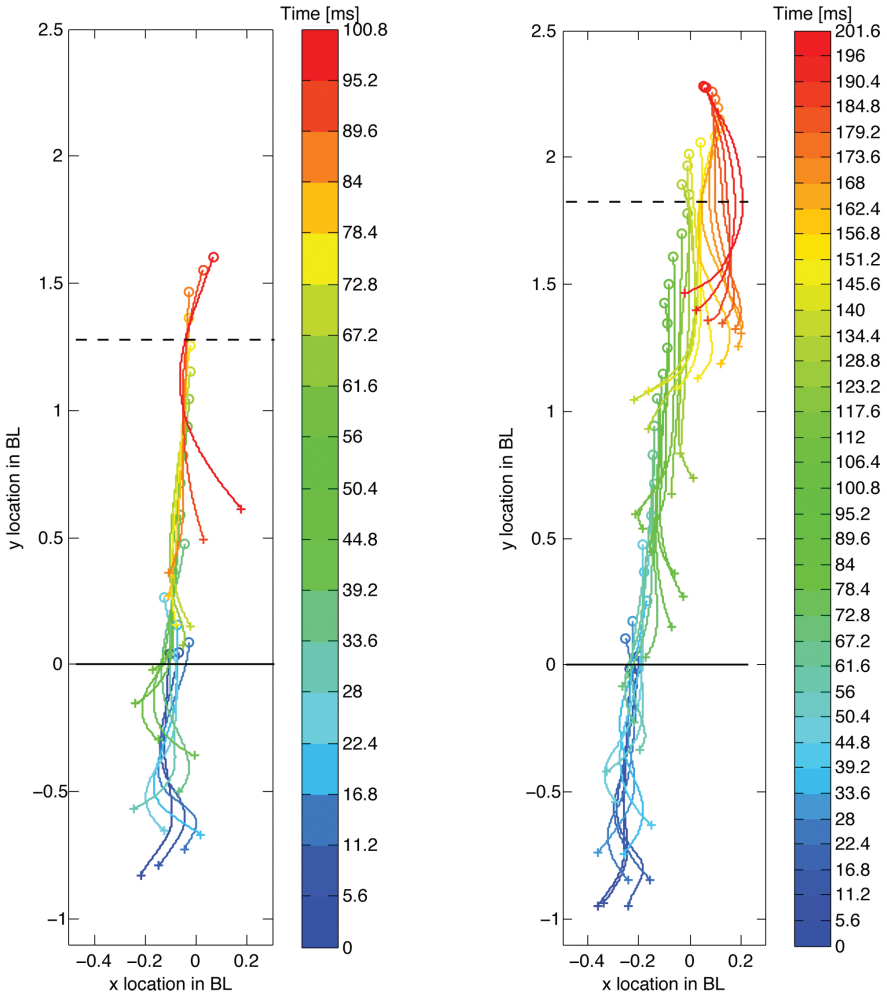

Figure 3-6: Both (a) and (b) present fish spine traces from high speed video sequences. Traces were captured every 5 frames, or 0.0056 seconds, until the fish reached its maximum height. The circles represent the nose of the fish, the cross is the tip of the tail. The black line is the water surface while the dotted line is at the height of the bait. Part (a) shows Archer 3 jumping with a glide portion, where the archer reaches a maximum height of 1.97 body lengths. Part (b) has Archer 10 jumping, without a glide portion to the jump. In this jump the archer reached 2.01 body lengths for its final height.

The traces for a particular run where the fish jumped 1.97 body lengths are shown in Figure 3-6(a). This particular jump showed the gliding portion, with the fish remaining relatively motionless in the horizontal direction while it moved through the air towards the bait. Traces for this run end when the fish started twisting its

body in order to reenter the water. Figure 3-6(b) shows body traces for a different fish when it jumps 2.01 body lengths above the water surface. Traces were only made up until the point at which the fish reached its maximum height, as after that there was significant turning that would have greatly confused the tracing. In this particular case, the glide portion of the run was missing, evidenced by the fact that the fish was always moving its caudal fin. For both of this videos, time equals zero is the first visible pectoral fin motion of the archer before jumping.

Figure 3-6(a) nicely illustrates how the archer flapped its tail from side to side before leaving the water and then after exiting the water was almost entirely motionless, evidenced by the fact that the body traces during the glide portion are extremely close to overlapping. This still body posture was only retained until after the fish has reached the bait.

Comparing the two plots of body traces over time it is also possible to see that even though these are two different fish, it takes roughly the same amount of time to reach 1.5 body lengths above the surface of the water. Timing of the jumps will be discussed more in the next chapter.

For completeness, body traces of each of the other fish used in this study are shown in Figure 3-7. In these figures, even though the bait height, number of tail strokes and archer changes from trace to trace, the glide portion of the jump is still visible once the fish has partially exited the water.

3.5.3 Angle of Initial Inclination

Video of the fish from a side angle before jumping allows the angle of initial inclination, β, between the fish and the vertical to be calculated. β, is illustrated in Figure 3-8, and was introduced in Chapter 2. While similar to the body axis that is referred to by Timmermans and Souren[28, 29] as B_s, it is not quite the same, since it does not run along the body (on the bottom of the stripes) from the bottom of the eye to the caudal peduncle. Instead, this angle is measured from the tip of the nose to the middle of the caudal peduncle because this is the only real possible measurement given that kinematic videos are all backlit so that stripes and eyes are not visible.

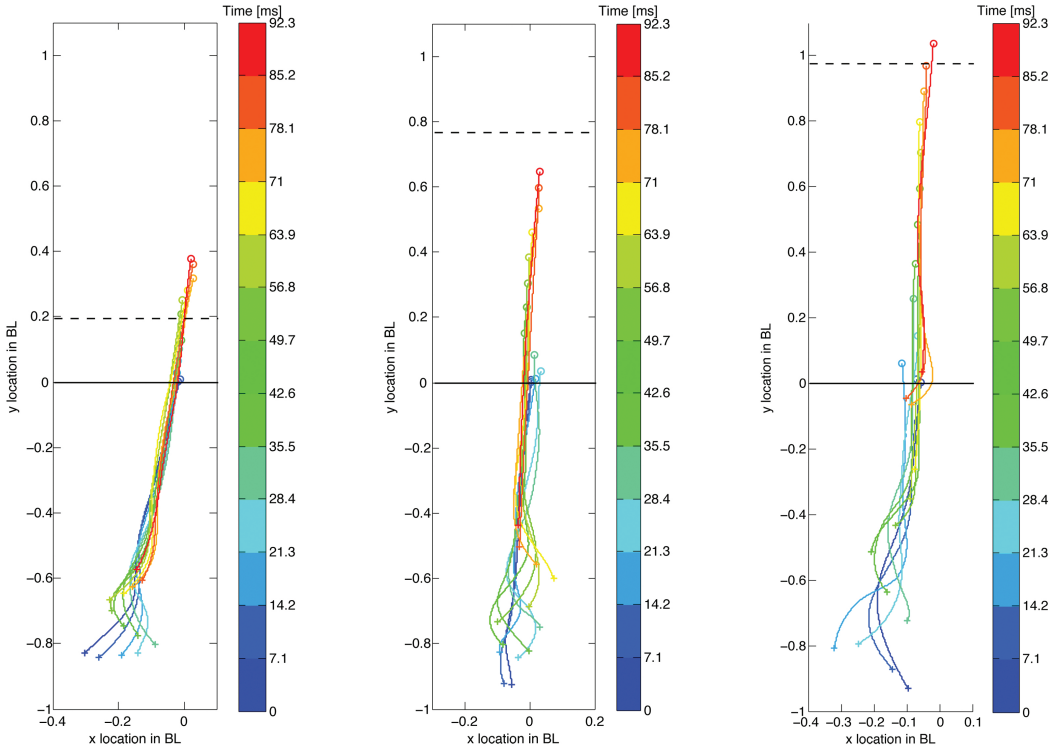

Figure 3-7: Body traces for the remaining archers. Once again, the circles represent the nose of the fish, the cross is the tip of the tail while the black line represents the water surface and the dotted line is at the height of the bait. In (a) Archer 1 jumped a maximum height of 0.41 body lengths, (b) depicts Archer 2 when it jumped 0.92 body lengths and (c) has Archer 4's body traces for a jump of 1.27 body lengths.

The overshoot and Δx displayed in the figure will be discussed in later sections. In order to calculate β, the image where fin motion started was viewed in Adobe Photoshop® where a line from the tip of the fish's nose to the middle of its caudal fin was calculated. Photoshop® then provided the angle of that line in degrees. A comparison of the average, maximum, and minimum β at which each fish jumped can be found in Table 3.1.

It is interesting to note from Figure 3-9 that the angle the fish is at immediately before it jumps seems to be correlated to the height of the bait for which the fish was jumping; however there is not enough data to make a strong conclusion about this. There is too wide of a variety in trends for a given fish and each fish does not have a sufficient number of trials to make any definite conclusions about overall trends.

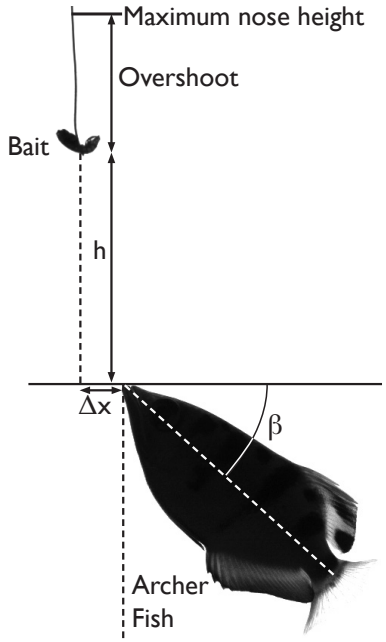

Figure 3-8: A schematic, showing the angle of inclination of the fish, over shoot height and distance between the fish and the middle of the bait.

Table 3.1: Inital Angles for Jumps

Archer No.	Average Angle [°] from horizontal	Minimum Angle [°] from horizontal	Maximum Angle [°] from horizontal	Number of Trials
1	55.0	52.8	56.2	3
3	53.3	42.4	65.4	6
4	54.2	47.6	63.6	5
10	54.5	43.4	59.6	5

It is, however, possible to see that the angle from which an archer fish will jump is definitely limited in range. None of the trials showed an archer jumping when its angle from the water surface was less than 40 degrees. Additionally, of the five archers, none were seen to jump from angles that were greater than 65 degrees. Timmermans and Souren [29] were able to correlate the body angle with the height of the prey that an archer was shooting for, with the end result being that for bait between 50 and 350 mm in height, the body angle could be described by $B_s = 63.4 - 0.11 * baitheight$. For their data range, this meant that angle varied between roughly 60 and 25 degrees from the horizontal. β, as found in this thesis, fits into this range, only without a

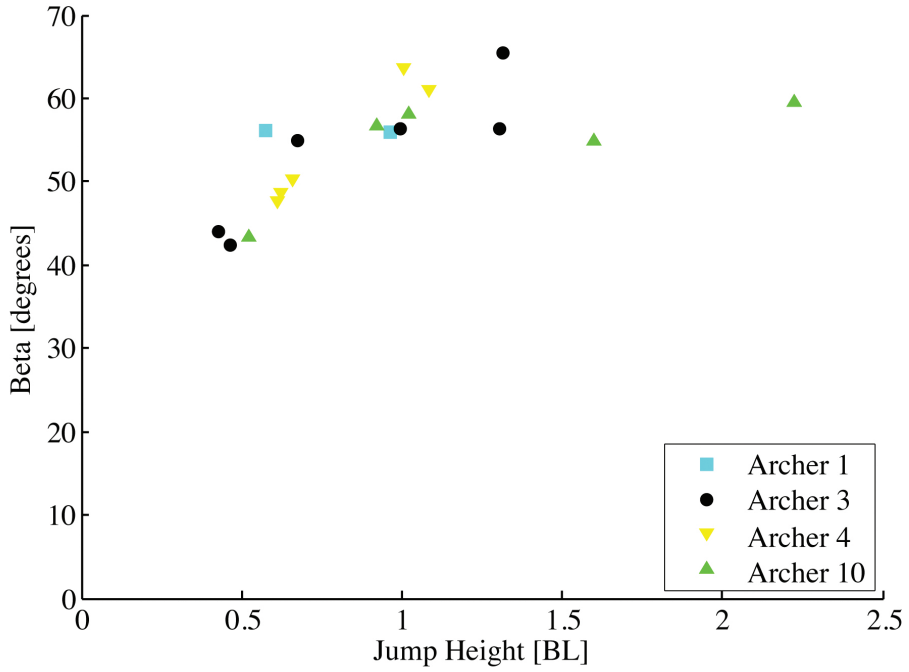

Figure 3-9: The angle that a fish is from vertical compared to the height of bait the fish was jumping for.

definite trend-line. This seems to indicate that these are not irrational angles for the archers to be orienting themselves at; there just is not enough data to draw a definite conclusion on whether or not this angle is related to the height of the bait when the archer is jumping instead of spitting.

3.5.4 Tail Strokes

Throughout this thesis one tail stroke was defined as when the archer's caudal fin moves from one peak displacement to the next, since this is hard to explain in words, an illustration of the start and end of one stroke is in Figure 3-10. If the tail only travels from one displacement maximum to the center position, where it is straight, this is considered half of a tail stroke. It is important to note that just because a certain number of strokes have been counted does not ensure that all of the strokes are the same length. A stroke just implies that the fish has moved its tail from the local position maximum on one side to a local position maximum on the other side.

To better quantify what role flapping the tail actually plays, the number of tail

(a) (b)

Figure 3-10: The difference between (a) and (b) is that of one full tail stroke. If the tail were to stop in the middle position, or start in the middle position and then end at either (a) or (b) that would be considered half a stroke.

strokes was considered as a function of jump height, seen in Figure 3-11. When trying to fit a relationship to this, there was better correlation if the height of the jump was given in terms of body lengths of the fish, rather than in centimeters.

Several conclusions can be drawn from this graph in its raw form. First of all, in order to jump out of the water, an archer has to perform at least one full flap of its tail. Secondly, there appears to be a linear relationship between the jump height achieved and the number of tail flaps required to reach that height. If linear relationships are fitted to the data for each archer individually, it results in a slope and intercept for each archer, as shown in Table 3.2. All of the archers have positive slopes and intercepts, but the only real discernible difference is between the two large archers (1 and 2) and the smaller archers (3, 4 and 10). When both the mass and the length are larger it seems that the slope of the data is higher, so physically this means that it will take a larger fish more tail flaps to get to higher elevations. This could be justified because of the additional mass that the fish has to propel out of the water or possibly because larger fish in a species are less flexible than smaller members of the same species (as evidenced by the linear relationship between size and turning radius [9]), so the tail strokes may not provide as much propulsion because they physically cannot reach the same comparative maximum amplitude. Another factor might be

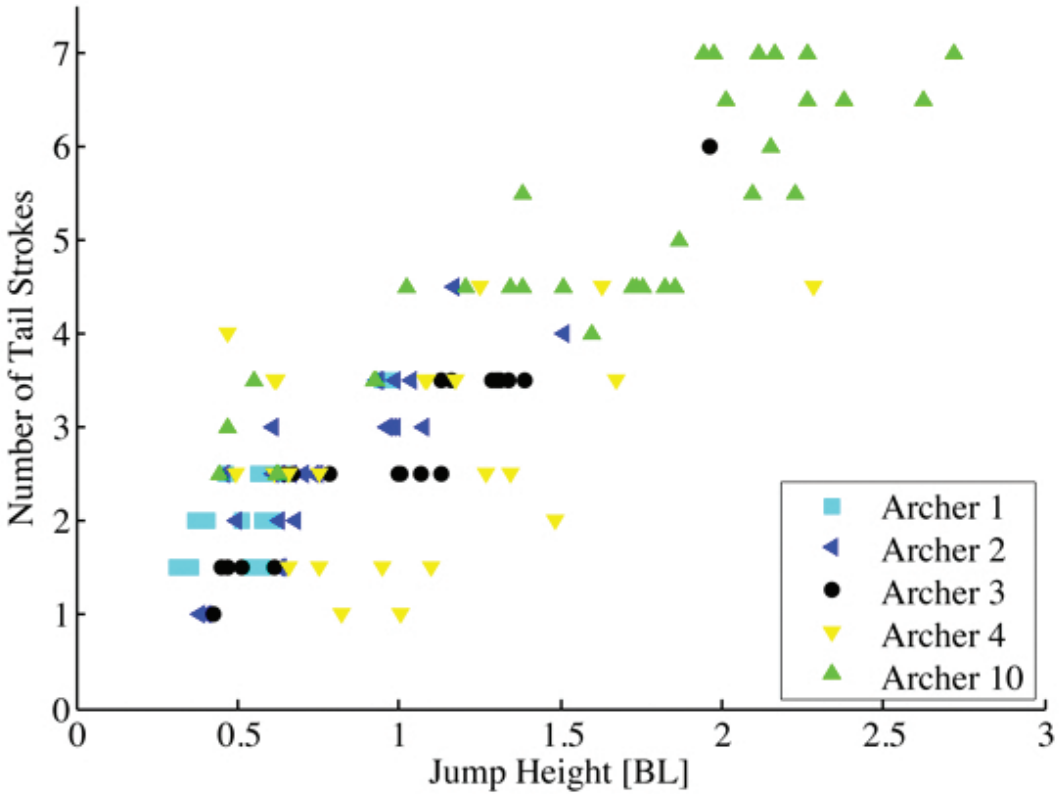

Figure 3-11: Jump height in body lengths vs the number of tail strokes.

that the larger fish were older, and performance degrades with age. However, since archer fish have not been known to be bred in captivity, this is impossible to judge accurately.

Table 3.2: Trend line information for archer maximum jump heights and the number of tail strokes to reach that height

Archer No.	Slope [strokes/BL]	Intercept [strokes]	Coefficient of determination [R^2]	Number of Trials	Mass [g]	Length [cm]
1	2.967	0.500	0.712	18	25.35	11.1
2	2.757	0.487	0.713	26	23.6	9.8
3	2.575	0.224	0.8978	24	7.9	7.0
4	1.842	0.878	0.546	24	10.2	6.8
10	2.001	1.746	0.783	35	9.3	7.6
All	2.479	0.641	0.827	127	N/A	N/A

To better understand the tail strokes that an archer fish utilizes to jump, it is interesting to look at the trends in size of the strokes and how long it takes an archer

to make them. Tables 3.3 through 3.7 give a detailed break down of one jump for each archer where the fish was viewed almost exactly head on, so that it was possible to quantify the maximum excursion of the tail as well as the time to reach that tail position. Additionally, Tables 3.8 and 3.9 provide a comparison between jumps of one larger and one smaller archer fish where the archers reach similar maximum heights (in centimeters, not body lengths).

Table 3.3: Stroke Information, Archer 1 jump of 0.41 BL

Stroke Number	Stroke Length [cm]	Stroke Length [BL]	Stroke Time [s]
1	2.633	0.237	0.0257
2	1.652	0.149	0.0300
3	1.210	0.109	0.0229

Table 3.4: Stroke Information, Archer 2 jump of 0.93 BL

Stroke Number	Stroke Length [cm]	Stroke Length [BL]	Stroke Time [s]
1	1.706	0.174	0.0300
2	2.389	0.244	0.0186
3	1.706	0.174	0.0214
4	0.504	0.051	0.0157

While this data only represents a single run for each archer, this is still enough to see some significant trends. The longest stroke always occurs in one of the first two strokes, and then after that stroke length gradually decreases. Additionally, stroke time tends to follow a similar decreasing pattern, although that does not come through as clearly in all of the runs.

These two phenomena are probably linked, and they could also be related to the velocity of the fish at that instant in time. If the archer is moving faster later in the jump then its possible that it doesn't have as much time to complete a tail stroke if it is trying to maintain a certain number of strokes. The significance of having a certain number of strokes will be touched on in the next chapter's discussion of particle image velocimetry data. However, if this is the case, and a archer needs to

Table 3.5: Stroke Information, Archer 3 jump of 1.97 BL

Stroke Number	Stroke Length [cm]	Stroke Length [BL]	Stroke Time [s]
1	1.846	0.264	0.0186
2	1.989	0.284	0.0171
3	1.613	0.230	0.0143
4	1.684	0.241	0.0143

Table 3.6: Stroke Information, Archer 4 jump of 1.27 BL

Stroke Number	Stroke Length [cm]	Stroke Length [BL]	Stroke Time [s]
1	1.946	0.286	0.0171
2	2.028	0.298	0.0129
3	1.112	0.164	0.0143
4	0.998	0.147	0.0114

make enough strokes while moving quickly out of the water, it could explain why there is a correspondingly shorter stroke length at times when the archer is traveling faster and about to leave the water. Also, since the stroke that takes the longest is also always one of the first, having to start from rest might also impact the time it takes to perform one stroke.

Table 3.7: Stroke Information, Archer 10 jump of 2.15 BL

Stroke Number	Stroke Length [cm]	Stroke Length [BL]	Stroke Time [s]
1	1.060	0.139	0.0157
2	1.987	0.261	0.0157
3	1.877	0.247	0.0143
4	1.612	0.212	0.0129
5	1.435	0.189	0.0129
6	0.972	0.128	0.0100

While it is interesting to look at the results of individual jumps, it can also be informative to compare jumps from different sized archers. Tables 3.8 and 3.9 do exactly that. They provide the jump of one of the larger archers (1 and 2), next to a jump from one of the smaller archers (4 or 10) that is of comparable height (in

Table 3.8: Stroke comparison between similar height jumps

(a) Archer 1, 5.72 cm jump

Stroke Number	Stroke Length [cm]	Stroke Length [BL]	Stroke Time [s]
1	2.762	0.249	0.0300
2	2.686	0.242	0.0214
3	1.190	0.107	0.0229

(b) Archer 4, 5.61 cm jump

Stroke Number	Stroke Length [cm]	Stroke Length [BL]	Stroke Time [s]
1	2.470	0.363	0.0200
2	1.885	0.277	0.0157
3	1.300	0.191	0.0129

centimeters).

Even though there are only two examples of this, some rough conclusions can still be reached. A similar number of strokes is needed to reach comparable heights, however the stroke length will vary as will the time for the strokes. This is similar to what is already known from comparing the strokes versus height of jump.

3.5.5 Dimensionless Parameters

To understand the fluid mechanics of the jump, all of the jumps were also quantified in terms of common dimensionless parameters that give insight into the environment in which jumping is taking place.

Reynolds Number

Reynolds number is a commonly used dimensionless parameter that can help determine the relative importance of inertial and viscous forces. It is defined as:

$$Re = \frac{\rho u L}{\mu}$$

Table 3.9: Another stroke comparison between similar height jumps

(a) Archer 2, 11.48 cm jump

Stroke Number	Stroke Length [cm]	Stroke Length [BL]	Stroke Time [s]
1	2.992	0.305	0.0300
2	2.480	0.253	0.0186
3	1.811	0.185	0.0186
4	1.142	0.116	0.0171
5	0.650	0.066	0.0129

(b) Archer 10, 11.48 cm jump

Stroke Number	Stroke Length [cm]	Stroke Length [BL]	Stroke Time [s]
1	1.886	0.248	0.0300
2	2.219	0.292	0.0186
3	1.469	0.193	0.0186
4	1.285	0.169	0.0171
5	0.484	0.064	0.0129

In terms of fish, for a stationary fish Anderson[1] says that for Re of order $3 * 10^3$ to $3 * 10^5$ based on length of the fish, the boundary layer profiles while remaining motionless in moving water suggested laminar flow for scup (carangiform swimmer) and dogfish (anguilliform swimmer). Swimming fish have higher friction drag than straight fish in a flow, so this might be slightly inaccurate when the fish is actually swimming or, in this case, jumping.

For the archers studied in this thesis, using the velocities calculated from the kinematic videos, a range of Reynolds numbers was calculated that varies from a minimum value of $1 * 10^3$ to a maximum of $3 * 10^3$. Since most of the fish is out of air at the time of the maximum velocity, the density and viscosity used to calculate Reynolds number were those of air at 20°C. Compared to the values from Anderson, this is well within the range for laminar boundary layers, however since the fish is not motionless and is also mostly in air, it is hard to tell. While further tests could be done to test the nature of the boundary layer, there was not time to study it in this thesis, so this must be a point of future work.

Froude Number

Froude number is used to, among other things, characterize the maneuverability of a fish [2] and can be generalized to the ratio of inertial and gravitational forces. In this thesis it is calculated as follows:

$$Fr = \frac{u}{\sqrt{gL}}$$

However, Bandyopadhyay calculates the internal Froude number as:

$$Fr = \frac{u}{gL}$$

Since both options include velocity in the definition, calculation of either was limited to only those runs where velocity was calculated. The calculated values for each fish shows the rough range for Froude number of this jumping behavior, as seen in Table 3.10. While the minimum and maximum are included in the table, they were not calculated the same way as for Bandyopadhyay. The only value that matches with his definition of Froude number is that of the average internal Froude number. From this though, it is possible to compare with his logic for flexibility of fish. Higher internal Froude numbers indicate a more flexible fish, and while he applied this to various species of fish, it also seems to make sense within the Toxotes species in this case. For example, Archer 1 is the largest used in this study, and it has the lowest internal Froude number. Since it is largest, it has the thickest body, which probably means that it is hardest for it to bend its tail and be successful at maneuvering.

Table 3.10: Froude Number

Archer No.	Minimum Fr No.	Maximum Fr No.	Average Fr No.	Average Internal Fr.	Fish Length [cm]	Number of Jumps
1	0.629	1.126	0.868	0.833	11.1	7
2	0.901	1.375	1.127	1.150	9.8	5
3	1.528	1.834	1.637	1.976	7.0	5
4	0.910	1.875	1.489	1.725	6.8	9
10	0.901	1.826	1.610	1.866	7.6	7

Overall, Froude number gives a picture of the archer fish jumping as an activity

where gravity plays a large part since it is the same order of magnitude as the inertia of the fish itself. This is perhaps unsurprising, since with a jumping fish it is expected that gravity will come to play an important role because of the vertical nature of the maneuver.

Strouhal Number

Strouhal number is used to describe oscillating flows such as the vortex shedding from a stationary object. It is also used to describe fish when they are swimming steadily, and in that context it is defined as:

$$St = \frac{fA}{u}$$

Where f is the frequency of the tail beat, A is the amplitude of the tail strokes and u is the forward velocity of the fish. Calculating Strouhal number in this fashion is really determining a property of the wake by using tail parameters. Most reduced data for swimming falls into the range of 0.20 to 0.40.

In this thesis Strouhal number was only calculated for four good runs where the fish had its belly parallel to the camera so that tail stroke amplitude could be calculated and also only runs where the velocity was known. Calculations were made using the average amplitude and frequency for a jump, this data, along with the Strouhal number itself, is in Table.3.11.

Table 3.11: Strouhal Number

Archer No	Strouhal Number	Jump Height [BL]	Average Amplitude [cm]	Frequency [Hz]	Fish Length [cm]
1	0.57	0.37	1.07	38.2	11.1
2	0.46	0.93	1.06	46.7	9.8
3	0.37	1.97	0.89	62.2	7.0
4	0.49	1.27	0.85	71.8	6.8

While Strouhal number was calculated for the purposes of comparing to swimming fish, this is a tough application for it. Not only is this not swimming, so the amplitude and frequency are not constant, but it is also an impulsive start, which falls under the

category of maneuvering rather than steady swimming. However Strouhal number was included for completeness of the analysis.

Weber Number

Weber number is a good measure of whether or not surface tension is important compared to inertial forces. Traditionally Weber number is defined as:

$$We = \frac{\rho u^2 L}{\sigma}$$

In order to determine whether or not surface tension is important in the case of an archer fish jumping out of water, the surface tension and density of the water in the 55 gallon home tank were measured over the course of one day at normal salinity (9.5 mS). Using the calculated density of 993.02 $\frac{kg}{m^3}$ and the maximum and minimum values of the surface tension (minimum of 60.048 $\frac{mN}{m}$, maximum of 67.732 $\frac{mN}{m}$) it was possible to calculate a range of possible Weber numbers for each fish based on the range of velocities obtained from kinematic videos, see Table 3.12 for these results.

Table 3.12: Length and Velocity Ranges

Fish Number	Minimum Weber No.	Maximum Weber No.	Fish Length [m]
Archer 1	699.5	2532.6	0.111
Archer 2	1119.9	2943.5	0.098
Archer 3	1644.5	2670.9	0.070
Archer 4	686.7	3290.6	0.068
Archer 10	673.6	3122.7	0.076

Since Weber number is basically calculated by dividing the effect of inertia by that of surface tension, a large Weber number indicates that inertia is going to dominate the fluid flow in question, where as a small Weber number would indicate that surface tension plays a very significant role. All the of the Weber numbers reported here are much greater than one, so the effects of surface tension are negligible for archer fish jumping out of water and sos surface tension will not be considered elsewhere.

Chapter 4

Kinematic Analysis

4.1 Introduction

The kinematic analysis focuses on the position, velocity and acceleration of the archer fish throughout the course of their jumps. This chapter starts out with an overview of the maximum velocity and acceleration before going into the more detailed descriptions of how velocity and acceleration vary over the course of the jump.

After establishing the velocity and acceleration trends, there is discussion of resultant trends, such as the jump duration and how much the archer overshoots the bait. Overshooting, throughout this thesis, refers to how far past the bait the fish jumps. This is consistently calculated in terms of percentages, so percent overshoot is how far past the bait the archer travelled with respect to height of the bait, normalized by bait height:

$$Overshoot = \frac{h_{final} - h_{bait}}{h_{bait}}$$

Where h_{final} is the maximum height of the archer's nose and h_{bait} is the height of the lowest portion of the bait.

The kinematic analysis is concluded with a discussion of the kinetic, potential, and total energies that are involved in the archer fish jumping.

4.2 Position, Velocity and Acceleration Data

In order to find the position, velocity and acceleration of the archer fish, high speed image sequences where the archer was backlit were taken. These images were then processed to extract the position, and from this data velocity and acceleration were calculated. This section shows that data in the form of maximum velocities and acceleration as well as showing the variation of velocity and acceleration over the course of various jumps.

4.2.1 Data Processing

Matlab® was used to process series of images in order to find the jump height of the fish. In order for this to program to run effectively, the runs that were processed were the ones where the fish had its nose out of the water before it started jumping. Then the program starts at the top left corner of each image and searches until it finds the first row where there is a dark region. Whether or not a pixel is dark is based on a thresholding criteria that can be changed by the user. Once a row is found where there is a dark pixel, the program then finds all of the dark pixels in that row and averages them to determine the middle of the nose. If there is anything in the top of the image, such as the bait, then the program requires a background image in order to remove this from images that are being processed. Any selected point is shown to the user who then has an opportunity to either accept the location or alter it by hand if there has been an error.

Once the position of the nose was located in each image for a jump, the next step was to fit a spline to the x position and the y position. This was done using the built in Matlab® function **spaps**, and with custom code to find the best error tolerance and roughness for a given set of data points [14]. Given the x or y positions, as a function of time, this combination of codes returns a series of splines to choose from. An example of the x and y spline as selected as the best fit can be seen in Figure 4-1, where the line is the fitted spline and the raw data is represented by crosses. After a spline has been fit to the position data, the first and second derivatives of the spline

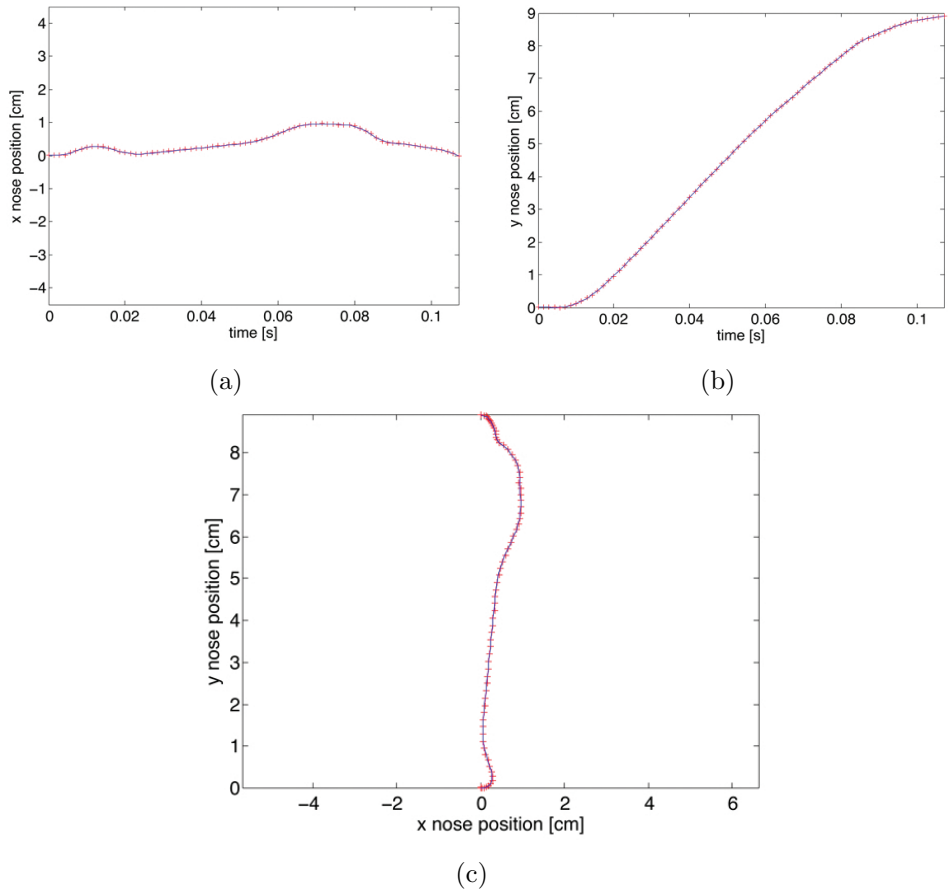

Figure 4-1: Nose position over time. The red 'x's represent data points while the blue line represents the spline that was fit to the data. X position in cm over time is in (a), while (b) has y position in cm over time and (c) has the combined position in cm with each position at an increasing time.

give the velocity and acceleration, respectively. The velocity and acceleration for the sample case can be seen in Figures 4-2 and 4-3 respectively.

When considering the velocity and acceleration of the fish, only the vertical component of position, velocity, and acceleration was considered since we are primarily concerned with vertical motion of the fish. Also, from the plots, its possible to see that the horizontal component only adds unnecessary noise to the data, especially when calculating vertical acceleration. All velocity and acceleration plots only show the vertical data for a given jump.

Finding the center of gravity while the fish is moving and changing its body orientation and fin locations would be ideal, but also extremely difficult. However,

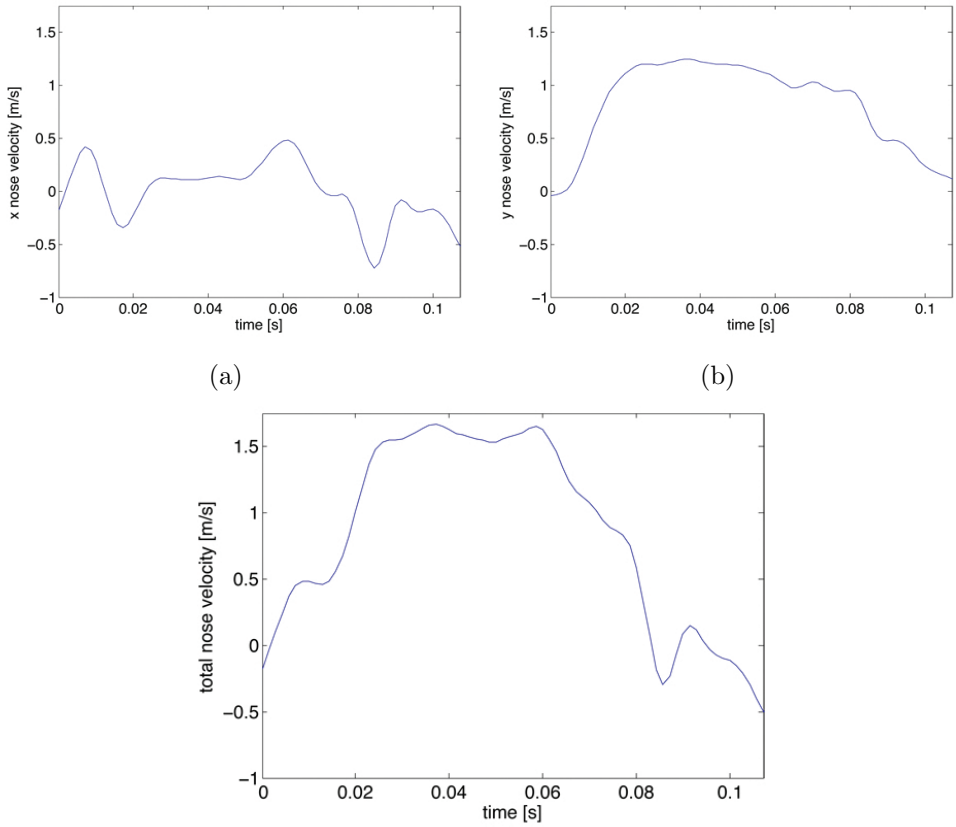

Figure 4-2: Nose velocity over time. The velocity was calculated by taking the derivative of the spline fit to the position data. X velocity in cm per second versus time is in (a), (b) has the y velocity in cm per second versus time and (c) has combined velocity in cm per second, versus time.

in a given jump there is minimal motion between the center of gravity of the fish (which is roughly located between the pectoral fins, found by modeling one of the archers in SolidWorks™ and then analyzing it) and the nose. As a result, tracking the nose instead of the center of gravity is a good alternative since it can be semi-automated. For certain video setups, which were not necessarily controllable due to the free swimming nature of the specimen, position data had error near the top extent of the jump as the fish opens its mouth. This results in an artifact in the position, velocity and acceleration data because the mouth is opening faster than the fish is moving, and it creates a peak in velocity near the time of bait capture. It does not effect the calculations for maximum velocity and acceleration as the behavior is

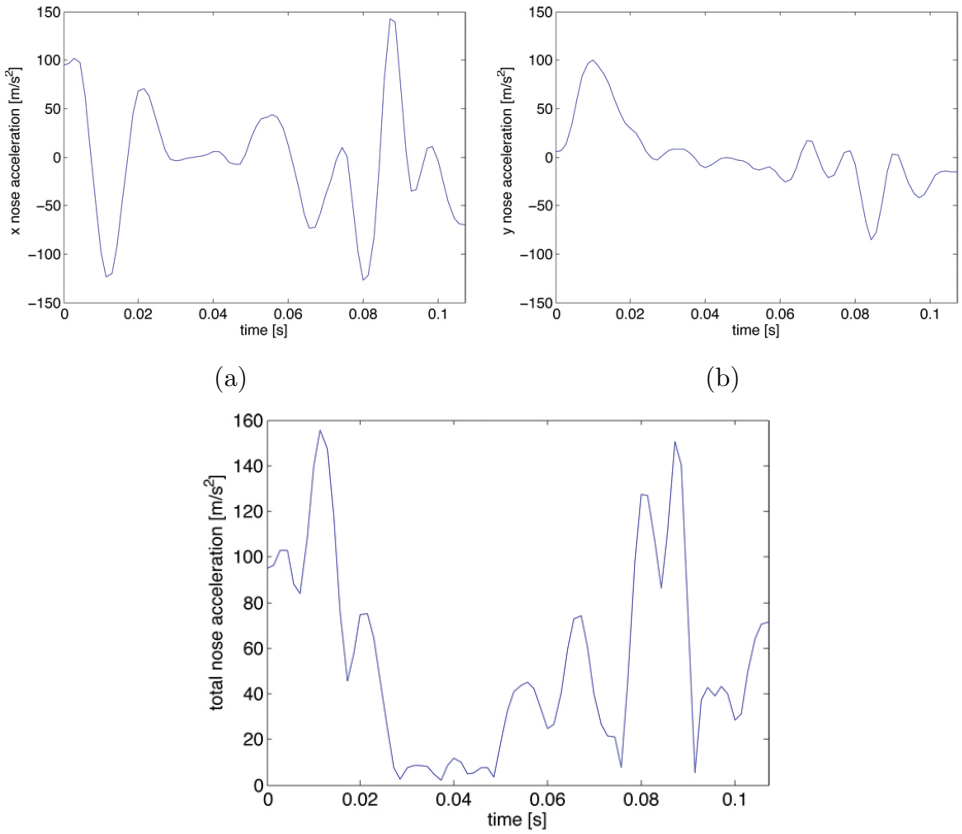

Figure 4-3: Nose acceleration over time. The acceleration was calculated by taking the second derivative of the spline fit to the position data. X acceleration in cm per second squared versus time is shown in (a), (b) has y acceleration in cm per second squared versus time while (c) is the combined acceleration in cm per second squared, versus time.

accounted for in post processing.

4.2.2 Maximum Velocity and Acceleration

Maximum velocities were calculated from the fit splines. They were checked manually to ensure they occurred before the fish had reached its prey, when velocity plots plateau. Individual maximum velocities for all of the archers are plotted versus jump height in Figure 4-4.

Clearly there is an increasing trend at work for maximum velocity and jump height. When there is a higher jump height there is also a higher maximum velocity, reflecting the need for more energy in order to reach higher bait. From the number of data

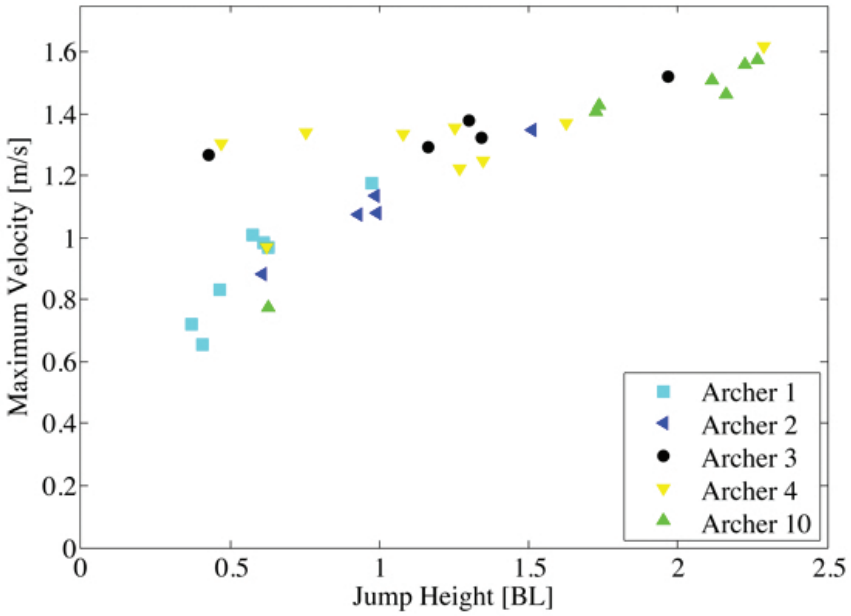

Figure 4-4: Maximum velocities of various fish with jump height.

points collected in this thesis it is hard to full characterize this trend. Table 4.1 shows data for both a linear regression between jump height and maximum velocity and a linear regression between the natural log of height and maximum velocity. However, it is hard to tell which is a best fit overall. Data from some of the archers are better described by the linear fit, while others are better described by the logarithmic fit.

Maximum acceleration for all of the archers' jumps were also verified to ensure that they occurred at a time before the fish captured the prey. Figure 4-5 shows maximum acceleration compared to final jump height for all runs and all fish. While there is a clear trend for maximum velocity, maximum acceleration does not obviously scale with jump height. For further understanding of the velocity and acceleration trends, they are plotted as a function of time so that they can be seen through the course of the jump.

4.2.3 Velocity and Acceleration Variation Throughout Jump

A better understanding of the motion of the fish can be gained by studying how the velocity and acceleration change throughout the course of the jump. For each fish

Table 4.1: Maximum velocity versus jump height trends

(a) Linear Regression

Archer No	Slope [(m/s)/BL]	Intercept [m/s]	Coefficient of determination [R^2]	Number of Trials	Mass [g]	Length [cm]
1	0.8223	0.4319	0.8448	7	25.35	11.1
2	0.5072	0.5957	0.9776	5	23.6	9.8
3	0.1609	1.1564	0.7764	5	7.9	7.0
4	0.2170	1.0470	0.5027	9	10.2	6.8
10	0.4692	0.5274	0.9554	7	9.3	7.6

(b) Linear Regression, Natural Log of Height

Archer No	Slope [(m/s)/ln(BL)]	Intercept [m/s]	Coefficient of determination [R^2]
1	0.5329	1.2245	0.9106
2	0.5079	1.1239	0.9796
3	0.1334	1.3416	0.5743
4	0.2153	1.2897	0.3902
10	0.6038	1.0639	0.9877

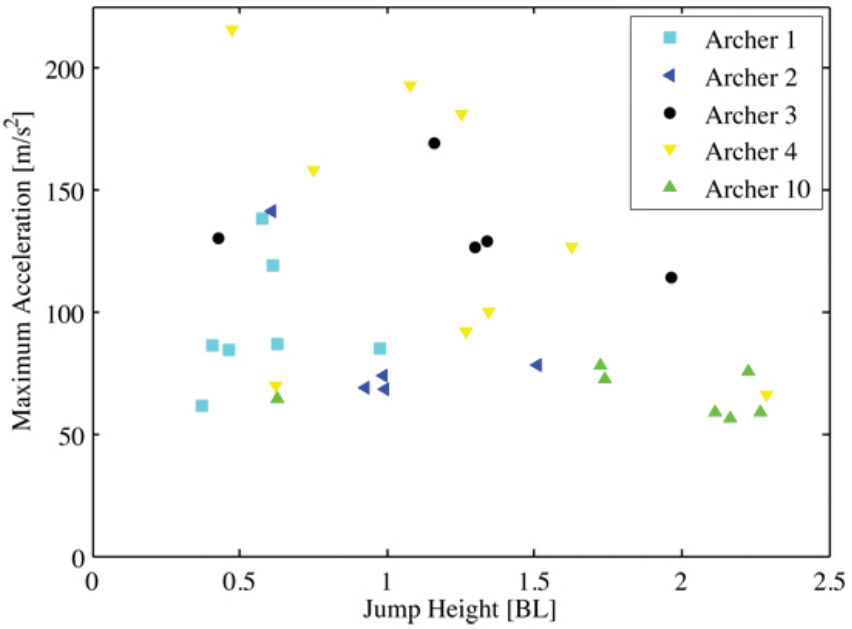

Figure 4-5: Maximum accelerations of various fish with jump height.

there is a plot that compares velocity and acceleration for runs that resulted in close to maximum jump heights, see Figures 4-6, 4-7, 4-8, 4-9 and 4-10. In all of these plots there is a circle on the velocity or acceleration data that indicates the point in

that run at which the fish's nose reached the same height as the bait.

In all of these comparison images the same trends are shown. The velocity of the jumping archer always starts off with a rapid increase and high acceleration. The initial positive slope of the velocity over time plot is roughly similar between all jumps that have results in close maximum heights, as is the time at which the slope levels out to zero. The velocity then stays relatively constant for a period of time before the fish reaches the bait, and then starts to decay as the fish grows closer to its prey.

This is all mirrored in the acceleration plots. The maximum acceleration occurs very shortly after the beginning of the jump, during the initial velocity increase. Then acceleration fades to zero around the time that the velocity has leveled off, and eventually becomes negative as the fish begins to fall back down into the water, reflecting the fact that gravity is now the only force acting on the archer. There is more noise in the acceleration data because it is the second derivative of a spline fit.

What the velocity and acceleration are showing can be translated into kinematics. The increase in velocity in the beginning of the jump, which is linked to the spike in acceleration, must occur during the thrust production since that is the portion of the jump when the archer fish is actively moving, flapping its tail in the water. Then, the velocity is relatively constant during what must be the glide portion of the jump, since during glide the fish holds itself in a rigid position, not contributing to thrust. Also during the glide, the acceleration often times comes to reflect the fact that only gravity is acting on the fish, as it drops to near negative 9.81 m/s^2. After the archer has captured the bait it often wiggles its body, causing spikes in both velocity and acceleration.

While the plots of velocity and acceleration for individual archers match well, comparisons between different archers should provide results that also match in order for this data to be truly repeatable. To that effect, velocity and acceleration for a variety of different jumps heights were plotted in Figure 4-11. These jumps came from multiple archer fish, but the final heights for all of them were within 0.02 body lengths of each other.

Rather than comparing different archers' jumps based on the final height in body

lengths, one could also compare in terms of final height in centimeters. Data for acceleration and velocity in this case is shown in Figure 4-12, where all the final jump heights are within 0.31 centimeters of each other. While the peak velocities and amount of noise in the data varies from one archer to the next, when comparing data either in body lengths or in centimeters, the overall trends are similar.

A summary of the variation between all of the jumps compared here is found in Table 4.2. It highlights the fact that each archer tends to have a similar velocity and acceleration profile for its jumps, as there is minimal variation in the peak variation and the time to the maximum acceleration. When the comparisons change to include multiple archers there is significantly more variation in the peak velocity and time to maximum acceleration. This is merely indicative of the variation of individuals, as all of the archers have velocity and acceleration profiles that resemble each other and it is only the timing and velocity values that are varying.

Table 4.2: Quantitative descriptions of the comparison of velocity and acceleration for various jumps, shown in Figure 4-6 through 4-12.

Archers compared	No. of jumps	Shown in figure	Variation of jump h_{max}	Variation of peak v [m/s]	Variation in time to a_{max} [s]
1	3	4-6	0.06 BL	0.0399	0.0015
2	3	4-7	0.07 BL	0.0572	0.0030
3	3	4-8	0.18 BL	0.0847	0.0014
4	3	4-9	0.36 BL	0.1409	0.0014
10	4	4-10	0.16 BL	0.1101	0.0089
1, 2, 4, 10	5	4-11	0.01 BL	0.5725	0.0099
2, 3, 4	5	4-12	0.31 cm	0.2703	0.0100

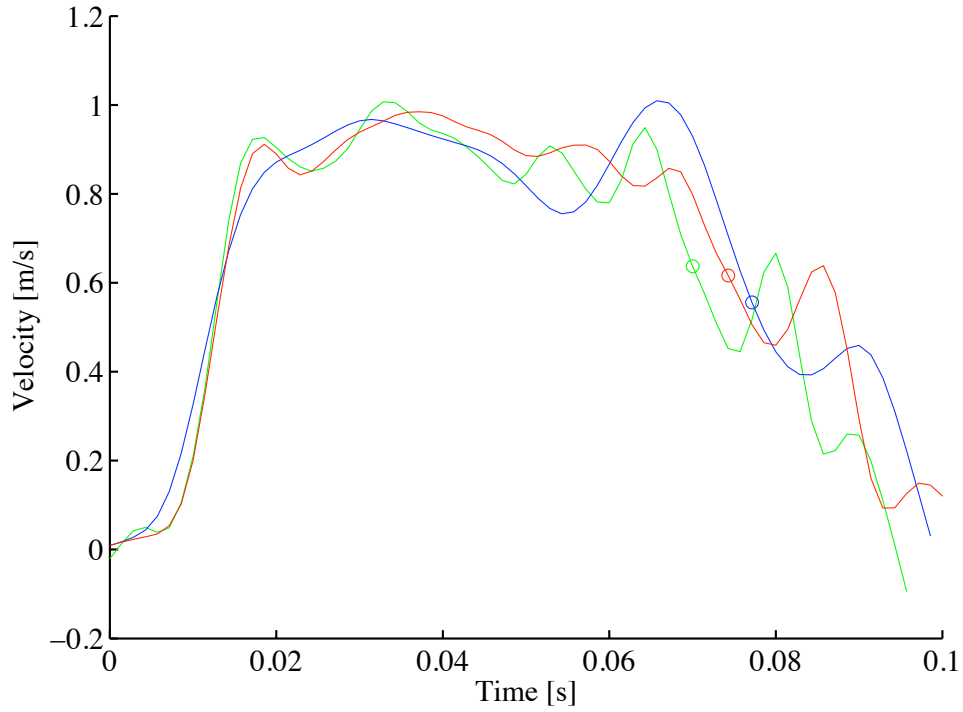

(a) Velocity over time.

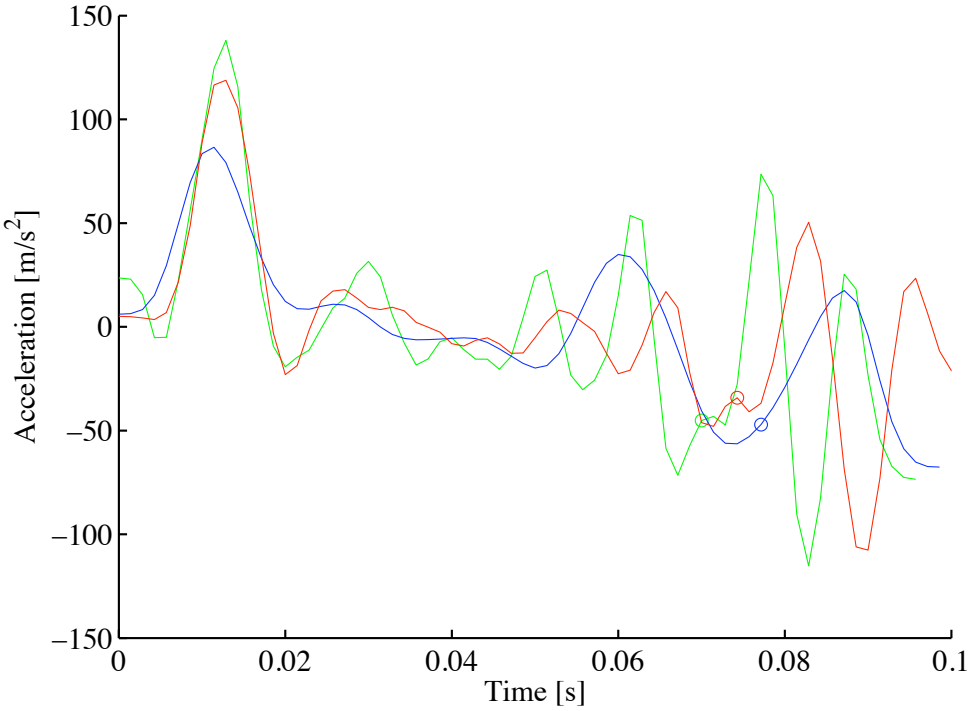

(b) Acceleration over time.

Figure 4-6: For both velocity and acceleration, three different jumps of Archer 1 are shown. The green trace is for a jump of 0.57 BL, blue is for a jump of 0.63 BL and red is for a jump of 0.61 BL. On each trace there is a circle at the point in time when the nose of the fish reached the bait.

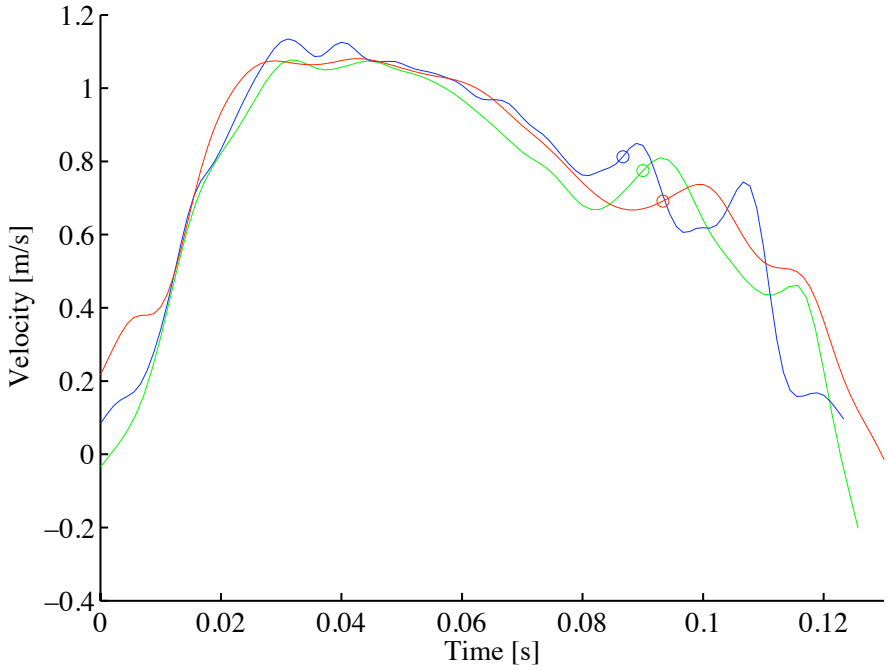

(a) Velocity over time.

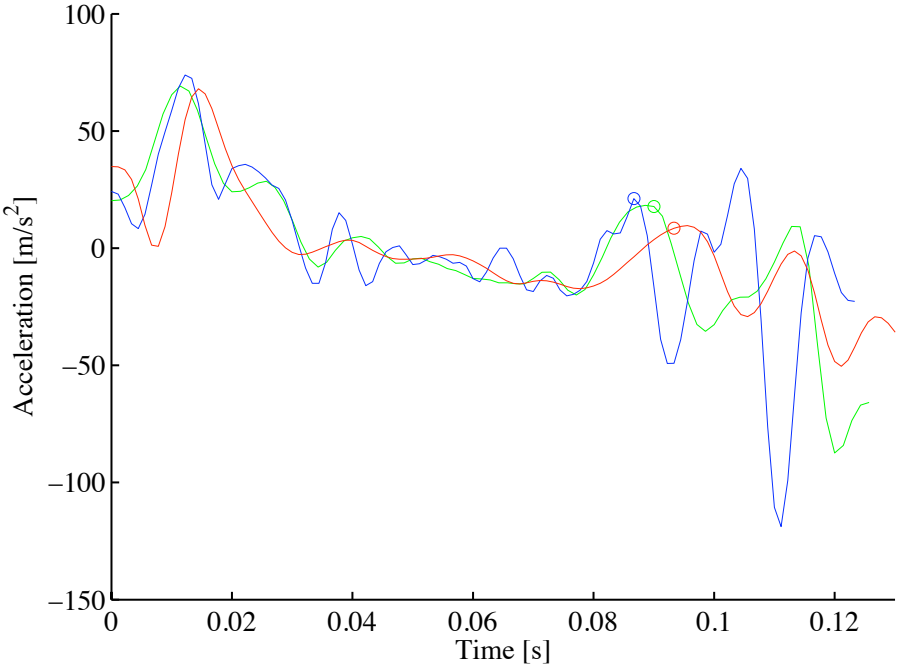

(b) Acceleration over time.

Figure 4-7: For both velocity and acceleration, three different jumps of Archer 2 are shown. The green trace is for a jump of 0.93 BL, blue is for a jump of 0.99 BL and red is for a jump of 0.99 BL. On each trace there is a circle at the point in time when the nose of the fish reached the bait.

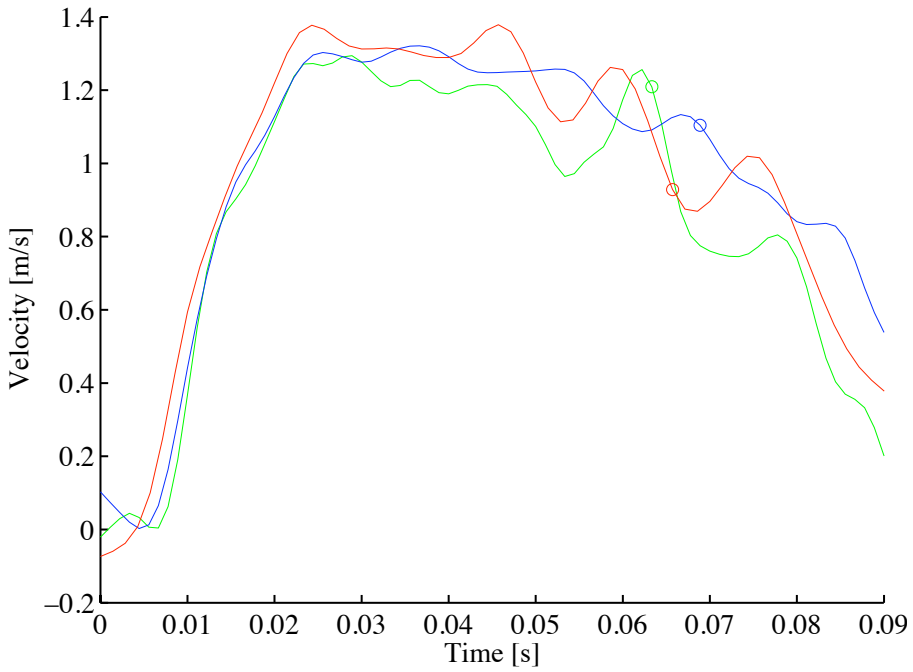

(a) Velocity over time.

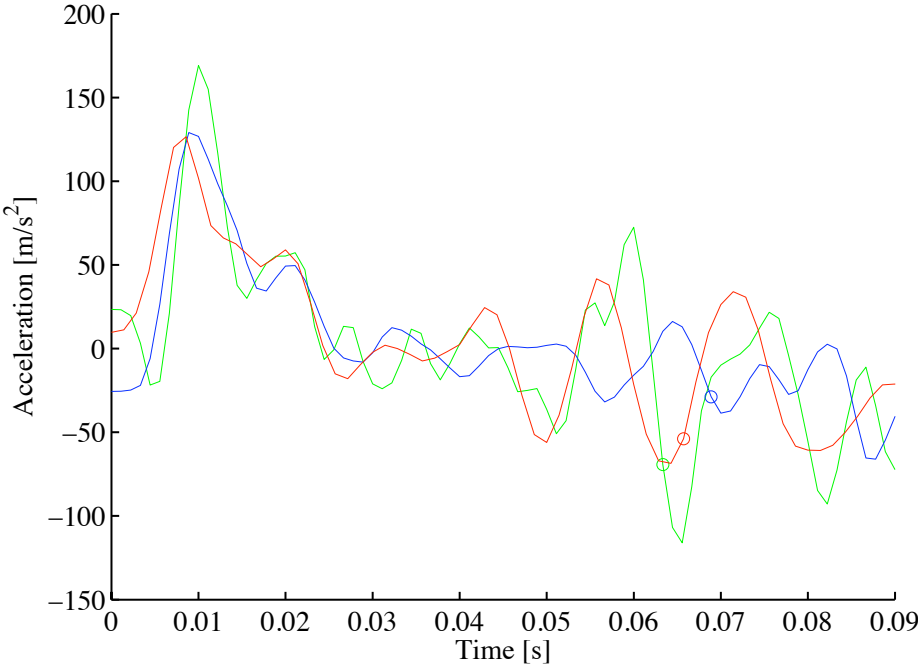

(b) Acceleration over time.

Figure 4-8: For both velocity and acceleration, three different jumps of Archer 3 are shown. The green trace is for a jump of 1.16 BL, blue is for a jump of 1.34 BL and red is for a jump of 1.30 BL. On each trace there is a circle at the point in time when the nose of the fish reached the bait.

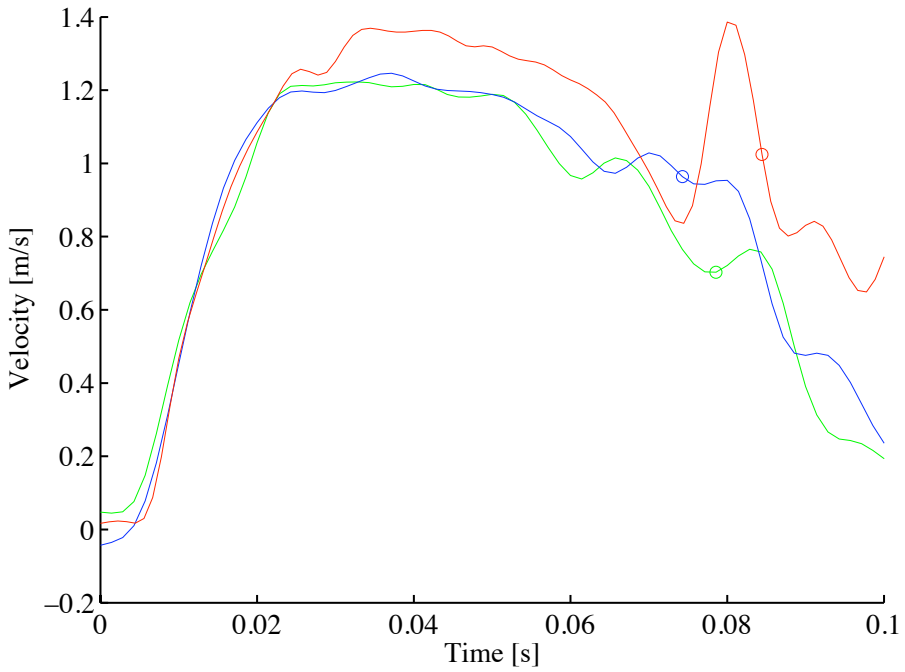

(a) Velocity over time.

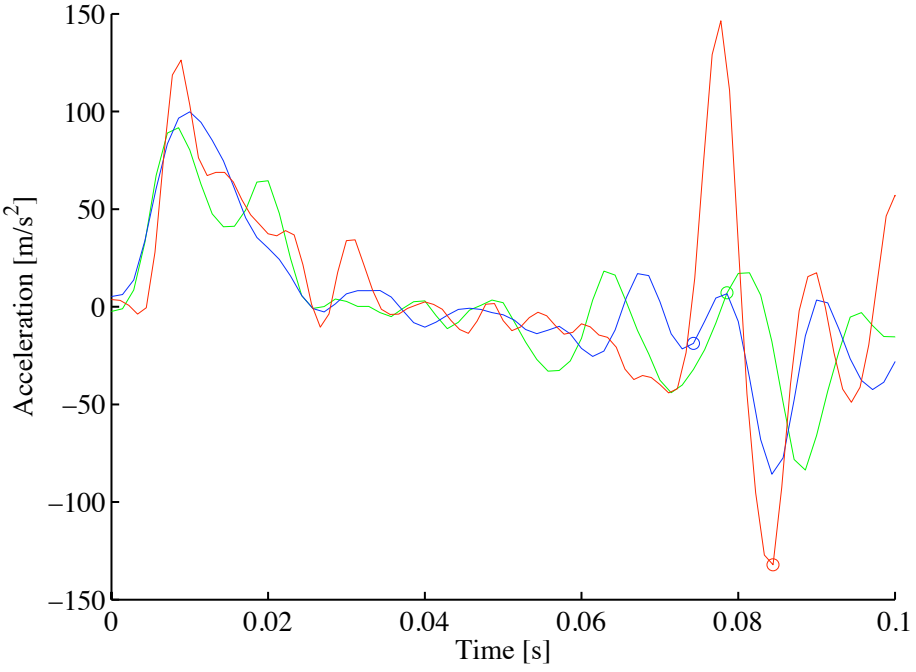

(b) Acceleration over time.

Figure 4-9: For both velocity and acceleration, three different jumps of Archer 4 are shown. The green trace is for a jump of 1.27 BL, blue is for a jump of 1.35 BL and red is for a jump of 1.63 BL. On each trace there is a circle at the point in time when the nose of the fish reached the bait.

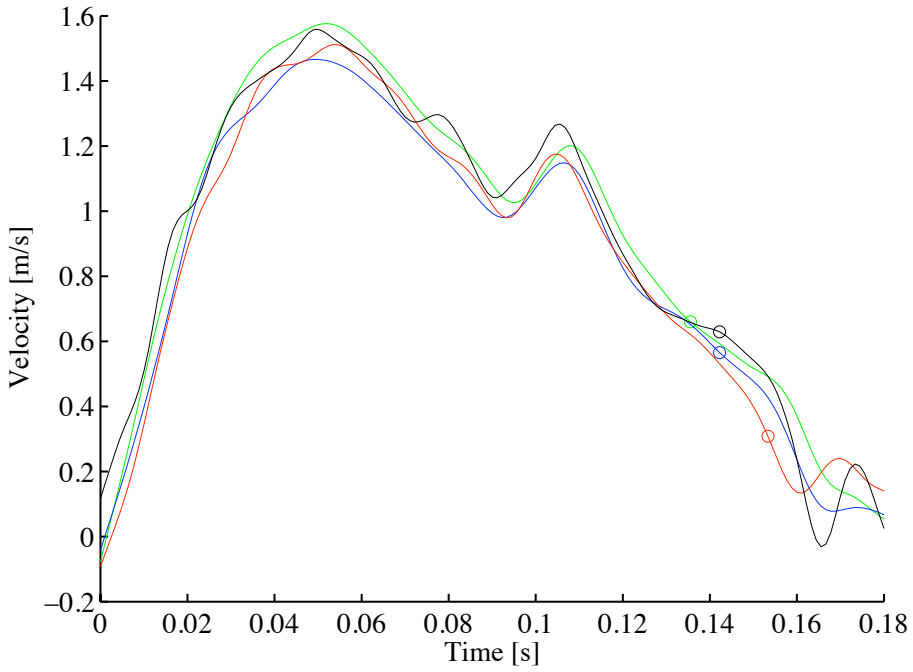

(a) Velocity over time.

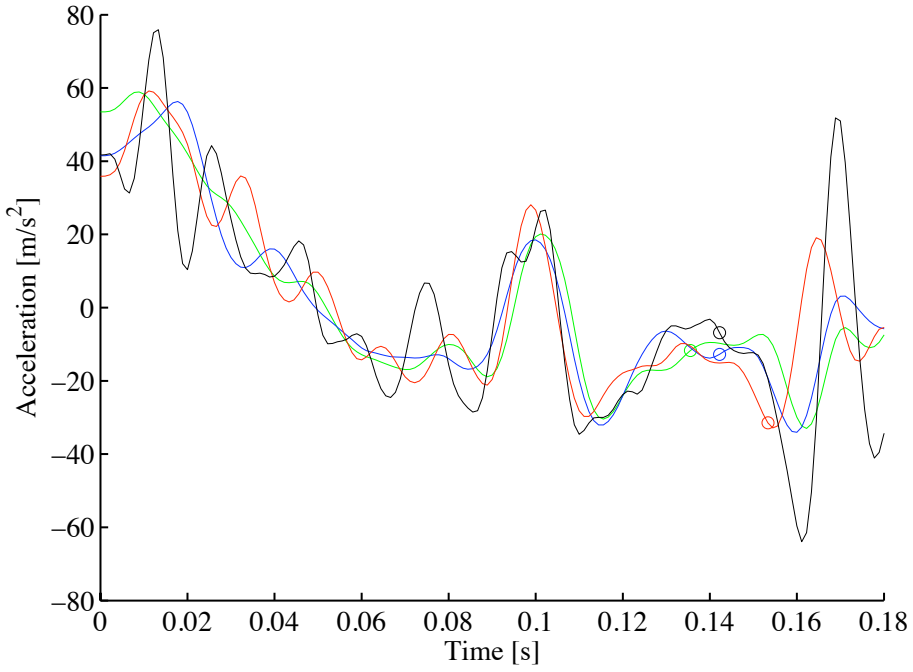

(b) Acceleration over time.

Figure 4-10: For both velocity and acceleration, four different jumps of Archer 10 are shown. The green trace is for a jump of 2.27 BL, blue is for a jump of 2.16 BL, red is for a jump of 2.11 BL and black depicts a jump of 2.23 BL. On each trace there is a circle at the point in time when the nose of the fish reached the bait.

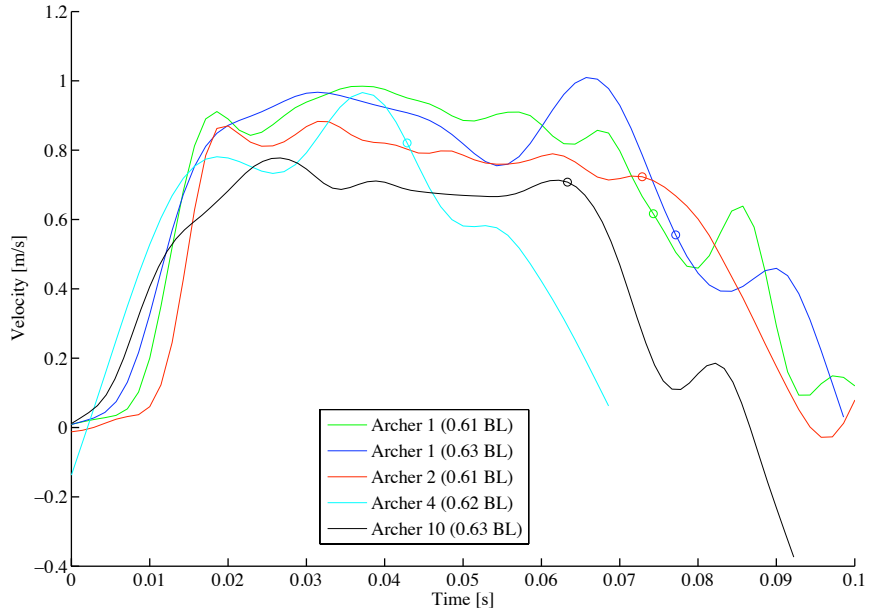

(a) Velocity over time.

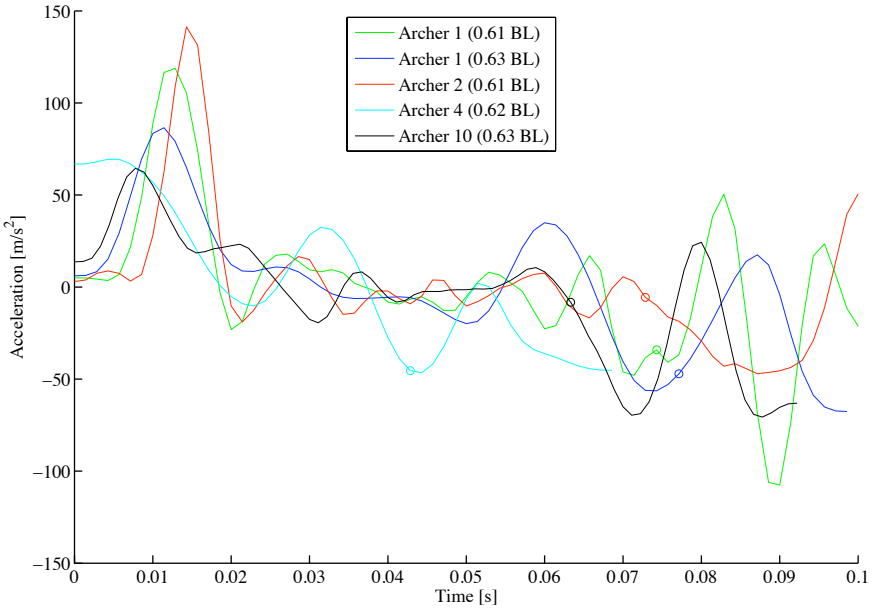

(b) Acceleration over time.

Figure 4-11: For both velocity and acceleration, 5 jumps are shown where the final height was comparable in terms of body lengths above the surface. Once again, the circles on each line show the point at which the archer reached the bait height.

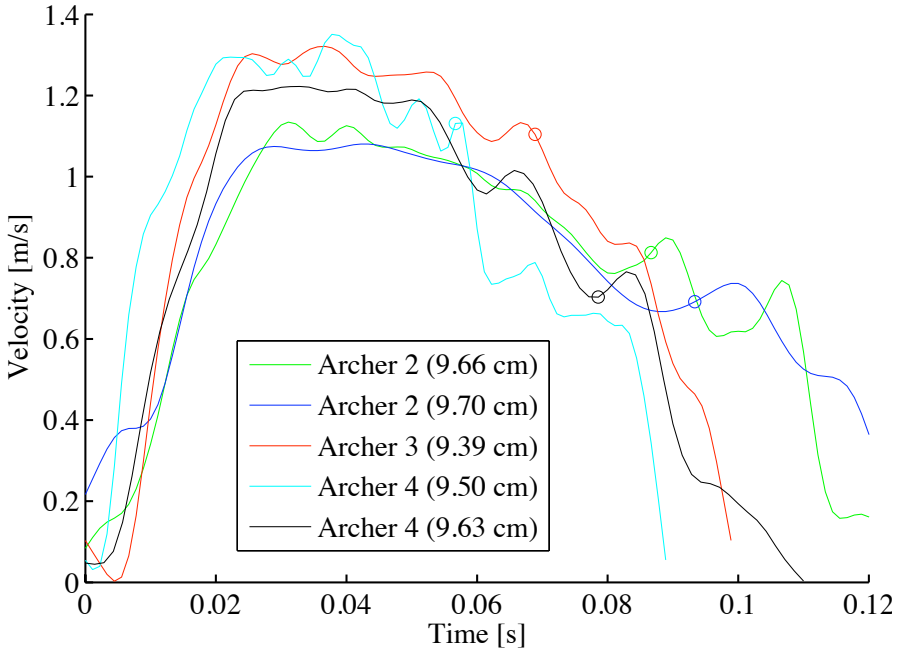

(a) Velocity over time.

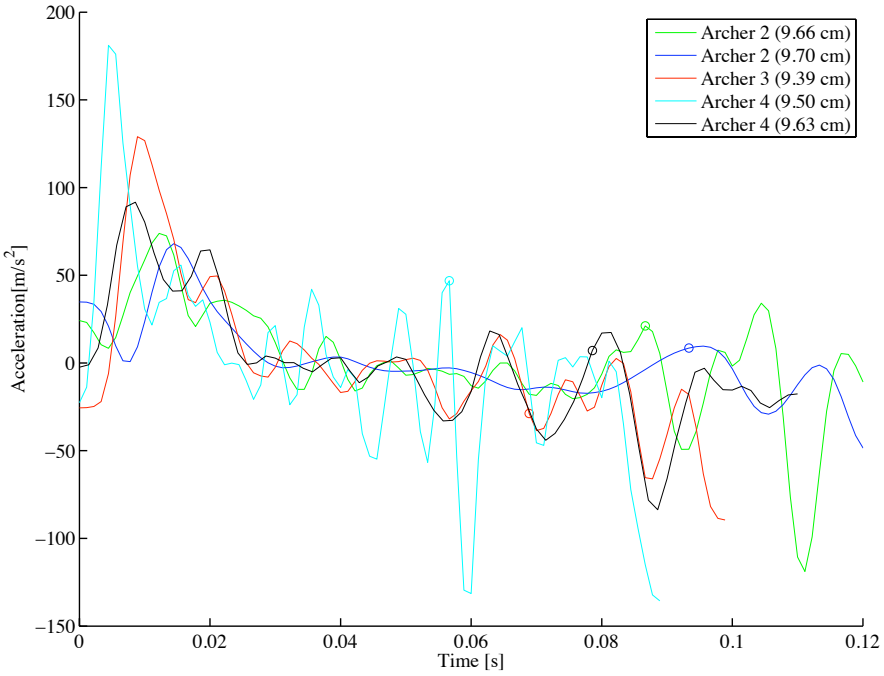

(b) Acceleration over time.

Figure 4-12: For both velocity and acceleration, 5 jumps are shown where the final height of the jumps were close to each other in terms of centimeters above the water surface. The circles on each line show the point at which the archer reached the bait height.

4.3 Jump Duration

Jumps were timed from the initial motion of the fish's pectoral fins until the moment when its mouth was determined to have reached the level of the bait. The data for each of the individual fish can be seen in combined in Figure 4-13. Error in the time recorded would be at most ± 2 frames (or between 0.002 and 0.004 seconds depending on the frame rate).

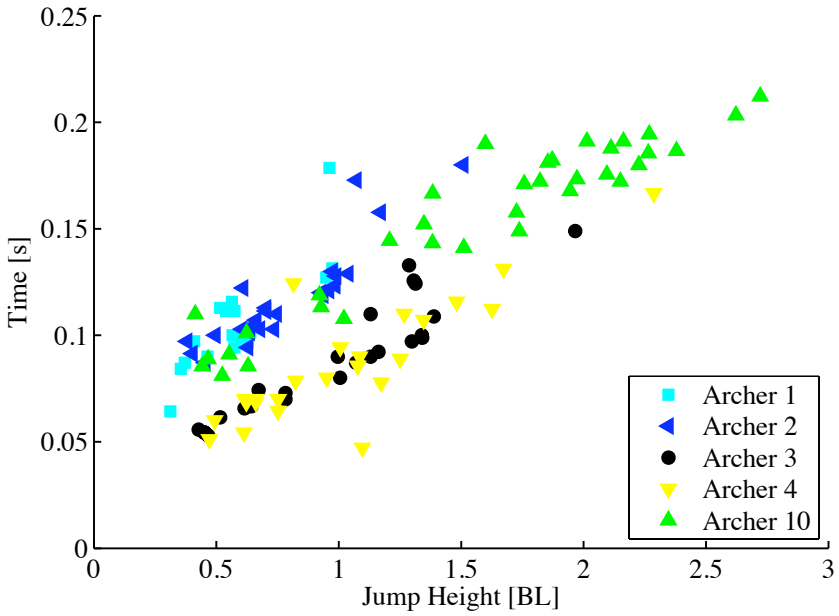

Figure 4-13: Fish maximum jump heights versus the time it took to reach maximum height.

The plot of jump height versus time demonstrates that all of the fish require more time to make higher jumps, in what appears to be a linear relationship. While the overall trend is the same for all of the archers, the individual relationship between height and time is fish dependent. Table 4.3 outlines the parameters of a linear fit to the data. The slope is representative of an average velocity for a jump, which increases with height of the bait. Theoretically this linear relationship should not exist past a cut off value, similar to what was discussed in the previous section. The archer has a minimum jump height, so the linear relationship for height and time should start at that minimum. Additionally, the larger archers have significantly higher slopes than

Table 4.3: Trend line information for archer maximum jump heights and the time it took to reach maximum height

Archer No.	Slope [BL/s]	Intercept [BL]	Coefficient of determination [R^2]	Number of Trials	Mass [g]	Length [cm]
1	0.1022	0.0455	0.7002	18	25.35	11.1
2	0.0797	0.0545	0.8094	26	23.6	9.8
3	0.0634	0.0259	0.8766	24	7.9	7.0
4	0.0556	0.0299	0.7159	24	10.2	6.8
10	0.0549	0.0673	0.9088	35	9.3	7.6
All	0.0571	0.054	0.673	127	N/A	N/A

the rest, which means that they will take longer to reach the same percent of their body length, so they are slower than the smaller fish.

4.4 Over Shooting

Whenever an archer fish captures prey by jumping, it overshoots the bait, or jumps beyond it. Here, overshoot is calculated as the difference between final height of the archer's nose and the bait height, normalized by the height of bait. Figure 4-14 plots overshoot in percentage; the top figure is for the larger fish and the bottom displays behavior of the smaller fish. If the archer completely missed the bait for a particular jump, that data point is shown in red and is only outlined, not solid. The larger fish demonstrate a significant amount of overshoot at low bait heights, however this trend is not seen as clearly for the smaller fish. Additionally, at larger bait heights, Archer 10 can be seen to have negative overshoot since it jumped to try to capture the bait, but missed because it could not get high enough.

When the data for all of the fish is combined together, as seen in Figure 4-15, it can be seen that the large fish tend to overshoot by 80 to 120% at lower bait heights, and there is a similar small increase in overshoot for the smaller archers. Also, at bait heights higher than roughly 1.5 body lengths there is less overshoot, which means that the archers are not wasting any energy to get to the bait. At the very extreme of the high bait, which is over around 2.5 body lengths ends, the two trials show that

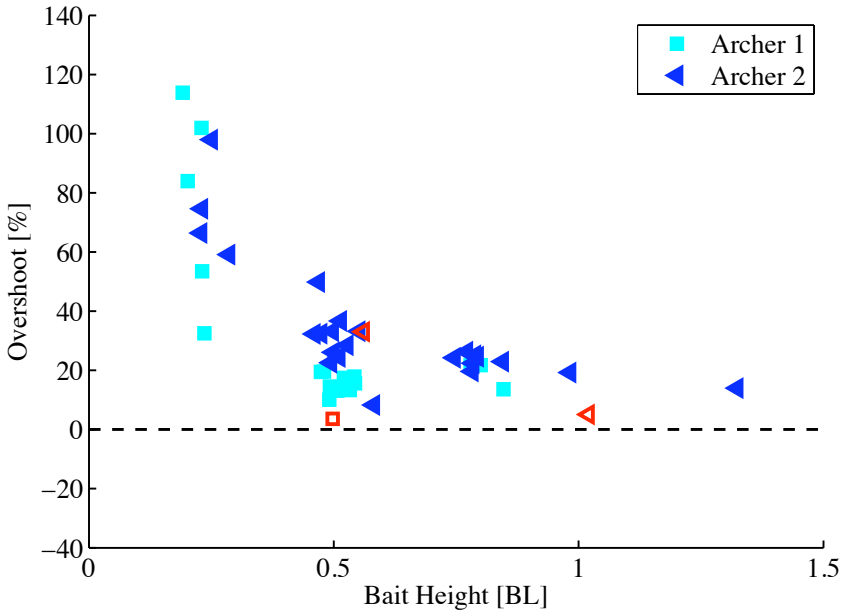

(a)

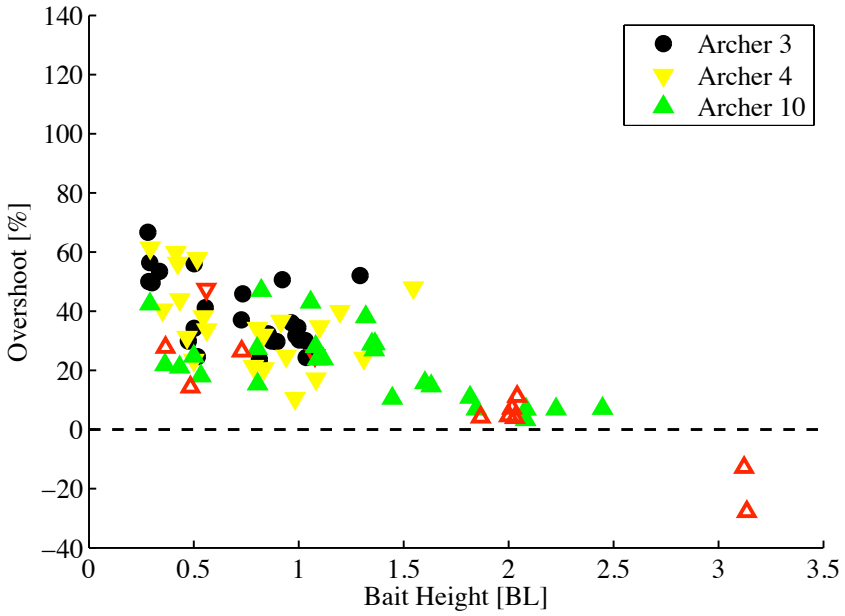

(b)

Figure 4-14: Both (a) and (b) show the percentage overshoot on a given jump compared to bait height, however (a) shows the two largest fish: Archer 1 (11.1 cm) and Archer 2 (9.8 cm) and (b) shows three smaller fish: Archer 3 (7.0 cm), Archer 4 (7.6 cm), Archer 5 (8.4 cm) and Archer 10 (7.6 cm). Red data points correspond to the archer not successfully capturing the bait.

attempts at this height end in misses. However, the middle region is much noisier with all of the archers plotted together. Examining the data for all fish when the bait height is between 0.5 and 1.5 body lengths gives a mean of 28.2% over shoot and a standard deviation of 11.2%.

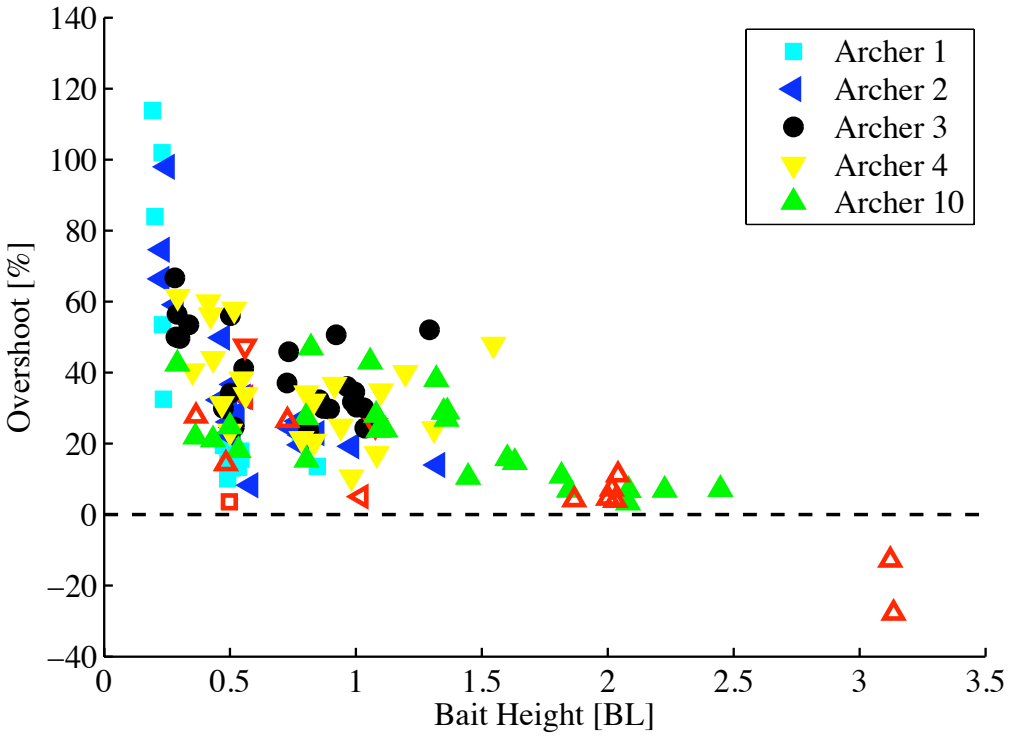

Figure 4-15: The percent of bait height that the fish overshot versus the bait height for all 5 fish. Data shown for all of the fish where red data points correspond to the archer not successfully capturing the bait.

While these trends could be explained by where the bait is located and how the archer sights it, [25] Schuster et al. suggest that the fish select angles that result in a wide variety of perceived distances, but the angle of inclination (for shooting at least) is based on the previous views that the fish had while swimming towards its prey. So while it could be possible that overshoot is a result of sighting, it is not an easy calculation to make.

A logical explanation for the large percentages of overshoot at low heights related to how many times the tail strokes the archers make. A tail stroke, as defined previously in Section 3.5.4, is one motion of the tail from a local maximum deflection

to another such maximum. At low heights the fish flaps its tail fewer times as was shown in Figure 3-11. If each tail stroke produces a set amount of thrust, then there will be a minimum jump height based on the fact that the fish can only produce set amounts of thrust. Even if the bait is very close to the surface, in order to escape at all the archer has to perform at least one tail stroke, which will propel it further out of water than it needs to travel to capture the prey, resulting in a large overshoot at a low bait height.

At higher bait heights the fish is subject to the same errors in judgement as it is when it shoots ([28]), however it eventually just can not produce enough thrust to reach the bait, at which point its overshoot turns negative. This was demonstrated by Archer 10 attempting to jump for bait at 2.5 body lengths above the water. When the bait is higher than 1.5 body lengths above the water there is still minimal overshooting, so using the theory that the archer gets sets amount of thrust from each tail stroke, this is the region where the archer is performing as many strokes as it can before leaving the water, and thus is near the limit of its jumping range. The middle region of the plot, where the bait is between 0.5 and 1.5 body lengths will not be subjected to the same stroke limitations, since these heights are not at either extreme of the number of tail strokes the archer can perform.

An interesting note is that some times failures results merely because the archer would not wait for the bait to be set in place and stop moving before jumping, especially for Archer 10. The history of missing the bait potentially has a large impact on overshoot, since it will alter future behaviors. Determining the true effect of missing is a very complicated topic that was not broached in this thesis.

4.5 Energy Analysis

In order to characterize the jump of an archer fish, the potential($PE = mgh$) and kinetic energy ($KE = \frac{1}{2}mv^2$) were calculated for each run. While potential energy could be calculated based on the final height for every jump, kinetic energy requires a maximum velocity value, so it was only found for runs presented in Figure 4-4. When

comparing the two forms of energy, the kinetic energy is expected to be greater than the potential energy, indicating that all of the energy required to jump is being accounted for in the change in velocity of the fish.

Initially potential energy was calculated based on the final nose position that had been found with the customized Matlab code described previously, however, this did not seem to properly account for the energy of the jump. If, instead, the potential energy was calculated based on the center of mass, the kinetic and potential energies balanced each other better. Calculation of the center of gravity of the fish was done for Archer 1 based on a SolidWorks model, shown in Figure 4-16. This model was

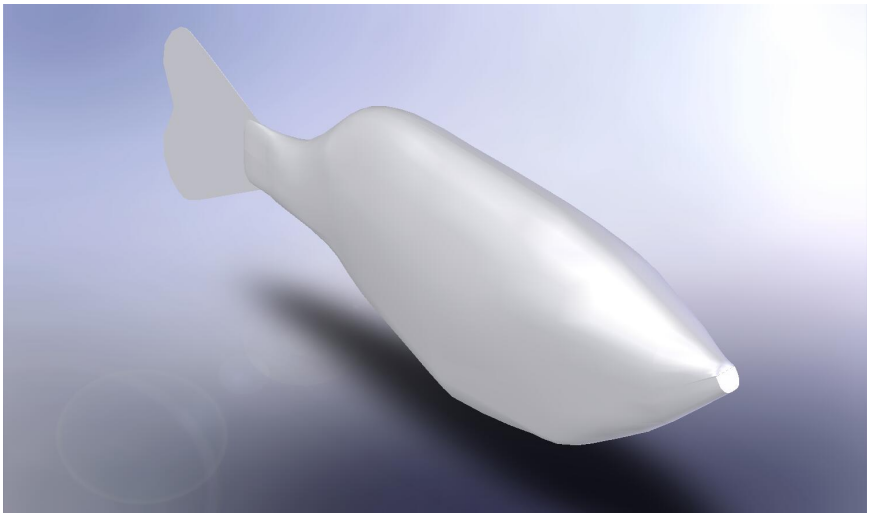

Figure 4-16: SolidWorks model of Archer 1 that allowed for center of gravity to be calculated.

made based on measurements obtained from images of the archer (dimensions were calculated using the same method as for overall length of the archer) and also relied on SolidWorks' ability to interpolate between sections of the fish. While not all of the archers are going to have exactly the same width as a function of length, in order to prevent having the necessity of modeling each fish individually, it was assumed that since the center of gravity of Archer 1 was 4.55 cm from the tip of its nose, or 41% of the distance along its body, the other archers would follow a similar trend. Therefore, all calculations based on center of gravity being located 40% of the way along the body of the archer in question.

The end result of all of these energy calculations can be seen for all archers in Figure 4-17, which nicely illustrates the significance of using the center of gravity instead of the nose for potential energy calculations. Based on the potential energy derived from center of gravity information, it appears that kinetic energy balances the maximum potential energy. Archer 10 has kinetic energy values that are slightly lower than potential energy, however these are within the error of the velocity calculation. From these plots it appears that the changing velocity of the archer is all that is needed to explain the final height of the jumps, even accounting for losses such as drag.

For each archer, the lowest and highest jump where nose position data had been processed were considered individually. Kinetic and potential energy were plotted over time for those jumps based on the prior definitions. Potential energy was calculated either as a function of time or as a function of distance out of the water. Total energy was assumed to just be the sum of kinetic and potential energies. On all of the energy plots shown in Figures 4-18 through 4-27, the time when the archer reached the bait was marked using a light blue solid line.

This set of figures also plots energy in two different ways; one compared to how much of the fish was out of water at a given instant in time, and the other compared to how much time had elapsed since the jump began. Velocity and acceleration plots are also given for reference. It is possible to see in some of those velocity plots the artifact that is left behind from the fish opening its mouth, and that can be seen carried over into the energy plots.

While potential energy is always increasing up until maximum jump height, kinetic energy can be broken into several different segments that apply for all of the cases shown here, similar to the velocity plots. The first portion is during thrust production, when the fish is accelerating out of the water. Then there is a phase where the kinetic energy has leveled out and is essentially constant, before the archer starts slowing down. Kinetic energy is roughly zero at the maximum height, since the fish is almost motionless at the top of its jump.

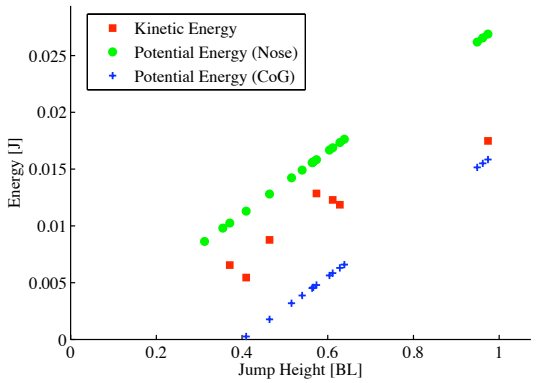

(a) Archer 1.

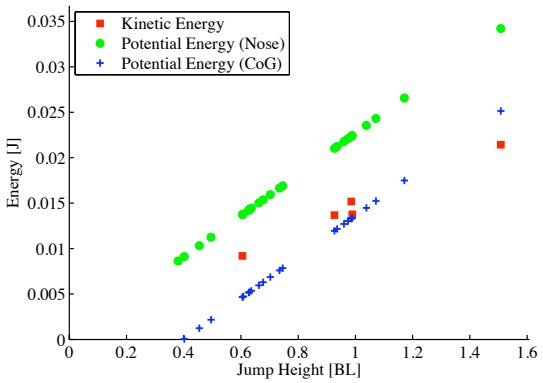

(b) Archer 2.

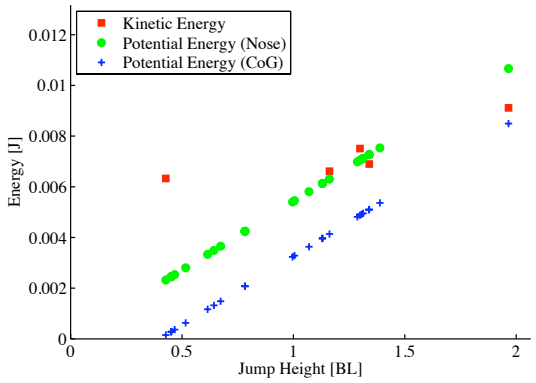

(c) Archer 3.

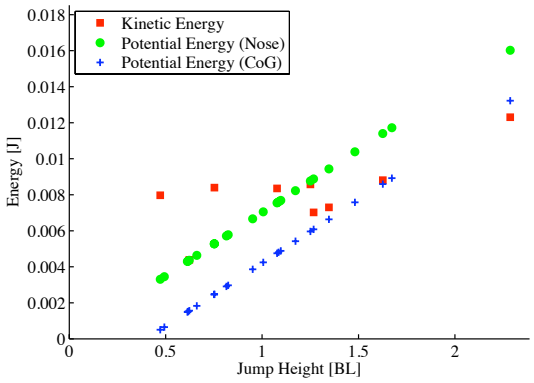

(d) Archer 4.

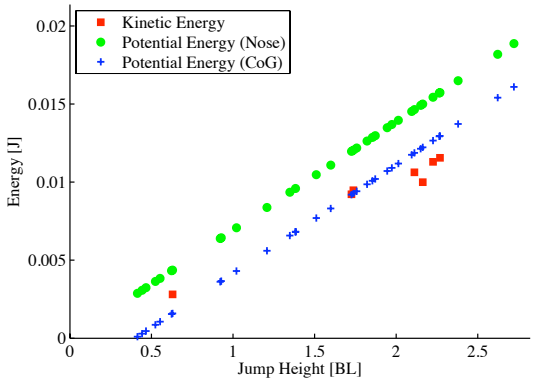

(e) Archer 10.

Figure 4-17: A comparison of the kinetic and potential energies needed for a jump. Potential energy of the nose is shown in green circles, while potential energy of the center of gravity is the blue crosses. Kinetic energy is only shown for jumps that had velocity data, and is represented by the green squares.

Looking at the variation of energy over time highlights an important aspects of power production. Maximum kinetic energy always occurs before the fish is entirely out of the water. This means that even if an archer flaps its tail in air, as happened for Figure 4-26, it is not significantly contributing to the total energy. All of the thrust production must occur when the fish still has its tail underwater where the density of the fluid, and thus the force, is 1000 times greater.

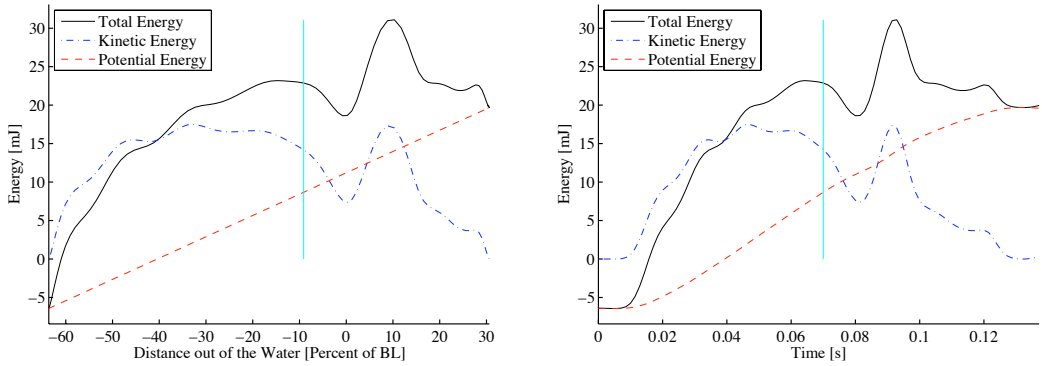

(a) Energy compared to % of fish out of water.

(b) Energy compared to time.

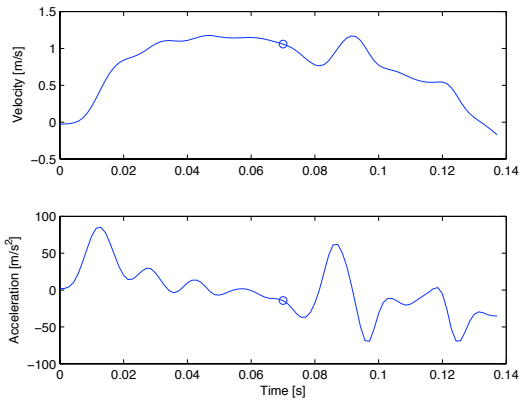

(c) Velocity and acceleration.

Figure 4-18: Energy analysis for Archer 1's highest jump that still had nose position data. This jump reached a maximum height of 0.97 BL (10.8 cm).

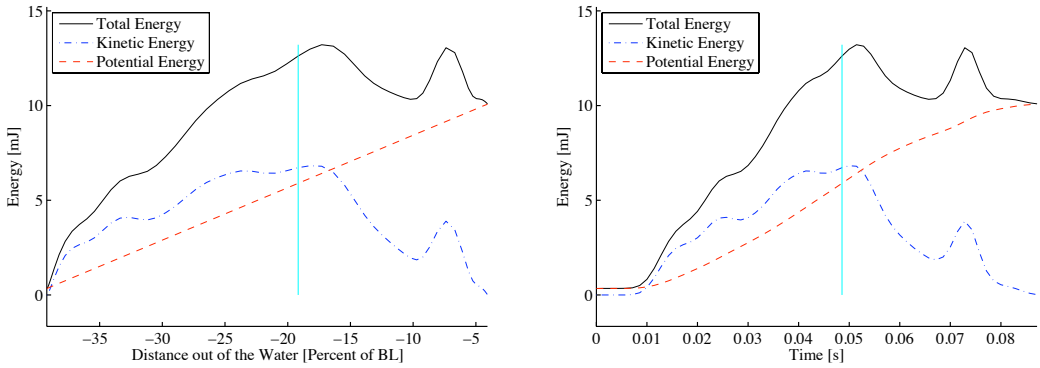

(a) Energy compared to % of fish out of water.

(b) Energy compared to time.

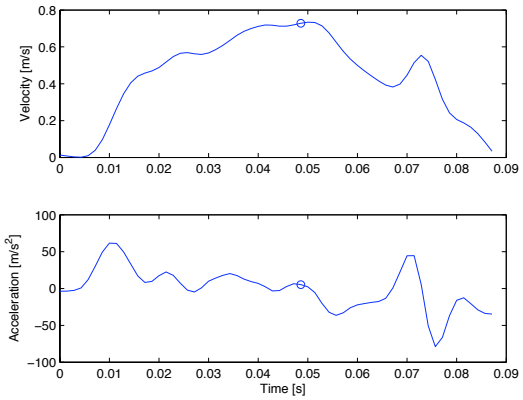

(c) Velocity and acceleration.

Figure 4-19: Energy analysis for Archer 1's lowest jump that still had nose position data. This jump only reached a maximum height of 0.37 BL (4.1 cm).

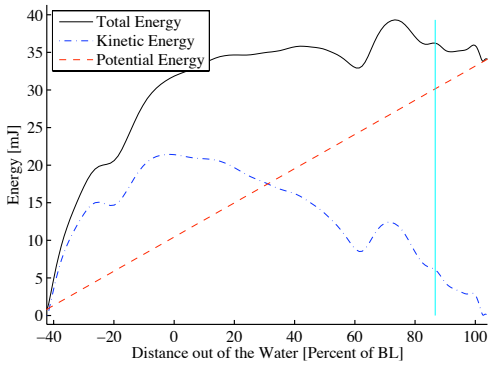

(a) Energy compared to % of fish out of water.

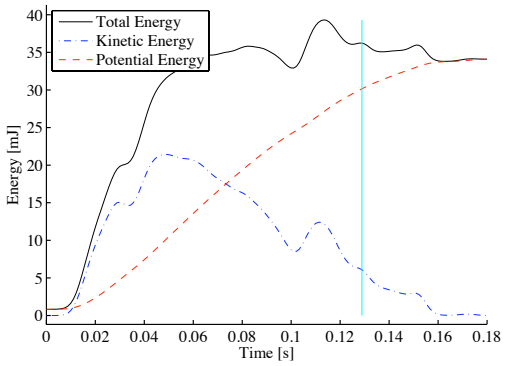

(b) Energy compared to time.

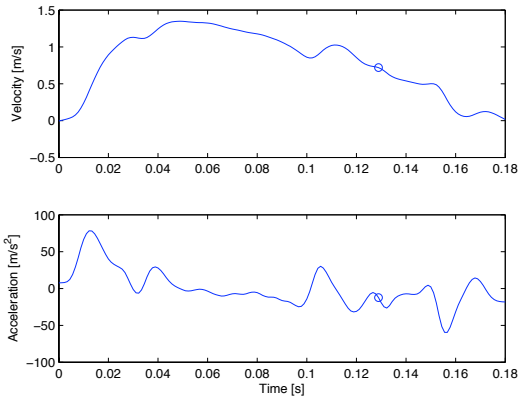

(c) Velocity and acceleration.

Figure 4-20: Energy analysis for Archer 2's highest jump that still had nose position data. This jump reached a maximum height of 1.51 BL (14.8 cm).

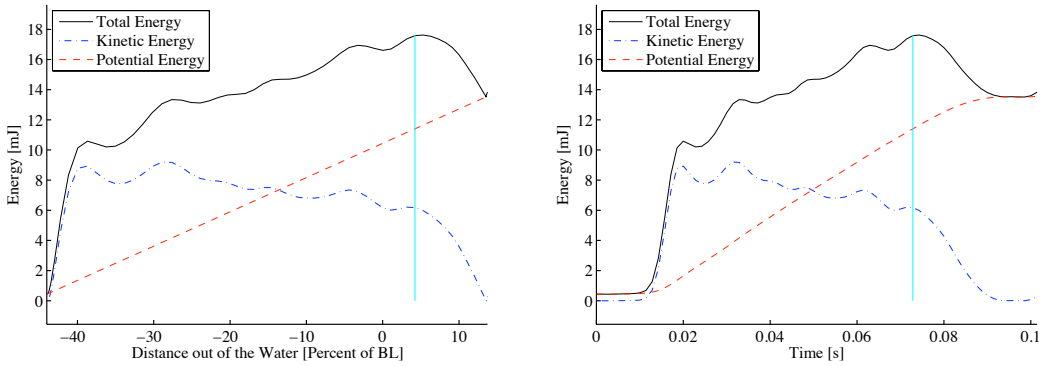

(a) Energy compared to % of fish out of water.

(b) Energy compared to time.

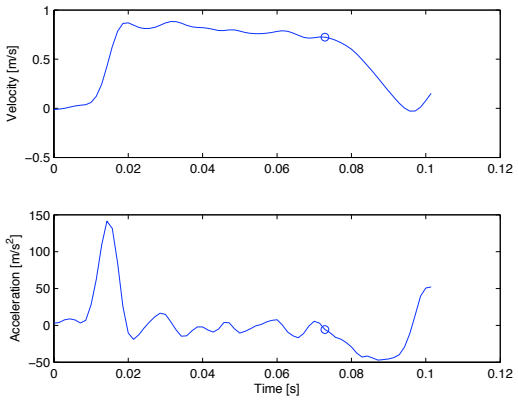

(c) Velocity and acceleration.

Figure 4-21: Energy analysis for Archer 2's lowest jump that that still had nose position data. This jump only reached a maximum height of 0.61 BL (5.9 cm).

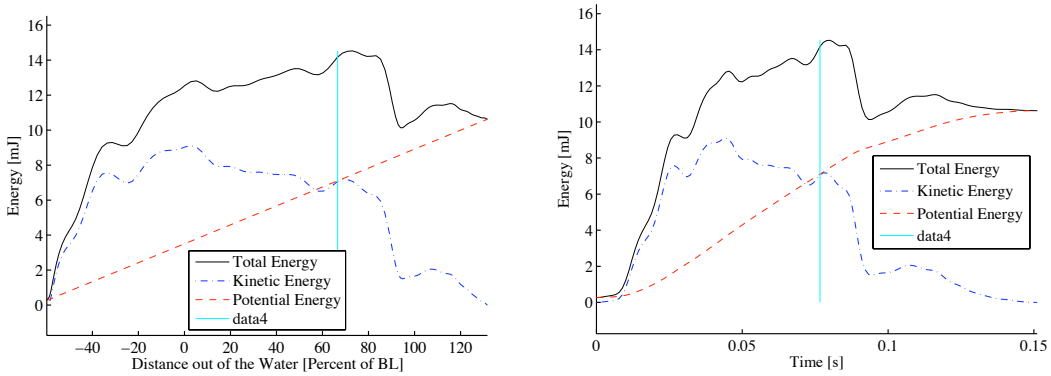

(a) Energy compared to % of fish out of water.

(b) Energy compared to time.

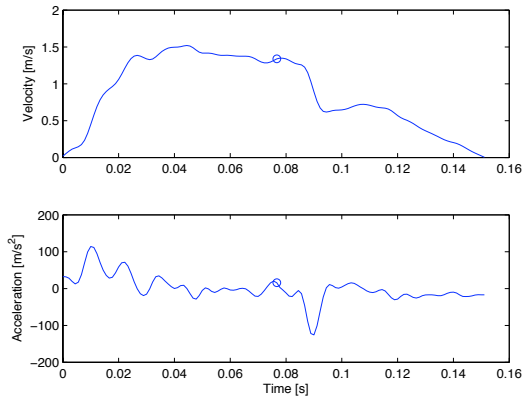

(c) Velocity and acceleration.

Figure 4-22: Energy analysis for Archer 3's highest jump that still had nose position data. This jump reached a maximum height of 1.97 BL (13.8 cm).

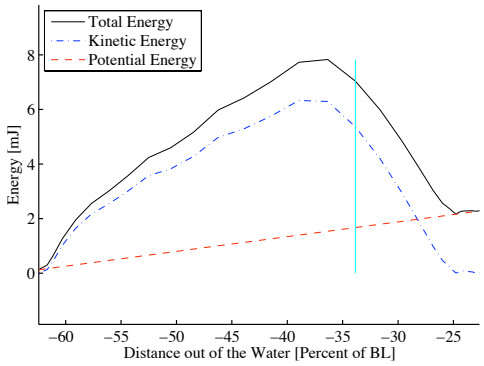

(a) Energy compared to % of fish out of water.

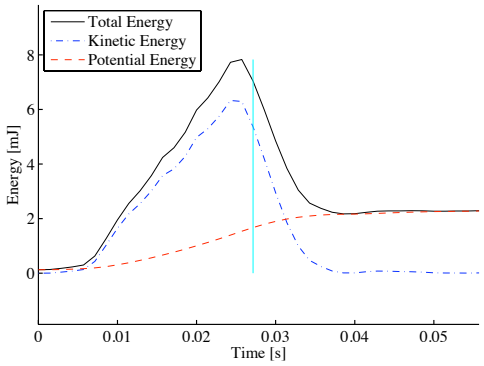

(b) Energy compared to time.

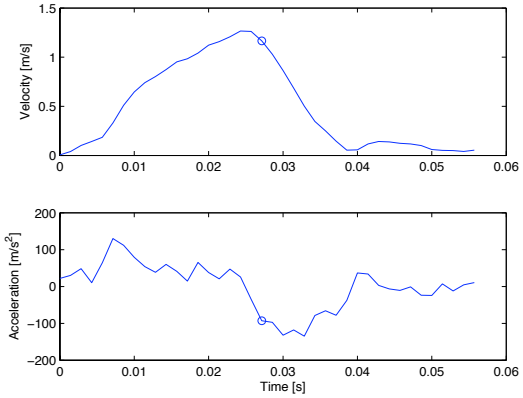

(c) Velocity and acceleration.

Figure 4-23: Energy analysis for Archer 3's lowest jump that that still had nose position data. This jump only reached a maximum height of 0.43 BL (3.0 cm).

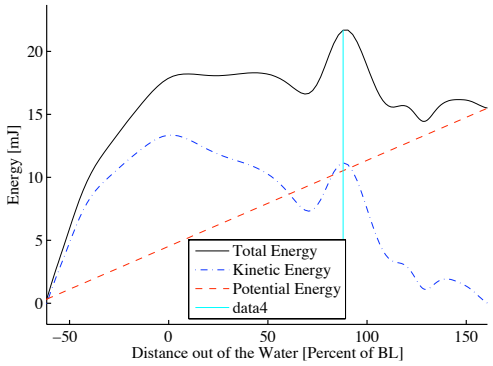

(a) Energy compared to % of fish out of water.

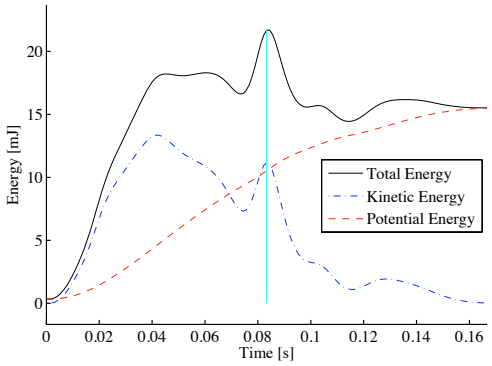

(b) Energy compared to time.

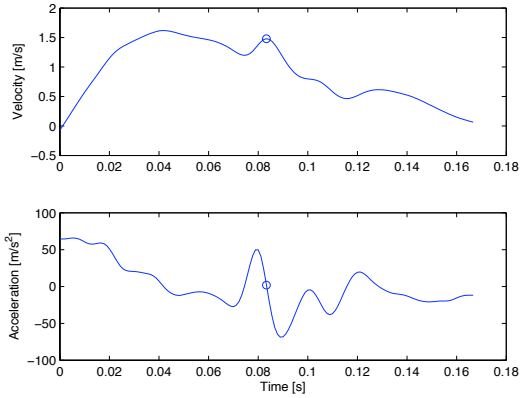

(c) Velocity and acceleration.

Figure 4-24: Energy analysis for Archer 4's highest jump that still had nose position data. This jump reached a maximum height of 2.29 BL (17.4 cm).

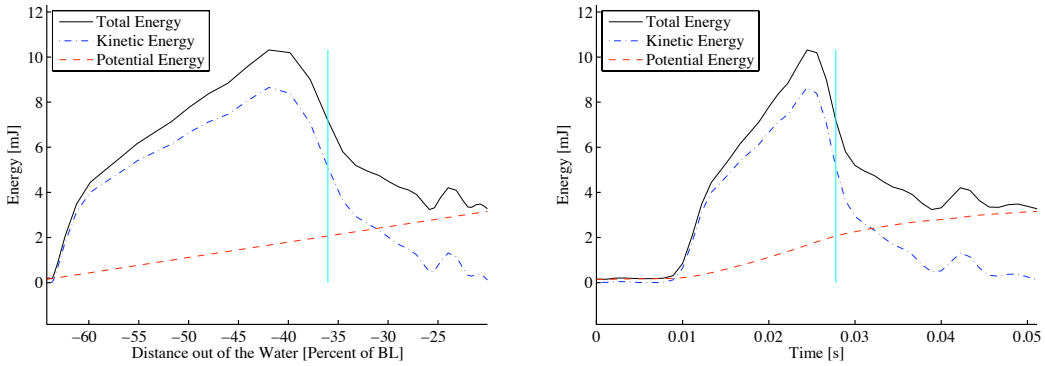

(a) Energy compared to % of fish out of water.

(b) Energy compared to time.

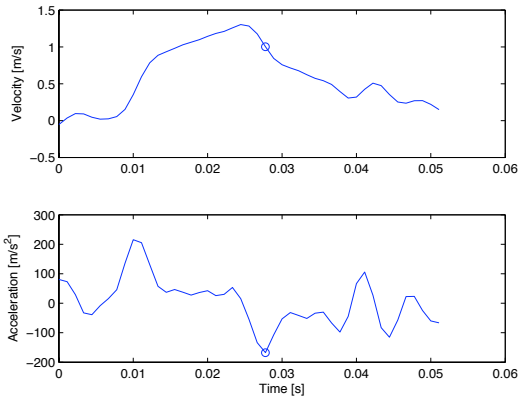

(c) Velocity and acceleration.

Figure 4-25: Energy analysis for Archer 4's lowest jump that that still had nose position data. This jump only reached a maximum height of 0.47 BL (3.6 cm).

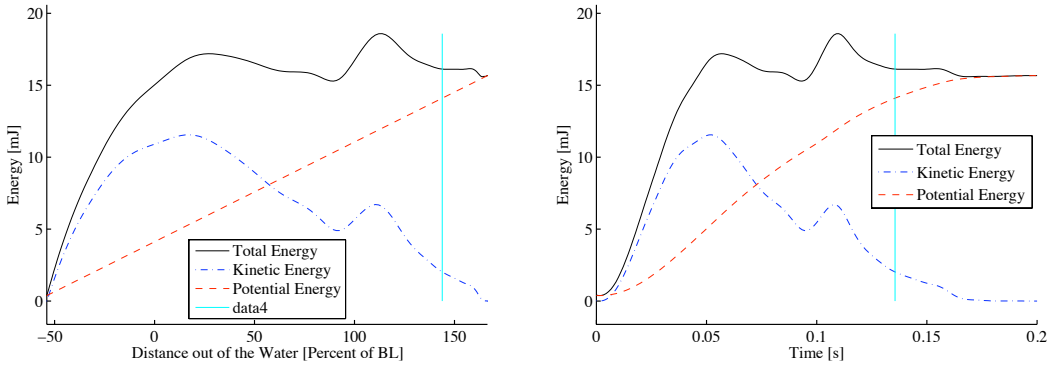

(a) Energy compared to % of fish out of water.

(b) Energy compared to time.

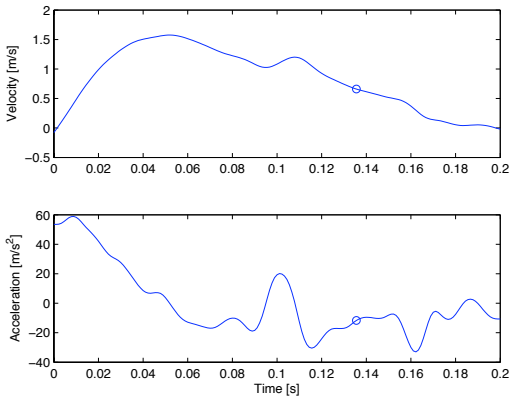

(c) Velocity and acceleration.

Figure 4-26: Energy analysis for Archer 10's highest jump that still had nose position data. This jump reached a maximum height of 2.27 BL (17.2 cm).

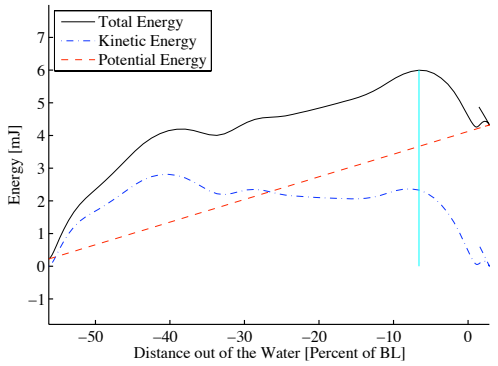

(a) Energy compared to % of fish out of water.

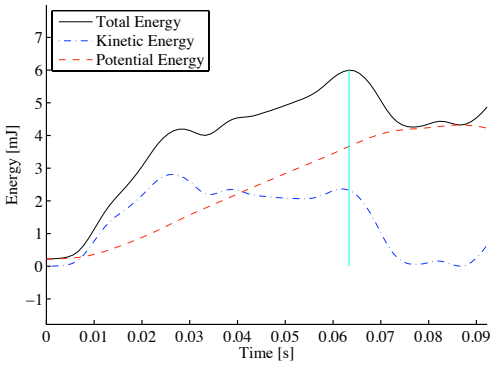

(b) Energy compared to time.

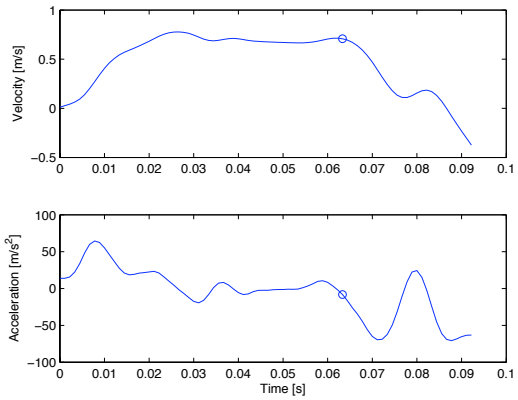

(c) Velocity and acceleration.

Figure 4-27: Energy analysis for Archer 10's lowest jump that still had nose position data. This jump only reached a maximum height of 0.63 BL (4.8 cm).

Generally the low jumps under half a body length tend to have more kinetic energy than what is ultimately needed, thus contributing to overshoot. In these graphs (Figures 4-19(c), 4-23(c) and 4-25(c)), the archer has a steep increase in kinetic energy that is almost always followed by prey capture and a corresponding sharp fall in kinetic energy. Not enough trials have been performed to say with certainty that the archers have a minimum jump height, but it is appears likely.

Chapter 5

Hydrodynamic Analysis

5.1 Introduction

In order to better understand how archer fish are able maneuver, PIV was used to perform a hydrodynamic analysis. The PIV analysis can be broken up into several portions. First there is a description of the first behavior involved in jumping; hovering. This is followed by PIV studies of the second stage of jumping, which is thrust production. To throughly examine how the archers jump, thrust production is looked at from two different angles; one where the fish is jumping mostly parallel to the laser plane, and another view where the fish is jumping perpendicular to the laser plane, so that its tail passes through the plane with time. Additionally, results are shown for when the anal fin is in the laser plane. In all of the PIV image sequences shown, positive vorticity is red (out of the page) while negative is blue. To further quantify some of these results of PIV, a final section describes the vorticity, circulation and impulse from the different runs.

5.2 Hovering

Hovering, as discussed in Chapter 3, is similar to station keeping, only with a different orientation of the archer's body. To get a better idea of what is occurring during station keeping, a series of PIV images as shown in Figure 5-1 was picked to shown

both the extremes of pectoral fin motion for the fin on the right. For the purpose of this image sequence time equal to zero was taken to be the first image shown, where the right hand pectoral fin is at the bottom of its range of motion.

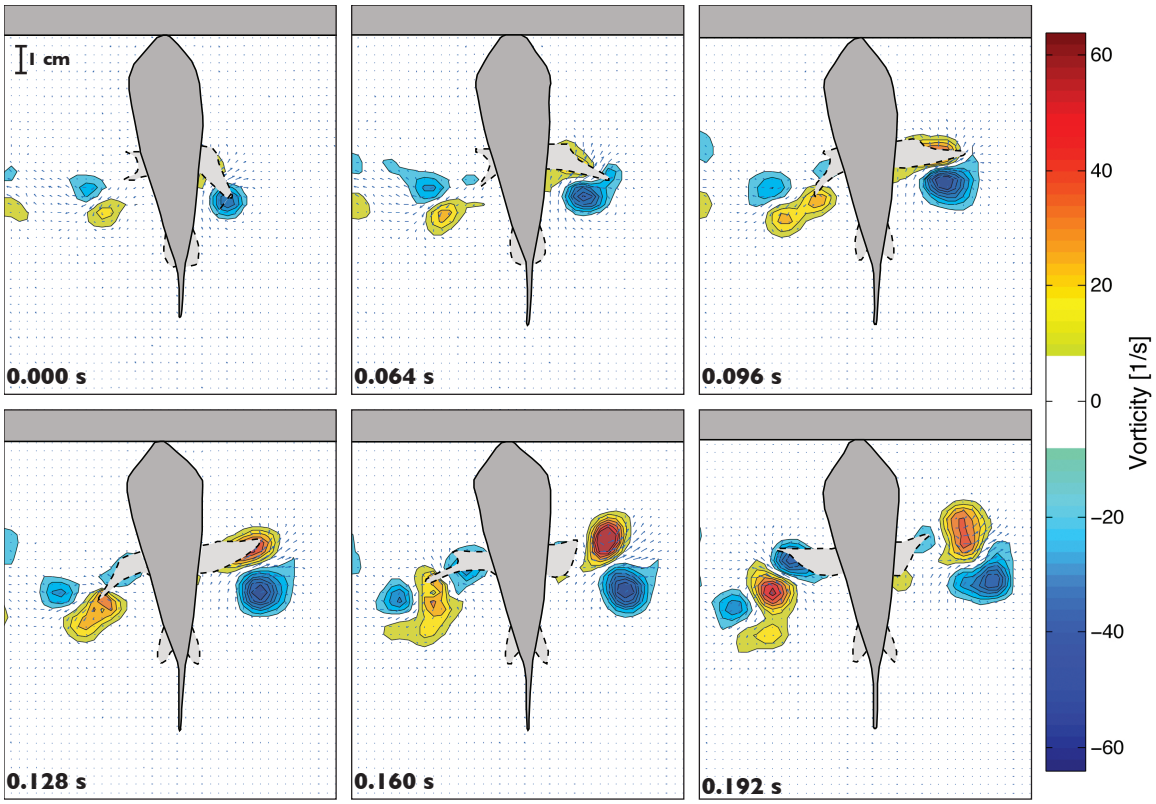

Figure 5-1: Vorticity and velocity vectors for an archer fish hovering, taken from a PIV image sequence.

As shown in the first image in the sequence, the pectoral fin has accumulated negative vorticity by the time it reaches this starting point for the image sequence. Then, as the archer moves its pectoral fin back up towards the surface of the water, it starts to have positive vorticity forming along its length. By the top the fin has shed the positive vorticity and is starting to form the negative vorticity that will be shed at the bottom of the range of motion. From this cut of vorticity there is a clear image of a jet moving away from the pectoral fin through the center of what appears to be a vortex ring, 65.0° from the body axis of the fish.

The fin on the left of the image sequences shows a similar jet formation, however with reversed vorticity so that the jet is still moving away from the body, at an angle

of 57.4° with respect to the fish's body axis. The fin creates the positive vorticity along its length through its downward stroke and then sheds it near the lowest point of its motion. Also, as it moves upwards the fin creates the negative vorticity that is shed when the fin is near the surface of the water.

Presumably this is indicative of what will happen throughout the course of station keeping, until the fish jumps or swims away. The pectoral fins produce opposing jets that hold the fish in place, although since this is only a two dimensional representation it is impossible to tell if any forward or backward thrust from the anal or dorsal fins would be needed to balance out any out of plane forces from the pectoral fins.

5.3 Thrust Production

Thrust production has multiple components that were explored through PIV. Tytell [33], suggested that the dorsal and anal fins provide force that is equal to that produced by the caudal fin. While it was difficult to position the laser plane precisely to see the contribution of all of the archer fish's fins, the tail and the anal fin were both examined in this thesis.

5.3.1 Anal Fin Contribution

The anal fin for the archer fish does contribute to the overall thrust production during a jump. This can be seen in Figure 5-2, where an image sequence taken at 900 frames per second of Archer 10 shows how the anal fin helps produce thrust. This particular data is for a jump where the bait was half a body length above the surface. Since this was one of the few jumps where the fish was positioned in such a manner that the vorticity from the anal fin was captured well by the PIV (but the anal fin still moves out of the laser plane after one and a half flaps) it is hard to make any definitive conclusions about how the anal fin contributes over the course of the jump.

This particular run nicely illustrates how the anal fin adds to the overall vorticity production by the archer during a jump. The fish rotates around its centerline axis throughout the course of the jump, so anything that is happening near the body is

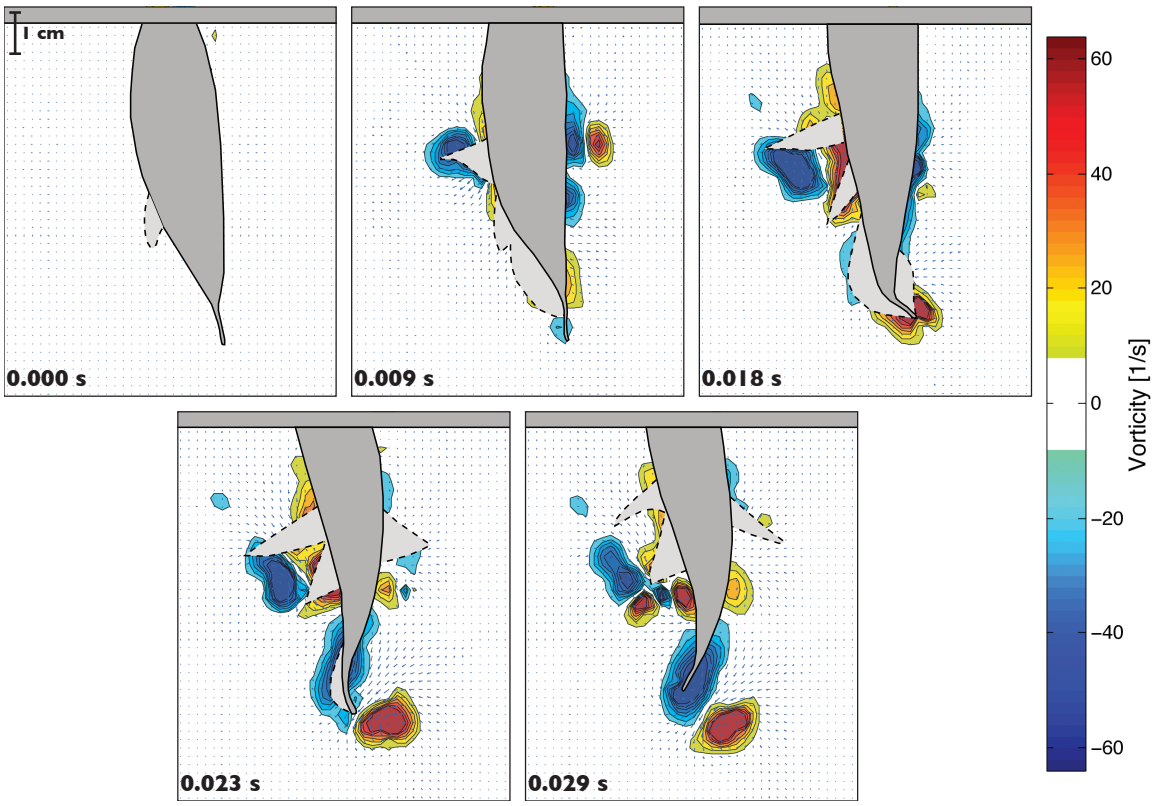

Figure 5-2: An image sequence showing vorticity and velocity vectors corresponding to evenly spaced portions of a PIV experiment. In this case the fish is being viewed head on, so the belly and body of the fish are the dark gray and the fins have dotted edges and are a lighter gray. The laser plane is aligned with the anal fin during the beginning of the jump.

harder to deciper. The frames were chosen to correspond with the peak excursion of the anal fin. The first frame is before any fin motion, the third when the anal fin is as at the maximum for that stroke, and the fifth is the maximum for the next stroke. Here it is important to remember that a stroke, as shown in Figure 3-10, is when the caudal fin moves between one set of peak displacements. Each of the intervening frames is at the middle of the stroke based on the time it took to complete the stroke. There is clearly positive vorticity that is shed off the anal fin in the third to fourth frame. Then, in the final frame negative vorticity has formed on the anal fin and looks like it will shed forthwith.

From this vorticity formation and release the conclusion to be drawn is that the anal fin produces at least one jet throughout the course of the jump. It is hard to

know if the anal fin will produce more than one jet, since there is no PIV where the anal fin is in the laser plane in the middle of a longer duration jump. In addition this jet is aligned at a fairly significant angle with respect to the vertical (35.9°), so it not only has downward momentum, but also transverse momentum to the left of the frame. Since the archer does not noticeably move to the side while jumping, this force must be balanced in the horizontal direction by some other force production. However, without 3-D PIV full field data with all other fins (e.g. dorsal or pelvic) in view there can be no further conclusions to be drawn about the transverse force production. Ideally, similar data should be seen for the dorsal fin as well.

5.3.2 Caudal Fin Contribution

In order to quantify the caudal fin contribution to force production, PIV was taken from two different angles, as discussed in Chapter 2. The first view was of the belly of the archer, using the same set up as when the anal fin was studied, and the second view was taken when the laser was parallel to the bottom of the tank. This way the fish's tail is cut by the laser plane, and the caudal fin will be seen moving through the laser plane as time progresses.

Head On View

For the first view, of the belly of the archer fish, two different runs are presented here. Both of the runs presented from this view are from Archer 10. The first sequence (Figure 5-3) is for a jump where the bait was half a body length above the water, while the second (Figure 5-4) has Archer 10 jumping for bait that is one body length above the water surface.

Looking at Figure 5-3, the tail is only in the laser plane for the course of two tail strokes. The first half stroke occurs from frame one to two, while the only complete stroke is between frames two and four, and the final half stroke occurs between frames four and six.

A jet like the one that is created by the anal fin is also seen here, only coming off

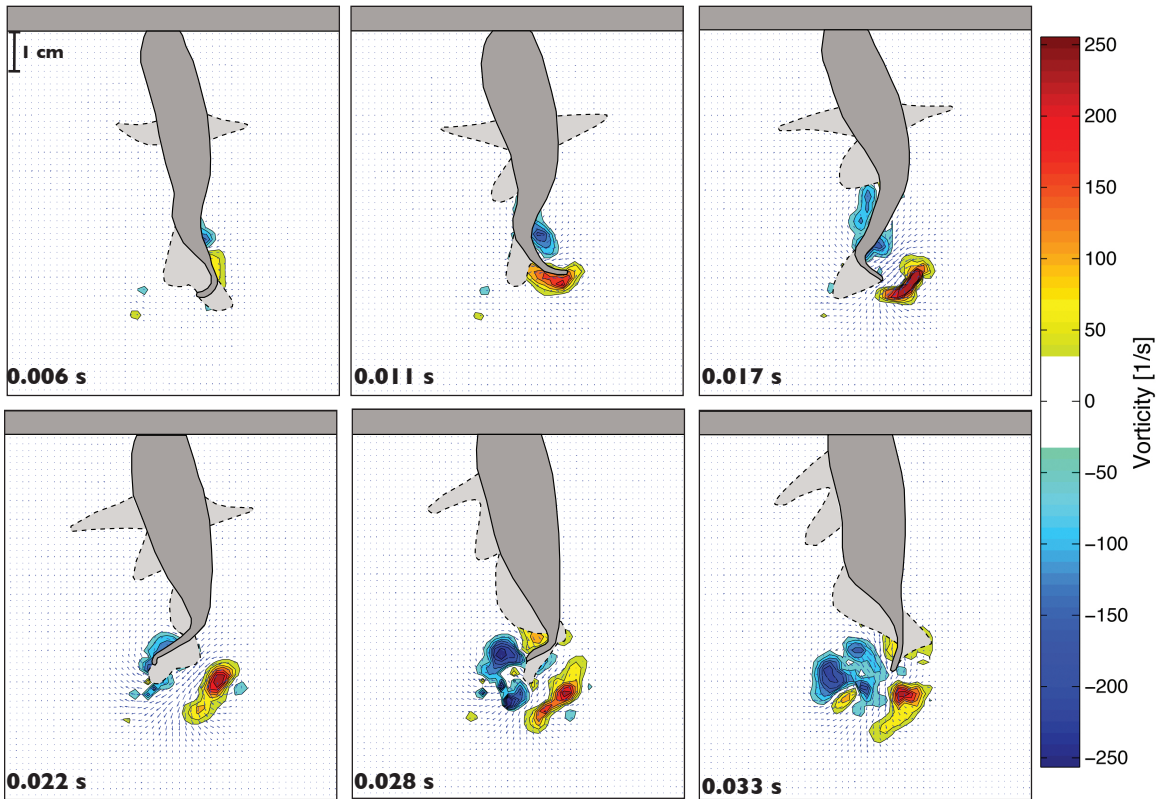

Figure 5-3: An image sequence showing vorticity and velocity vectors corresponding to evenly spaced portions of a PIV experiment. In this case the fish is being viewed head on, so the belly and body of the fish are the dark gray and the fins have dotted edges and are a lighter gray. The laser plane lines up with the caudal fin initially.

the caudal fin at an angle of 42.3° from horizontal, but still oriented away from the fish and towards the left of the frame. Once again the positive vorticity is shed first after forming along the lower portion of the caudal fin, after the first half a stroke. Even before the positive vorticity is shed there is still the gradual build up of negative vorticity further up the body of the archer. This stays on the body until after the positive vorticity has been shed and the tail has moved through the rest of its only full stroke. At the end of that stroke the negative vorticity is released from the body and the apparent vortex ring begins to move away.

Since this jump only reaches a final height around half a body length, the archer will not perform as many tail strokes as it would if it were jumping higher. In order to compare the thrust production for a small number of tail strokes to a jump with more tail strokes, we turn to Figure 5-4.

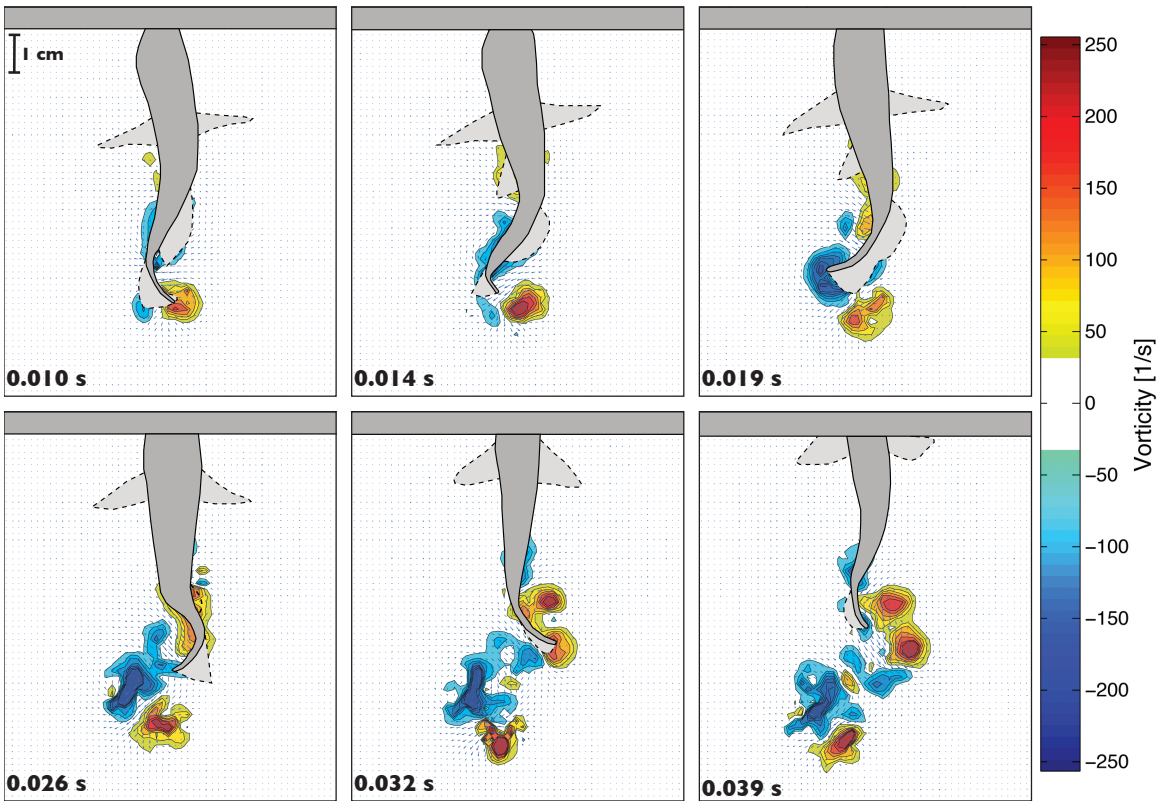

Figure 5-4: An image sequence corresponding a PIV experiment where the bait height was one body length. In this case the fish is being viewed head on, so the belly and body of the fish are the dark gray and the fins have dotted edges and are a lighter gray. To begin with, the laser plane is aligned with the caudal fin.

This figure also shows multiple tail strokes, however this time two and a half strokes are visible throughout the run. The first stroke goes from time equal to zero to the second frame, while the second stroke is from frame two to five. A final half a stroke occurs from frame five to six. Once again there is the formation of a first vortex ring, with a jet through its center at 44.8°. This occurs from 0.0 to 0.026 seconds, in the same manner as for the half a body length jump, with the positive vorticity being shed before the negative vorticity.

In this case, however, there is also the formation of a second jet, depicted in the fifth frame of the image sequence. This jet is inclined at 38.9° from the horizontal, and is found to the right of the fish, instead of the left as all previous jets have been located. It is impossible to tell for sure if the positive vorticity that is being produced in the last three frames will be shed, as well as the negative vorticity that makes

an appearance in the last two frames. If this is shed though, the wake formation will begin to resemble that of the vortex wake when a fish is swimming, with jets alternating directions through the center of interconnected vortex rings.

While these are only two cases, they show that not only does the caudal fin create vortex rings, but also that those rings are shed in time with tail strokes; one positive and negative pair per stroke. Since there are more strokes for higher jumps, and each stroke seems to be producing a distinct jet moving away from the body of the archer, this means that the addition of more strokes for higher jumps correlates to an increase in thrust production for higher jumps.

Another important note is that in both of these cases the vorticity that is produced moves away from the body in a direction parallel to the position of the tail at the end of the stroke. For the archer to move straight up from the water there must be a balancing force somewhere along the body that is not being captured by these PIV images.

Bottom View

To get another picture of the nature of the vorticity being created by an archer fish jumping, PIV was taken from an alternative angle where the tail is moving through the laser plane, as described in Chapter 2. There are two runs presented in this section, from different archers. It is impossible to see the first pectoral fin motion in these video sequences. However, as discussed in Section 2.2.1 the first motion of the pectoral fin is synchronous with the first motion of the tail, so time equals zero for both cases should be similar.

The first of these two bottom view sequences (Figure 5-5) shows Archer 3 jumping for bait that is half a body length above the surface of the water. The tail is apparent in the first two frames, which occur during the first tail stroke. After that the caudal fin moves out of the laser plane and all that remains in frame is the in plane vorticity. When the caudal fin is moving through this image sequence, it is traveling towards the top right of the frame at approximately 28.5° above the horizontal.

In the first image in this sequence the larger grayed out region is the caudal fin,

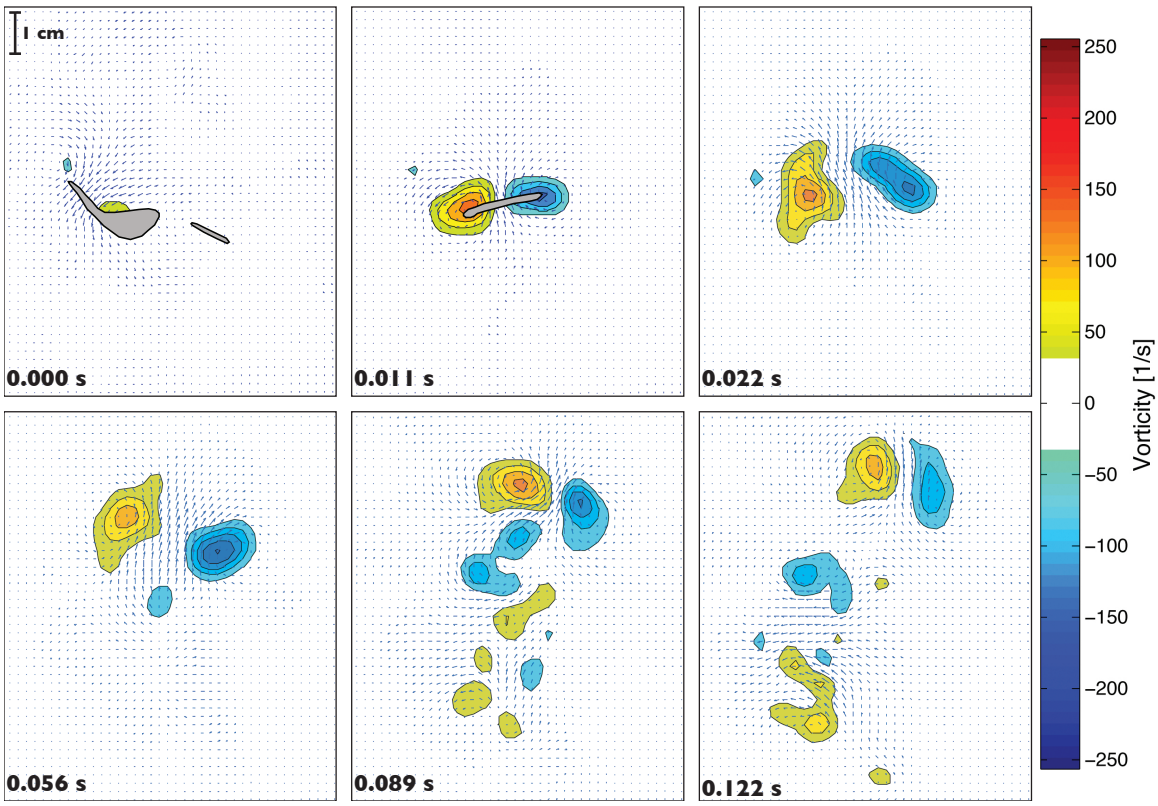

Figure 5-5: An image sequence showing vorticity and velocity vectors corresponding to evenly spaced portions of a PIV experiment, where the bait was half a body length above the surface. All grayed out sections are slices of the tail.

while the smaller such region is part of the anal fin. There is little vorticity formation at this point, but by the next image, which is partially through the first caudal fin stroke, there is a definite jet coming off the tail, between regions of positive and negative vorticity. The jet's direction is almost perpendicular to the caudal fin itself, but not quite; there is a 1.2° difference.

After the caudal fin has passed from the plane (this occurs at 0.0211 seconds) the jet is still readily apparent and moving in the same direction. This vortex ring configuration remains cohesive for a considerable length of time after the tail has left the region. In the fifth frame there is the addition of other vorticity in the frame. Since the previous images have lacked spurious bits of vorticity that would represent noise in the PIV, this new vorticity seems significant. The last frame nicely displays what appears to be another vortex ring passing through the plane. This second patch of vorticity must have been created later in the jump, and thus is being viewed after

it has been shed and convected downward, so it is impossible to conclusively say that it was generated by another tail flap or the dorsal fin. The lack of noise later frames and the previous PIV views both suggest that it is from a separate stroke.

In comparison, Figure 5-6 shows Archer 4 jumping for bait at a full body length above the surface. For this particular run the fish had more of its body in the laser plane to begin with, resulting in a shadow to the right of the archer. In terms of the fins that are in the laser sheet, the top portion is a slice of the anal fin, while the region on the lower right is the caudal fin.

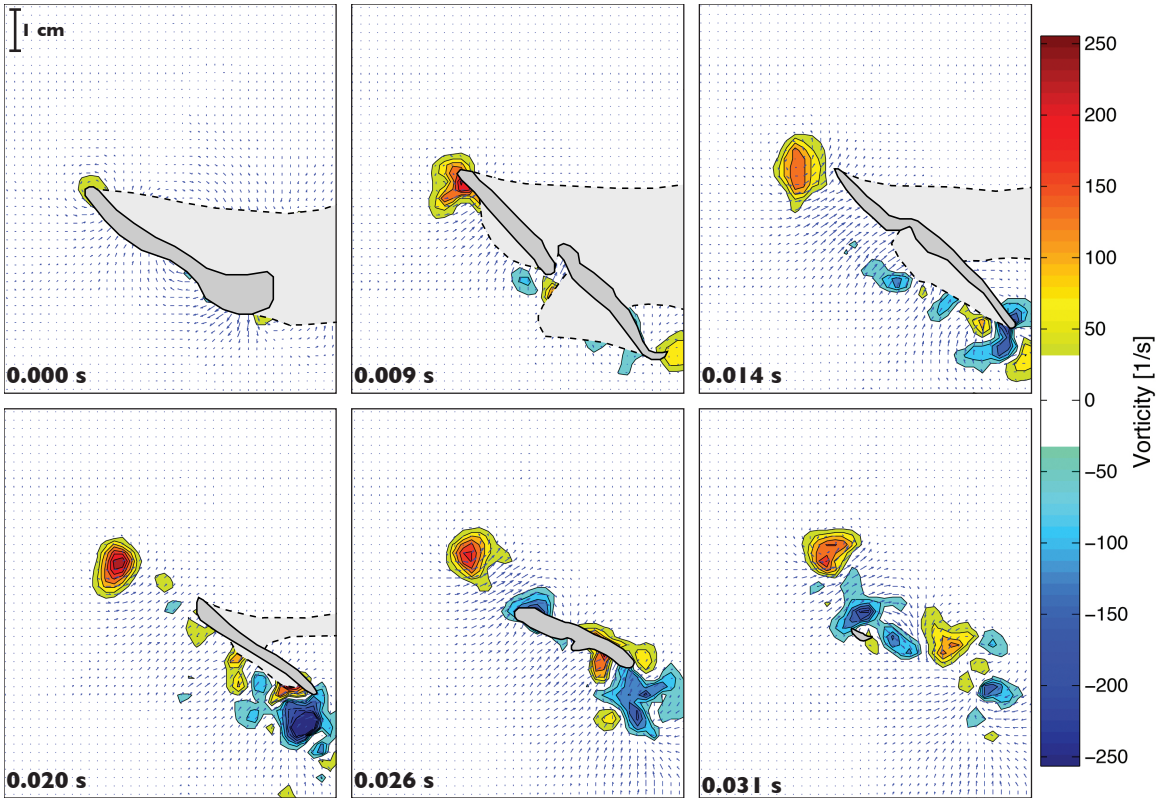

Figure 5-6: An image sequence showing vorticity and velocity vectors corresponding to evenly spaced portions of a PIV experiment, where the grayed out sections with solid lines are slices of the tail in the laser plane. Lighter gray regions with the dashed borders are either shadowed regions or areas where fins were blocking the laser plane. For this run the bait was one body length above the water surface.

In the first two frames the shadowed region appears to be covering the beginnings of vorticity production, but it is still possible to see a very concentrated region of positive vorticity that forms at the edge of where the anal fin is in the laser plane. As

the anal fin moves out of plane the positive vorticity is still left behind. Additionally, a contribution from the caudal fin starts to make an appearance at the same time (frame three). For this jump height the data is less clear cut, there is no distinct jet being produced by the tail. However there is a jet between the positive vorticity created by the anal fin and the negative vorticity on the adjacent edge of the caudal fin. This jet, which is angled at 33.9° with respect to horizontal, is separated from the line of the caudal fin by 58.6°. On the other end of the caudal fin there appears to be a similar phenomenon taking place. It is entirely possible that part of the vorticity shown on the bottom right is from the dorsal fin, in which case this jump would show characteristics of the theory put forth by Tytell [33], where the the caudal fin vorticies potential interact with those produced by the anal and dorsal fins.

For the lower body length jump from this same view point, PIV was shown for enough time frames to show the appearance of what appeared to be vorticity from another tail stroke. In this particular case that was not done because the level of coherence decreases too much with increasing time.

5.4 Circulation

For each of the PIV images shown above, the circulation was calculated for the vortex ring that is shed, except for Figure 5-6, since there is no coherent vortex ring shown in this series of images. Calculation of circulation was done using a custom Matlab program that numerically evaluates Stokes theorem:

$$\Gamma = \sum_{i,j} \omega_{i,j} \delta A$$

Where $\omega_{i,j}$ is the curl of the velocity field at a point specified by (i,j) and δA is the box size, or in this case (32 pix)^2, converted to centimeters based on the calibration image for each run. From the diameter of the vortex ring and the circulation, impulse

could be calculated as for a vortex ring moving steadily ahead:

$$\underline{I} = \rho\Gamma\frac{\pi D^2}{4}\underline{e}_z$$

In this equation, Γ is the circulation that was calculated previously, D is the diameter of the vortex ring, and ρ is the density of the fluid, which for this trials was taken to be 99.84 g/cm^3 based on measurements made on water from the archers' home tank.

To put the circulation and impulse values in perspective, when Epps and Techet [15] looked at a Giant Danio fast starting, for a fish of length 7.4 cm and mass of 4.3 g, the "maneuvering" vortex had a circulation of 17 cm^2/s while the "propulsive" vortex had a circulation of 34 cm^2/s. Those same vortices had an impulse of 25 and 91 gcm/s, respectively.

Hovering

For the hovering PIV image sequence shown in Figure 5-1, circulation and impulse were calculated for both the vortex ring shed from the pectoral fin on the left of the image (Table 5.1) as well as the vortex ring shed from the fin on the right of the image (Table 5.2). Both of these tables illustrate the increasing circulation and impulse throughout the formation of the vortex ring; however comparing the values for the vortex rings from the two sides of the archer shows a discrepancy in circulation, diameter, and impulse. The vortex ring that is formed to the right of the archer has a large impulse associated with it, however this is to be expected as the image sequence was chosen to coincide with the formation of this vortex ring.

Ideally, these vortices should have the same impulse in order to balance each other. However, as was mentioned before, the vortices being shed are coming off the pectoral fins are different angles with respect to the body axis, so it is not surprising that the vortices are not perfectly balanced, since they would not cancel even if they had the same impulse.

Even though the hovering vortex rings are not equal but opposite, they still show significant impulse production by the pectoral fins of the archer fish, indicating that

Table 5.1: Hovering circulation and impulse data for the vortex ring that is shed off the pectoral fin that appears on the left of the images.

Frame No.	Time [s]	Γ [cm^2/ s]	D [cm]	Impulse [g cm/ s]
1	0.000	23.7	0.79	11.5
2	0.064	40.3	0.76	18.1
3	0.096	65.4	0.92	43.1
4	0.128	74.0	1.00	56.9
5	0.160	97.7	1.32	132.6
6	0.192	145.7	1.17	156.27

Table 5.2: Hovering circulation and impulse data for the vortex ring that is shed off the pectoral fin that appears on the right of the images.

Frame No.	Time [s]	Γ [cm^2/ s]	D [cm]	Impulse [g cm/ s]
1	0.000	34.9	0.97	25.6
2	0.064	83.9	1.03	70.1
3	0.096	141.6	0.80	70.6
4	0.128	154.3	1.15	161.1
5	0.160	178.6	1.34	250.0
6	0.192	163.2	1.39	245.7

it is reasonable for the pectoral fins to be the primary force behind the hovering behavior. The fact that the rings are not perfectly balanced could either show that other fins are minimally involved in hovering, or it could be an artifact of the vortex rings not being caught at the same point in their respective cycles.

Anal Fin Contribution

Results from calculations of circulation and impulse for the PIV run that caught the anal fin (image sequence shown in Figure 5-2) are found in Table 5.3. An important note is that for frame 5 the circulation, diameter and impulse presented are actually interpolated from surrounding frames due to a processing error. Additionally, for the first two frames of the PIV sequence that capture the contribution of the anal fin, there was no significant vortex ring, so circulation was not reported.

For this run, the circulation and impulse are seen to increase as vorticity increases

Table 5.3: Jumping circulation and impulse data for anal fin vortex, bait height 0.5 BL. Note that frame 5 is interpolated from the surrounding frames due to an error with the Matlab processing code.

Frame No.	Time [s]	Γ [cm^2/ s]	D [cm]	Impulse [g cm/ s]
3	0.018	320.3	1.28	414.2
4	0.023	340.4	1.42	538.5
5	0.029	367.7	1.05	318.3

along the length of the body. For the last frame the vorticity and impulse have begun to drop again as the ring is being shed from the body. Comparatively, this is a greater amount of impulse than what is formed during hovering. Having a high impulse as a result of the anal fin's motion is a indicator that the anal fin must play a significant role in the jumping behavior. However since the vortex ring moves off at an angle from the vertical, this raises the question of what is balancing it. This is a question that will be very difficult to answer without the help of a 3-D PIV system.

Caudal Fin Contribution

Contributions from the caudal fin were similarly analyzed in Matlab. The circulation, diameter of vortex rings, and impulse can be found in Table 5.4 for the jump where the bait was 0.5 body lengths above water, and Table 5.5 for the jump where bait was a full body length out of water. For both runs, the vortex ring analyzed was the one that was shed during the first full tail stroke. In the half body length case this vortex was shed near the time of the fifth image (Figure 5-3), while for the one body length case the vortex in question was shed close to the time of the fourth image (Figure 5-4).

For the case where the bait was half a body length above the free surface, a maximum impulse of 885.5 g cm/s was calculated for the last image in the sequence, after the vortex had been shed from the tail. Once again the circulation and impulse are seen to grow as the vorticity forms, and peak when it has been shed into the surrounding fluid. Comparing this to the vorticity shed by the anal fin shows that it is almost twice as great, so while the anal fin does contribute, it is the caudal fin that

Table 5.4: Jumping circulation and impulse data for caudal fin vortex, bait height 0.5 BL.

Frame No.	Time [s]	Γ [cm^2/ s]	D [cm]	Impulse [g cm/ s]
1	0.006	146.2	0.53	32.7
2	0.011	273.1	1.00	216.0
3	0.017	261.0	1.26	323.6
4	0.022	326.2	1.40	499.9
5	0.028	387.0	1.43	618.8
6	0.033	476.8	1.54	885.5

is producing more of the impulse required for the jump.

Table 5.5: Jumping circulation and impulse data for caudal fin vortex, bait height 1.0 BL.

Frame No.	Time [s]	Γ [cm^2/ s]	D [cm]	Impulse [g cm/ s]
1	0.010	385.4	1.60	776.7
2	0.014	481.0	1.31	649.0
3	0.019	505.7	1.22	589.1
4	0.026	721.5	1.27	915.4
5	0.032	561.6	1.15	584.2
6	0.039	545.0	1.23	651.1

The impulse data for the jump of one body length shows a very similar trend, only with even higher peak impulse and circulation. This vortex ring has a higher circulation and smaller diameter that result in the increased impulse (again, reached after the vortex is shed). Since the circulation, diameter and impulse trends are only being compared for two runs it is impossible to tell whether or not the change in diameter and circulation is the result of differing behaviors for jumps of varying heights, or is merely a result of natural variation. What these two runs do prove is that a large amount of impulse is gained from each tail stroke and contributes to the archer fish's ability to jump out of water.

While the jets produced by these jumps are also at a significant angle with respect to vertical and since the tail often performs multiple strokes during the course of a jump, the horizontal components of the multiple jets could potentially cancel each

other out. This is something that will require either more well placed 2-D PIV studies, or a 3-D study in order to determine.

Circulation and impulse were also calculated for the case where a jump of half a body length is viewed from the bottom of the tank, however not the run where the archer jumps one body length and is viewed from the bottom, since in that case there is not the formation of one clear vortex ring. The data for the jump of half a body length is shown in Table 5.6. When viewing this data it is important to remember that the archer used for this run (Figure 5-5) is different from the archer used for the front view runs.

Table 5.6: Jumping circulation and impulse data for caudal fin vortex as viewed from below, bait height 0.5 BL.

Frame No.	Time [s]	Γ [cm^2/ s]	D [cm]	Impulse [g cm/ s]
1	0.000	3.4	1.14	3.5
2	0.011	211.4	1.39	321.5
3	0.022	305.3	1.59	607.3
4	0.056	258.6	1.61	522.7
5	0.089	206.9	1.23	244.4
6	0.122	157.0	1.11	151.5

The processed impulse and circulation show that the maximum for both can be found in the third image in the sequence, which is when the tail is passing out of the laser plane and appears to be at the end of its first stroke. Since it is impossible to tell if this is the true point at which the vortex is being shed, it is impossible to compare values between runs. However, this data reinforces the fact that the caudal fin is producing vorticity contributing to the propulsion of the fish out of water. It also highlights the fact that the caudal fin is not producing a jet that is moving straight down through the water, but like the anal fin is at an angle, even if it is not as extreme.

Chapter 6

Conclusions

Analysis of how archer fish jump out of water has been presented for the first time. The analysis makes use of both high speed imaging as well as high speed digital particle image velocimetry to enable visualization of the kinematics and fluid mechanics of the jumping behavior. The major results from both the kinematic and the hydrodynamic analysis are summarized below.

6.1 Kinematics of Jump

The archer fish's jump can be broken up into three main parts:

- **Hovering** relies on out of phase pectoral fin motions to keep the archer in place before it jumps. This takes place at the angle of initial inclination, which is generally in the range of 40 to 65 degrees from the horizontal.

- **Thrust Production** occurs once the archer begins its first fin motions (t =0) and continues as long as the archer is performing tail strokes. As the jump height increases, there is a linear increase in the number of strokes the archer performs during the thrust production phase. During this phase the archer's velocity is steadily increasing, while the acceleration experiences a sharp peak in the beginning of the thrust production. The maximum velocity reached here will increase with the increasing height of the bait.

- **Glide** occurs after the archer has partially exited the water and is no longer performing tail strokes. During this portion of the jump, which is optional, the archer holds its body still as it glides towards the prey. The glide ends when the archer reaches its prey. During this phase the archer's velocity is relatively constant, while the acceleration drops until it reflects the fact that gravity is pulling the archer down.

When an energy balance is performed for these archer fish, the kinetic and potential energy were found to balance each other, with the kinetic energy being higher in certain cases, potentially explaining the phenomenon of overshooting (when the fish jumps higher than it needs to in order to capture the bait). Overshooting occurs more at lower heights (bait lower than 0.5 body lengths above the surface) and less when the bait is higher than 1.5 body lengths above the surface. For the fish used in this thesis the upper limit of jumping was found to be around 2.5 body lengths above the free surface.

6.2 Fluid Mechanics of Jump

There were three main runs which particle image velocimetry was used to study:

- **Hovering**: Opposing vortex rings are produced by the pectoral fins. While these are angled with respect to the body, they provide enough impulse to explain how the archer is able to hold itself stationary. Contributions from the caudal, anal or dorsal fin may provide small stabilization forces.

- **Anal Fin Contribution to Jump**: The anal fin produces at least one jet which comes off the body at an angle with respect to the body axis. The resultant jet produces a significant amount of impulse, and thus cannot be ignored when considering the propulsive mechanisms. Horizontal impulse produced by the anal fin may be balanced by the action of the dorsal fin, but that cannot be determined without performing 3 dimensional PIV.

- **Caudal Fin Contribution to Jump**: The caudal fin produces a jet each time it performs a tail stroke. While the anal fin does contribute to the impulse needed to jump, the caudal fin vortex ring results in more impulse. This thesis examined the impulse that results from the first tail stroke, but further studies are needed to establish a pattern for the rest of the tail strokes that the archer performs.

Overall, this thesis looked at the never before studied jumping behavior of archer fish. It established the main mechanisms of this unique ability, and highlighted some of the key hydrodynamic points in the jumping maneuver. Hopefully this will lay the ground work for future studies on the archer fish as well as make people more aware of the archer's unique ability.

6.3 Consideration for Future Studies

The ability of archer fish to jump is a very complex skill. While this these touched on some of the major aspects of the jumping behavior, there are items left for future work, such as:

- **Neural Control**: Many fast start maneuvers have been studied further to figure out the neural pathways that are associated with their control. This could be extended to archer fish as well, to see if this fast starting maneuver is also a Mauthner-initiated response.

- **Operant Control**: Goldstein and Hall [16] studied whether or not a variable ratio schedule of reinforcement could change the archer's spitting behavior. This could be extended to the jumping behavior as well so that it is easier to predict if the impact of this control has the same effect on jumping as it does on spitting. Additionally, this could be used to determine when the archer is going to spit or when it will jump.

- **Swim Bladder**: During this study it was assumed that the swim bladder was not changing throughout the course of the jump, so that buoyancy effects were

always the same. However, this is not necessarily true, so it should be further examined in order to determine whether or not the variable buoyancy of the swim bladder comes into play.

- **Fish Tracking**: To clean up the position, velocity and acceleration data, a more complex algorithm could be developed to track the center of gravity of the fish instead of just the nose. While this is not expected to change the velocity and acceleration plots significantly, it should eliminate some of the noise that is due to the fish opening and closing its mouth.

- **Three Dimensional Imaging**: In order to fully understand the motion of all of the fins, it would be best to take three dimensional particle image velocimetry data. This way the interaction between the fins will be captured, as well as the data for one fin through time, since the fin will no longer move out of the plane being studied.

Bibliography

[1] Erik J. Anderson, Wade R. McGillis, and Mark A. Grosenbaugh. The boundary layer of swimming fish. *The Journal of Experimental Biology*, 204:81–102, 2001.

[2] Promode R. Bandyopadhyay. Maneuvering hydrodynamics of fish and small underwater vehicles. *Integrative and comparative biology*, 42(1):102–117, 2002.

[3] Marc Bekoff and Robert Door. Predation by "shooting" in archer fish, toxotes jaculatrix: accuracy and sequences. *Bulletin of the Psychonomic Society*, 7(2):167–168, 1976.

[4] Charlie R. Braekevelt. Photoreceptor fine structure in the archerfish (toxotes jaculatrix). *American Journal of Anatomy*, 173(2):89–98, 1985.

[5] Juerg M Brunnschweiler. Water-escape velocities in jumping blacktip sharks. *Journal of the Royal Society Interface*, 2:389–391, 2005.

[6] Maurice Burton and Robert Burton. *The international wildlife encyclopedia*. Marshal Cavendish Corp, New York, 1970.

[7] John O. Dabiri. On the estimation of swimming and flying forces from wake measurements. *The Journal of Experimental Biology*, 208:3519–3532, 2005.

[8] Lawrence M. Dill. Refraction and the spitting behavior of the archerfish (toxotes chatareus). *Behavioral Ecology and Sociobiology*, 2:169–184, 1977.

[9] Paolo Domenici. The scaling of locomotor performance in predator-prey encounters: from fish to killer whales. *Comparative Biochemistry and Physiology: Part A*, 131:169–182, 2001.

[10] Paolo Domenici and Robert W. Blake. The kinematics and performance of fish fast-start swimming. *Journal of Experimental Biology*, 200:1165–1178, 1997.

[11] Eliot G. Drucker and George V. Lauder. Locomotor forces on a swimming fish: three-dimensional vortex wake dynamics quantified using digital particle image velocimetry. *The Journal of Experimental Biology*, 202:2393–2412, 1999.

[12] Robert C. Eaton, Rocco A. Bombardieri, and Dietrich L. Meyer. The mauthner-initiated startle response in teleost fish. *Journal of Experimental Biology*, 66:65–81, 1977.

[13] G.C.A Elshoud and P. Koomen. A biomechanical analysis of spitting in archer fishes (pisces, perciformes, toxidae). *Zoomorphology*, 105:240–252, 1985.

[14] Brenden P. Epps. *An impulse framework for hydrodynamic force analysis: fish propulsion, water entry of spheres, and marine propellers*. PhD thesis, Massachusetts Institute of Technology, 2010.

[15] Brenden P. Epps and Alexandra H. Techet. Impulse generated during unsteady maneuvering of swimming fish. *Experiments in Fluids*, 43(5):691–700, 2007.

[16] Stephen R Goldstein and David Hall. Variable ratio control of the spitting response in the archer fish (toxotes jaculator). *Journal of Comparative Psychology*, 104(4):373–376, 1990.

[17] David G. Harper and Robert W. Blake. Prey capture and the fast-start performance of northern pike esox lucius. *Journal of Experimental Biology*, 155:175–192, 1991.

[18] M.C. Kondratieff and C.A. Myrick. How high can brook trout jump? a laboratory evaluation of brook trout jumping performance. *Transcations of the American Fisheries Society*, 135(2):361–370, 2006.

[19] Dayv Lowry, Alpa P Wintzer, Michael P Matott, Lisa B Whitenack, Daniel R Huber, Mason Dean, and Philip J. Motta. Aerial and aquatic feeding in the silver arawana, osteoglossum bicirrhosum. *Environmental Biology of Fishes*, 73:453–462, 2005.

[20] Oliver Milburn and R. McN. Alexander. The performance of the muscles involved in spitting by the archerfish toxotes. *Journal of Zoology*, 180:243–251, 1976.

[21] U.K. Muller, B.L.E. van den Heuvel, E.J. Stamhus, and J.J. Videler. Fish foot prints: morphology and energetics of the wake behind a continuously swimming mullet (chelon labrosus risso). *The Journal of Experimental Biology*, 200:2893–2906, 1997.

[22] Samuel Rossel, Julia Corlija, and Stefan Schuster. Predicting three-dimensional target motion: how archer fish determine where to catch their dislodged prey. *The Journal of Experimental Biology*, 205:3321–3326, 2002.

[23] William M. Saidel, Gabriel F. Strain, and Shannon K. Fornari. Characterization of the aerial escape response of the african butterfly fish, pantodon buchholzi peters. *Environmental Biology of Fishes*, 71:63–72, 2004.

[24] Thomas Schlegel, Christine J. Schmid, and Stefan Schuster. Archerfish shots are evolutionarily matched to prey adhesion. *Current Biology*, 16(19):R836–R837, 2006.

[25] Stefan Schuster, Samuel Rossel, Annette Schmidtmann, Ilonka Jager, and Julia Poralla. Archer fish learn to compensate for complex optical distortions to determine the absolute size of their aerial prey. *Current Biology*, 14:1565–1568, 2004.

[26] Stefan Schuster, Saskia Wohl, Markus Griebsch, and Ina Klostermeier. Animal cognition: how archer fish learn to down rapidly moving targets. *Current Biology*, 16:378–383, 2006.

[27] S. E. Temple. Effect of salinity on the refractive index of water: considerations for archer fish aerial vision. *Journal of Fish Biology*, 70:1626–1629, 2007.

[28] P.J.A. Timmermans. Prey catching in archer fish: angles and probability of hitting an aerial target. *Behavioural Processes*, 55(2):93–105, 2001.

[29] P.J.A. Timmermans and P.M. Souren. Prey catching in archer fish: the role of posture and morphology in aiming behavior. *Physiology and Behavior*, 81:101–110, 2004.

[30] P.J.A. Timmermans and J.M.H. Vossen. Prey catching in archer fish: does the fish use a learned correction for refraction? *Behavioural Processes*, 52(1):21–34, 2000.

[31] M.S. Triantafyllou, G.S. Triantafyllou, and D.K.P. Yue. Hydrodynamics of fish-like swimming. *Annual Review of Fluid Mechanics*, 32:33–53, 2000.

[32] T.C. Tricas. Feeding ethology of the white shark, carcharodon carcharias. *Memoirs of the Southern California Academy of Sciences*, 9:81–91, 1985.

[33] Eric D. Tytell. Median fin function in bluegill sunfish lepomis macrochirus: streamwise vortex structure during steady swimming. *The Journal of Experimental Biology*, 209(8):1516–1534, 2006.

[34] Eric D. Tytell and George V. Lauder. Hydrodynamics of the escape response in bluegill sunfish, lepomis macrochirus. *Journal of Experimental Biology*, 211:3359–3369, 2008.

[35] P. W. Webb. Fast-start performance and body form in seven species of teleost fish. *Journal of Experimental Biology*, 74:211–226, 1978.

[36] D. Weihs. A hydrodynamical analysis of fish turning manoeuvres. *Proceedings of the Royal Society B*, 182:59–72, 1972.

[37] F.C. Wiest. The specialized locomotory apparatus of the fresh-water hatchetfish family gasteropelecidae. *Journal of Zoology*, 236(4):571–592, 1995.

[38] Saskia Wohl and Stefan Schuster. The predictive start of hunting archer fish: a flexible and precise motor pattern performed with the kinematics of an esape c-start. *The Journal of Experimental Biology*, 210:311–324, 2007.